SSC-265

A STUDY OF SHIP HULL CRACK ARRESTER SYSTEMS

SHIP STRUCTURE COMMITTEE
1977

SHIP STRUCTURE COMMITTEE

AN INTERAGENCY ADVISORY
COMMITTEE DEDICATED TO IMPROVING
THE STRUCTURE OF SHIPS

MEMBER AGENCIES:
United States Coast Guard
Naval Sea Systems Command
Military Sealift Command
Maritime Administration
American Bureau of Shipping

ADDRESS CORRESPONDENCE TO:
Secretary
Ship Structure Committee
U.S. Coast Guard Headquarters
Washington, D.C. 20590

SR-226

15 APR 1977

The development of new materials and the increased sophistication of computer assisted stress-analysis techniques provided an opportunity for the Ship Structure Committee to review and evaluate current and proposed ship hull crack arresting systems. Major emphasis was put upon dynamic fracture mechanics for the proper classification and evaluation of the crack arrester systems investigated. Results have also been compared with a static arrest toughness analysis.

The results contained in this report indicate that 1) there is no general type of crack arrest system completely superior to all others in all circumstances; 2) an exact quantitative evaluation must be performed for each application; and 3) insufficient fundamental work has been done to provide a fully rational or scientific approach for crack arrester design. A five element research program has been proposed to remedy these deficiencies. This will be considered by the Ship Structure Committee in the future.

W. M. Benkert
Rear Admiral, U.S. Coast Guard
Chairman, Ship Structure Committee

FINAL TECHNICAL REPORT

on

Project SR-226

"Hull Crack Arrester Systems"

A STUDY OF SHIP HULL CRACK ARRESTER SYSTEMS

by

M. Kanninen
E. Mills
G. Hahn
C. Marschall
D. Broek
A. Coyle
K. Masubushi*
K. Itoga*

BATTELLE COLUMBUS LABORATORIES

under

Department of the Navy
Naval Sea Systems Command
Contract No. N00024-75-C-4325

*MIT, Consultants to BATTELLE

U. S. Coast Guard Headquarters
Washington, D.C.
1976

ABSTRACT

A world-wide survey of marine engineers, shipyards, and regulating agencies was conducted to ascertain both current and contemplated approaches to arresting cracks in ship hulls. As a result of this survey, a crack arrester classification system was developed. The classification was used to aid in a systematic investigation aimed at determining the most attractive practical schemes for arresting cracks in ship hulls. In addition to describing the classification system, example calculations showing quantitatively the effect of imposing various kinds of mechanical arrester devices in the path of a fast-moving crack are given in the report. Considerable background material on the theoretical concepts and material characterizations required for the arrest of fast fractures and fatigue is also given. Taken together the work described in the report can be used as a first step in developing guidelines for ship designers in situations where structural perturbations for the purpose of arresting unstable crack propagation are envisioned.

TABLE OF CONTENTS

TABLE OF CONTENTS (Continued)

LIST OF FIGURES

LIST OF FIGURES (Continued)

LIST OF FIGURES (Continued)

LIST OF TABLES

SHIP STRUCTURE COMMITTEE

The SHIP STRUCTURE COMMITTEE is constituted to prosecute a research program to improve the hull structures of ships by an extension of knowledge pertaining to design, materials and methods of fabrication.

RADM W. M. Benkert, USCG
Chief, Office of Merchant Marine Safety
U.S. Coast Guard Headquarters

Mr. P. M. Palermo
Asst. for Structures
Naval Ship Engineering Center
Naval Ship Systems Command

Mr. M. Pitkin
Asst. Administrator for
Commercial Development
Maritime Administration

Mr. J. L. Foley
Vice President
American Bureau of Shipping

Mr. C. J. Whitestone
Maintenance & Repair Officer
Military Sealift Command

SHIP STRUCTURE SUBCOMMITTEE

The SHIP STRUCTURE SUBCOMMITTEE acts for the Ship Structure Committee on technical matters by providing technical coordination for the determination of goals and objectives of the program, and by evaluating and interpreting the results in terms of ship structural design, construction and operation.

NAVAL SEA SYSTEMS COMMAND

Mr. C. Pohler - Member
Mr. J. B. O'Brien - Contract Administrator
Mr. G. Sorkin - Member

U.S. COAST GUARD

LCDR E. A. Chazal - Secretary
CAPT C. B. Glass - Member
LCDR S. H. Davis - Member
LCDR J. N. Naegle - Member

MARITIME ADMINISTRATION

Mr. N. Hammer - Member
Mr. F. Dashnaw - Member
Mr. F. Seibold - Member
Mr. R. K. Kiss - Member

MILITARY SEALIFT COMMAND

Mr. D. Stein - Member
Mr. T. W. Chapman - Member
Mr. A. B. Stavovy - Member
CDR J. L. Simmons - Member

NATIONAL ACADEMY OF SCIENCES
SHIP RESEARCH COMMITTEE

Mr. R. W. Rumke - Liaison
Prof. J. E. Goldberg - Liaison

AMERICAN BUREAU OF SHIPPING

Mr. S. G. Stiansen - Chairman
Mr. I. L. Stern - Member
Dr. H. Y. Jan - Member

SOCIETY OF NAVAL ARCHITECTS & MARINE ENGINEERS

Mr. A. B. Stavovy - Liaison

WELDING RESEARCH COUNCIL

Mr. K. H. Koopman - Liaison

INTERNATIONAL SHIP STRUCTURES CONGRESS

Prof. J. H. Evans - Liaison

U.S. COAST GUARD ACADEMY

CAPT W. C. Nolan - Liaison

STATE UNIV. OF N.Y. MARITIME COLLEGE

Dr. W. R. Porter - Liaison

AMERICAN IRON & STEEL INSTITUTE

Mr. R. H. Sterne - Liaison

U.S. NAVAL ACADEMY

Dr. R. Bhattacharyya - Liaison

METRIC CONVERSION FACTORS

Approximate Conversions to Metric Measures

Symbol	When You Know	Multiply by	To Find	Symbol
		LENGTH		
in	inches	*2.5	centimeters	cm
ft	feet	30	centimeters	cm
yd	yards	0.9	meters	m
mi	miles	1.6	kilometers	km
		AREA		
in^2	square inches	6.5	square centimeters	cm^2
ft^2	square feet	0.09	square meters	m^2
yd^2	square yards	0.8	square meters	m^2
mi^2	square miles	2.6	square kilometers	km^2
	acres	0.4	hectares	ha
		MASS (weight)		
oz	ounces	28	grams	g
lb	pounds	0.45	kilograms	kg
	short tons (2000 lb)	0.9	tonnes	t
		VOLUME		
tsp	teaspoons	5	milliliters	ml
Tbsp	tablespoons	15	milliliters	ml
fl oz	fluid ounces	30	milliliters	ml
c	cups	0.24	liters	l
pt	pints	0.47	liters	l
qt	quarts	0.95	liters	l
gal	gallons	3.8	liters	l
ft^3	cubic feet	0.03	cubic meters	m^3
yd^3	cubic yards	0.76	cubic meters	m^3
		TEMPERATURE (exact)		
°F	Fahrenheit temperature	5/9 (after subtracting 32)	Celsius temperature	°C

*1 in = 2.54 (exactly). For other exact conversions and more detailed tables, see NBS Misc. Publ. 286, Units of Weights and Measures, Price $2.25, SD Catalog No. C13.10:286.

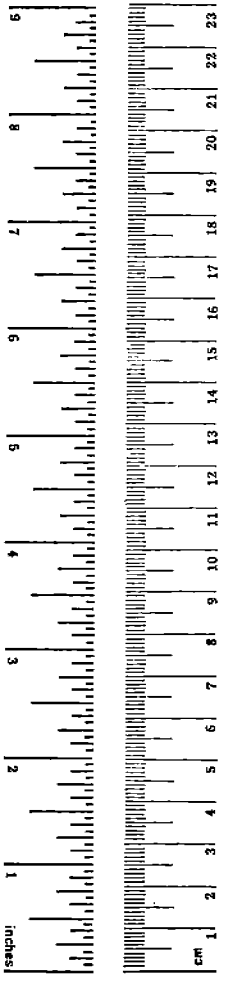

Approximate Conversions from Metric Measures

Symbol	When You Know	Multiply by	To Find	Symbol
		LENGTH		
mm	millimeters	0.04	inches	in
cm	centimeters	0.4	inches	in
m	meters	3.3	feet	ft
m	meters	1.1	yards	yd
km	kilometers	0.6	miles	mi
		AREA		
cm^2	square centimeters	0.16	square inches	in^2
m^2	square meters	1.2	square yards	yd^2
km^2	square kilometers	0.4	square miles	mi^2
ha	hectares (10,000 m^2)	2.5	acres	
		MASS (weight)		
g	grams	0.035	ounces	oz
kg	kilograms	2.2	pounds	lb
t	tonnes (1000 kg)	1.1	short tons	
		VOLUME		
ml	milliliters	0.03	fluid ounces	fl oz
l	liters	2.1	pints	pt
l	liters	1.06	quarts	qt
l	liters	0.26	gallons	gal
m^3	cubic meters	35	cubic feet	ft^3
m^3	cubic meters	1.3	cubic yards	yd^3
		TEMPERATURE (exact)		
°C	Celsius temperature	9/5 (then add 32)	Fahrenheit temperature	°F

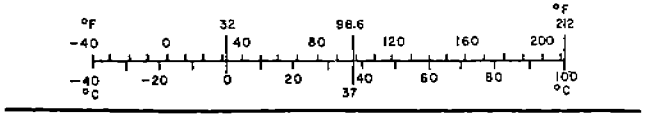

A STUDY OF SHIP HULL CRACK ARRESTER SYSTEMS

1.0 INTRODUCTION

Early instances in which the catastrophic failure of a ship hull was averted by the arrest of a rapidly propagating crack occurred in the 1920's. The liners Majestic and Leviathan both came perilously close to breaking in two at sea in the winter North Atlantic. In each case, cracks propagated across the strength deck and down the ships' sides and stopped at circular air port openings[1] . While these somewhat fortuitous cases might have served to stimulate research on fracture, intensive action was not initiated until after the epidemic of ship failures originating with the Schenectady and the Esso Manhattan [2,3] during World War II. Substantially, as a result of these and other serious brittle fractures in Liberty ships and T-2 tankers, a program of research was begun. This work has developed into the present-day technical discipline of fracture mechanics.

Fracture mechanics opens the way to analyze enegineering structures that will experience predetermined amounts of stable and unstable crack growth. Structures can then be made "damage tolerant" in 3 different ways:

(1) Through the selection of relatively high-toughness materials, cracks are not allowed to grow to a critical size. Periodic inspections are carried out to ensure that cracks are detected before they can cause fast fracture. In order to schedule the inspection interval, an accurate characterization of fatigue crack-growth behavior is required.

(2) Moderate or low-toughness materials are employed and cracks are allowed to grow to a critical size and cause fast fracture. However, the structure is designed redundant such that a fast crack is arrested without causing complete loss of the structure. This can be achieved by building a structure consisting of parallel members, one of which may completely fail, or by the use of crack arresters.

(3) Moderate or low-toughness materials are employed and cracks are permitted to grow to critical size as in (2) but the structure is not redundant. Instead, crack arresters are installed in critical locations. These are designed to stop the crack before excessive damage is sustained and to contain the structure until repairs can be made.

Presently, damage-tolerant concepts 1 and 2 are successfully used in aircraft design. Some of the methodologies developed in the aircraft industry will be discussed later in this report.

Fracture mechanics, damage-tolerant strategies have not been applied in detail in the design of ship hulls and thus may have contributed to such recent

fractures as the large integrated tug/barge M.V. Martha R. Ingram in New York harbor in 1972[4]. But the use of fracture-mechanics concepts has been advocated. Rolfe et al[5] have proposed that the most economical damage-tolerant strategy for ship hulls is the use of materials with "moderate levels of notch toughness with properly designed crack arresters".

In returning to the consideration of crack arrester systems to prevent ship hull fracture, the problem has come full circle. The original solution to the all-welded Liberty ship dilemma during World War II was to incorporate crack arresters where advancing brittle failures were to be stopped. These consisted of flame-cut longitudinal slots along the whole midship portion that were covered with riveted straps. Many cases are on record of cracks being arrested by these devices, and it is almost certain that several ships were saved from complete rupture by their presence[2]. More refined concepts such as arresting a brittle fracture with a strake of notch-tough steel welded between strakes of standard ship steel are currently favored by ship designers. However, crack arrester design procedures are still not well developed in general.

The general objectives of this report are as follows. First, the extent to which crack arrester systems are considered in present-day ship designs, as determined by surveying marine engineers, shipyards, and regulating agencies, both in the U.S. and abroad, will be discussed. Second, a study, identifying the basic material and theoretical concepts required for crack arrest design and setting the stage for more advanced research into the design of effective crack arresters for ship hulls, is given. Third, the current state of the art of crack arrester schemes was classified and evaluated to identify concepts involved in their design. Fourth and last, recommendations for the research needed in this technological problem are set out and discussed.

2.0 DESCRIPTION OF EXISTING CRACK ARRESTER DESIGN PRACTICES

2.1 BASIC PRINCIPLES AND CLASSIFICATION OF ARRESTERS

The basic principle behind the use of a crack arrester is to reduce the crack-driving force below the resisting force that must be overcome to extend a crack. The crack-driving force is the energy (strain energy, kinetic energy and external work) released by the structure at the crack tip as fracture extends. The resisting force is fracture energy which is closely related to the fracture toughness of the material. This principle--which underlies the new discipline of fracture mechanics--can be used to classify the different crack arrester configurations.

(1) Arresters that decrease the crack driving force of a propagating crack

(2) Arresters that increase the fracture toughness of the material encountered by a propagating crack

(3) Arresters that simultaneously change both the driving force and the toughness.

A more detailed description of this classification together with some numerical examples are given in Chapter 6 of this report. A quantitative discussion of the fracture mechanics parameters is given in Chapter 3.

In the remainder of the section, brief descriptions of the various kinds of crack arresters will be given.

Riveted Seam Type of Crack Arrester. (Figure 2.2.1) The continuous structure of an all-welded ship makes crack arresters very essential. In the case of a riveted discontinuous hull structure, a crack obviously cannot continue to propagate over a riveted seam. The easiest and simplest type of crack arrester system would be to use riveted seams at the vital portion of welded structures. However, the economic and labor conditions existing today preclude them because of the scarcity of qualified riveters.

Inserted Type of Crack Arrester. (Figure 2.2.2) In this type of crack arrester, tougher steel is used just at vital locations in the structure. It is not economical to use high quality material in the whole structure. The basic idea is that a tough arrester strake elevates the crack resisting force above the level of the crack-driving force. This is the most common type employed in marine applications[6]. Also, experimental evaluations of this type of arrester have been carried out rather extensively.[7,8]

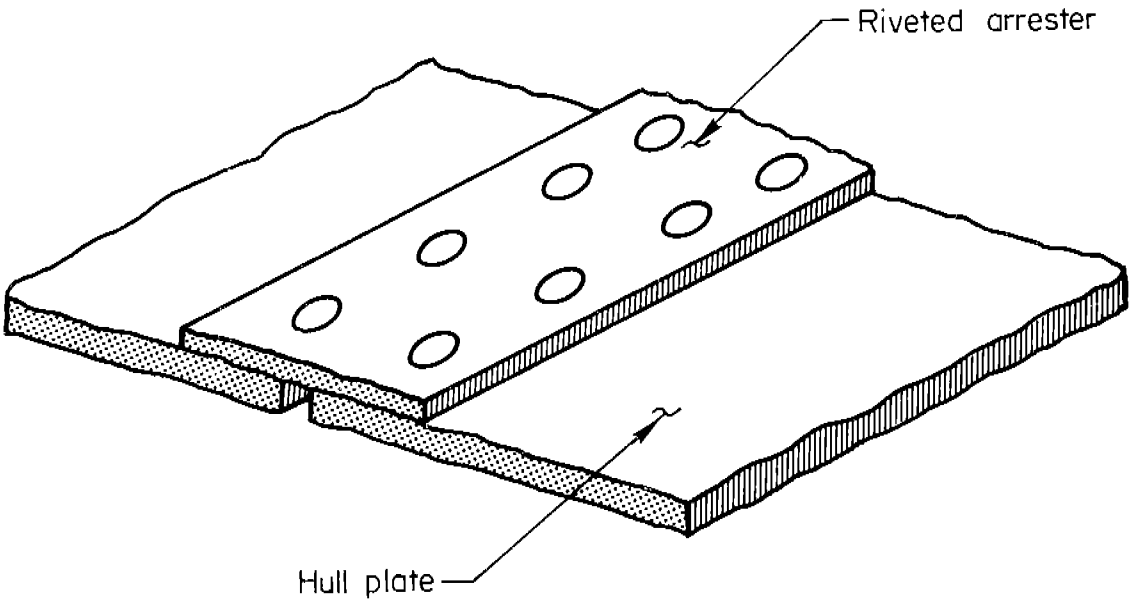

FIGURE 2.2.1. RIVETED SEAM TYPE OF CRACK ARRESTER

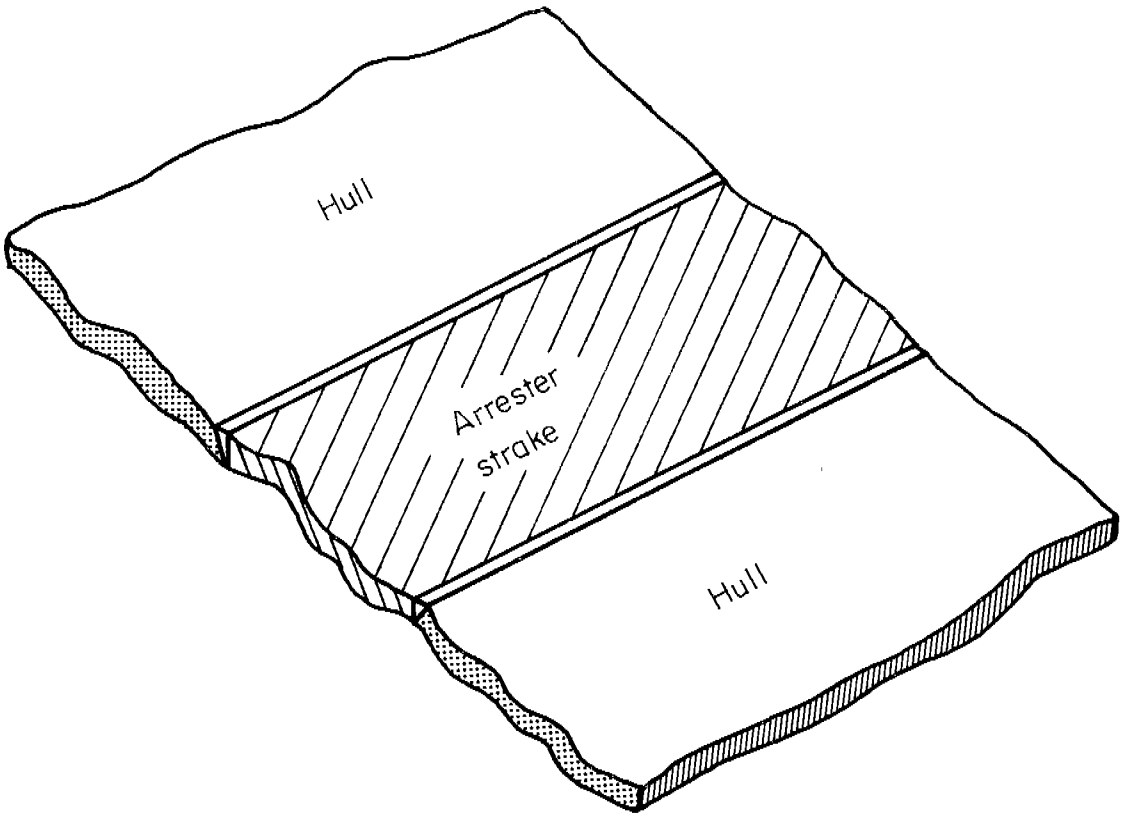

FIGURE 2.2.2. INSERTED TYPE OF CRACK ARRESTER

Patch Type of Crack Arrester. (Figure 2.2.3) The idea in this type of arrester is to suppress the crack-driving force by introducing a compression load from a patch. In some experimental investigations, the effect of the patch reveals a decrease in K near the patch.[9,10,11] Thus, when a crack runs into this region, it will be arrested even though the basic fracture toughness is not changed.

Stiffener Type of Crack Arrester. (Figure 2.2.4) The mechanism of arresting a running crack in this system is similar to the patch-type model. Calculations have shown that if the main crack passes through the stiffener, the accompanying displacement would be resisted by the stiffener, causing compressive stress at the crack area and a reduction in the driving force. Test results from various combinations of a stiffeners, materials, and heat-treat conditions indicate that cracks can be arrested using this concept. A T-type integral stiffener is also shown on Figure 2.2.4.

Ditch Type of Crack Arrester. (Figure 2.2.5) In this type of crack arrester, the base material thickness is thinned by machining a groove along the plate in a direction perpendicular to the anticipated running crack. The basic idea is that the fracture mode can be made to change at the reduced section by producing a shear lip there. The effect of the shear lip is to increase the energy dissipation mode and to change the crack propagation direction to eventually arrest the crack.

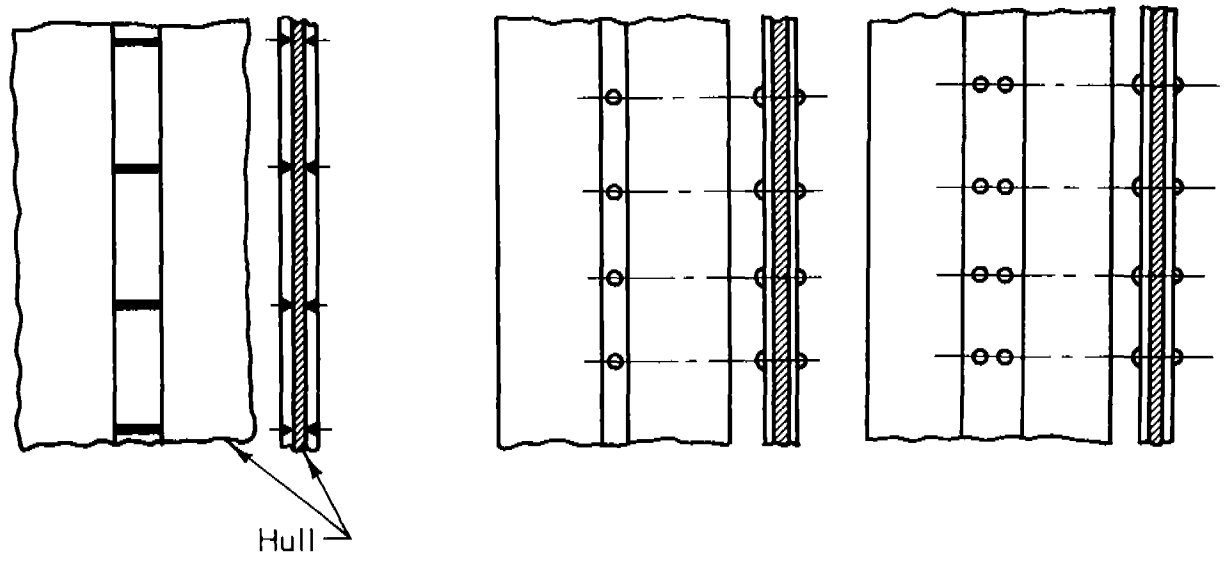

FIGURE 2.2.3. PATCH TYPE CRACK ARRESTER

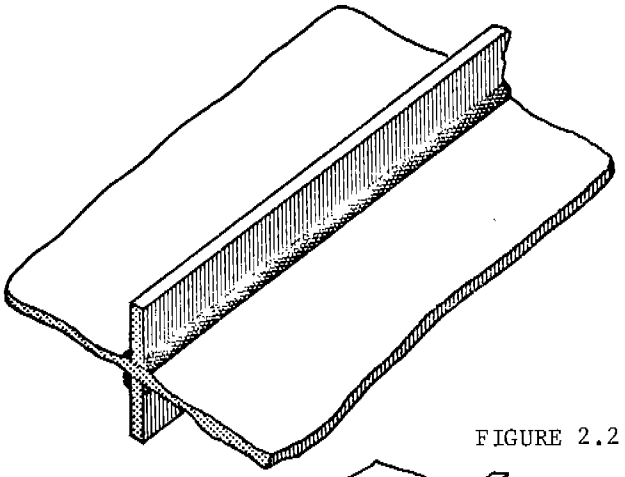

FIGURE 2.2.4. STIFFENER TYPE CRACK ARRESTERS

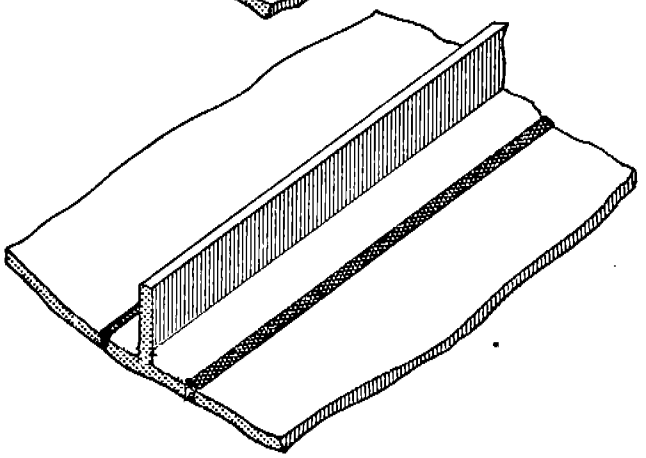

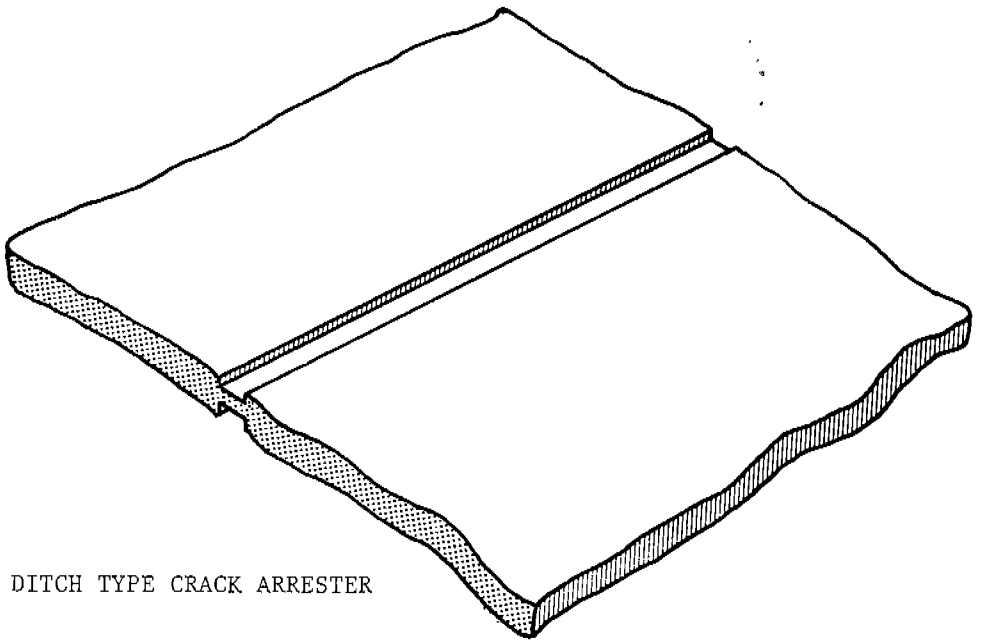

FIGURE 2.2.5. DITCH TYPE CRACK ARRESTER

2.2 SHIP CLASSIFICATION SOCIETY RULES

The problem of brittle fracture in ship structures has been addressed by the classification societies mainly by using three simultaneous approaches:

1. Improvement in steels in general and the use of special steels in certain areas of the ship

2. Improvement in the stress analysis of ship structures

3. Improvement in detail design to reduce stress concentration effects.

In the post-WWII era when the brittle fracture problem became most crucial, the classification societies first took independent action. As a result, a large number of specifications were instituted, sometimes of a conflicting nature. In 1959, however, the societies* joined in a unification of their rules which was welcomed by both shipbuilders and steelmakers.

The steels are specified by the societies with the intention of providing grades at strength levels with the necessary toughness for their intended use. The gradation of toughness is obtained by specifying the appropriate requirements for control of chemical composition, process of manufacture, melting practice and, in some cases, verification by Charpy V-notch testing. The American Bureau of Shipping steel grade specifications are shown in Tables 2.3.1 and 2.3.2[12]. For comparison, Table 2.3.3 shows the specifications for some of the same steels from Lloyd's Register of Shipping[13]. These specifications differ essentially only in the area of Charpy V-notch testing temperatures. The ABS specifications require a lower testing temperature.

The applications for each steel are indicated in the various sections of the Rules to assure that the quality of each steel is suitable for the steel thickness, ship size, and particular application involved. For example, the ABS requirement for Grade A steel (the lowest toughness category) may be used up to 51 mm (2 in) thickness in low stress areas, but would not be permitted in any thickness for the sheer strake of an ocean going vessel in excess of 137 meters (450 feet) in length. For this type of service, a Grade B steel would be required up to a thickness of 16 mm (0.63 in), a Grade D normalized up to 27.5 mm (1.08 in) and a Grade CS, E, or DS normalized up to 51 mm (2.0 in). These relationships between steel grades and ship applications are based primarily on proven service experience under a wide variety of conditions encountered by merchant ships over the past years.

While the Society Rules do not use the terminology of crack arrester, they do specify that the tougher grades (Grade E, for example) be used where the arrester strakes are usually applied. Lloyd's, for example, specifies Grade E steel at the sheerstrake, over the longitudinal bulkheads, and at the

---

*American Bureau of Shipping, Bureau Veritas, Germanischer Lloyd, Lloyd's Register of Shipping, Nipon Kaiji Kyoiai, Det Norske Veritas, and Registro Italianno Navale.

ORDINARY STRENGTH HULL STRUCTURAL STEEL

GRADES	A	B	D	E	CS	DS
PROCESS OF MANUFACTURE	FOR ALL GRADES OPEN HEARTH, BASIC OXYGEN, OR ELECTRIC FURNACE					
DEOXIDATION	ANY METHOD EXCEPT RIMMED		SEMI-KILLED OR KILLED	KILLED, FINE GRAIN PRACTICE	KILLED, FINE GRAIN PRACTICE	KILLED, FINE GRAIN PRACTICE
CHEMICAL COMPOSITION (LADLE ANALYSIS)						
CARBON, %	0.23 MAX	0.21 MAX	0.21 MAX.	0.18 MAX.	0.16 MAX.	0.16 MAX.
MANGANESE, %	—— *	0.80-1.10	0.70-1.40	0.70-1.50	1.00-1.35	1.00-1.35
PHOSPHORUS, %	0.04 MAX.	0.04 MAX.	0.04 MAX.	0.04 MAX	0.04 MAX	0.04 MAX.
SULFUR, %	0.04 MAX	0.04 MAX.	0.04 MAX	0.04 MAX.	0.04 MAX.	0.04 MAX
SILICON, %	——	0.35 MAX.	0.10-0.35	0.10-0.35	0.10-0.35	0.10-0.35
HEAT TREATMENT	——	——	NORMALIZED OVER 35.0 MM (1.375 IN.)	NORMALIZED	NORMALIZED	NORMALIZED OVER 35.0 MM (1.375 IN.)
TENSILE TEST						
TENSILE STRENGTH	FOR ALL GRADES: 41-50 KG/MM^2; 53,000-71,000 PSI					
YIELD POINT, MIN.	FOR ALL GRADES: 24 KG/MM^2; 34,000 PSI					
ELONGATION, MIN	FOR ALL GRADES: 21% IN 200MM (8 IN.); 24% IN 50MM (2 IN.); 22% IN. $5.65\sqrt{A}$ (A EQUALS AREA OF TEST SPECIMEN)					
IMPACT TEST STANDARD CHARPY V-NOTCH						
TEMPERATURE	——	——	-20 C (-4 F)	-40C (-40F)	——	——
ENERGY, MIN. AVG.	——	——	2.8 KGM (20 FT. LBS.)	2.8 KGM (20 FT. LBS.)	——	——
NO. OF SPECIMENS	——	——	3 FROM EACH 40 TONS	3 FROM EACH PLATE	——	——

* GRADE A PLATES OVER 12.5MM (0.50 IN.) THE Mn SHALL BE 2.5 x C% (MIN.)

TABLE 2.3.1. ABS STEEL GRADES

HIGHER STRENGTH HULL STRUCTURAL STEEL

GRADES	AH32 OR AH36	DH32 OR DH36	EH32 OR EH36
PROCESS OF MANUFACTURE	FOR ALL GRADES: OPEN HEARTH, BASIC OXYGEN, OR ELECTRIC FURNACE		
DEOXIDATION	SEMI-KILLED OR KILLED	KILLED, FINE GRAIN PRACTICE	KILLED, FINE GRAIN PRACTICE
CHEMICAL COMPOSITION (LADLE ANALYSIS)	FOR ALL GRADES:		
CARBON %	0.18 MAX.		
MANGANESE %	0.90–1.60		
PHOSPHORUS %	0.04 MAX.		
SULFUR %	0.04 MAX.		
SILICON %	0.10–0.50 { AH TO 12.5 MM (0.50 IN.) MAY BE SEMI-KILLED IN WHICH CASE 0.10% MIN. Si DOES NOT APPLY		
NICKEL %	0.40 MAX.		
CHROMIUM %	0.25 MAX		
MOLYBDENUM %	0.06 MAX.		
COPPER %	0.35 MAX.		
ALUMINUM % (ACID SOLUBLE)	0.06 MAX.		
COLUMBIUM % (NIOBIUM)	0.05 MAX.		
VANADIUM	0.10 MAX		
HEAT TREATMENT	NORMALIZING REQ'D. OVER 12.5 MM (0.50 IN.) IF Nb TREATED	NORMALIZING REQ'D OVER 25.5 MM (1.0 IN.) IF Al TREATED OVER 12.5 MM (0.50 IN.) IF Nb TREATED OVER 19.0 MM (0.75 IN.) IF V TREATED	NORMALIZED
TENSILE TEST			
TENSILE STRENGTH	FOR 32 GRADE: 48–60 KG/MM^2 (68,000–85,000 PSI) FOR 36 GRADE: 50–63 KG/MM^2 (71,000–90,000 PSI)		
YIELD POINT, MIN	FOR 32 GRADE: 32 KG/MM^2 (45,500 PSI) FOR 36 GRADE: 36 KG/MM (51,000 PSI)		
ELONGATION, MIN	FOR ALL GRADES: 19% IN 200 MM (8 IN.), 22% IN 50 MM (2 IN.) 20% IN $5.65\sqrt{A}$ (A EQUALS AREA OF TEST SPECIMEN)		
IMPACT TEST STANDARD CHARPY V-NOTCH			
TEMPERATURE	———	-20C (-4F)	-40C (-40F)
ENERGY, MIN AVG	———	3.5 KGM (25 FT LBS)	3.5 KGM (25 FT LBS)
NO OF SPECIMENS	———	3 FROM EACH 40 TONS	3 FROM EACH PLATE

TABLE 2.3.2. ABS STEEL GRADES

TABLE 2.3.3. LLOYD'S STEEL GRADES

GRADE	A	B	D	E
DEOXIDATION	Any method (For rimmed steel *see* Note 1)	Any method except rimmed steel	Fully killed, fine grain practice (Aluminium treated) *see* Note 2	Fully killed, fine grain practice (Aluminium treated)
CHEMICAL COMPOSITION (ladle analysis)				
Carbon	0,25% max.	0,21% max.	0,21% max. } Notes	0,18% max. } Note
Manganese	*See* Notes 3 and 5	0,80% min. } Notes	0,70% to 1,40% } 5 and 6	0,70% to 1,50% } 5
Silicon	0,50% max.	0,50% max. } 4 and 5	0,10% to 0,50% max.	0,10% to 0,50%
Sulphur	0,040% max.	0,040% max.	0,040% max	0,040% max.
Phosphorus	0,040% max.	0,040% max.	0,040% max.	0,040% max.
Aluminium (acid soluble)	—	—	0,015% min. Note 7	0,015% min. Note 7
TENSILE TEST				
Yield Stress (min.)				
N/mm²	230	230	235	235
kg mm.²	23·5 (Note 8)	23·5 (Note 8)	24	24
ton/in²	14·9	14·9	15·2	15·2
TENSILE STRENGTH				
N/mm²	400 to 490	400 to 490	400 to 490	400 to 490
kg/mm²	41 to 50	41 to 50	41 to 50	41 to 50
ton in.²	26 to 31·7	26 to 31·7	26 to 31·7	26 to 31·7
ELONGATION % min. Standard Test Piece Thickness (mm)				
More than / Less than or equal to				
— / 5	15	15	15	15
5 / 10	16	16	16	16
10 / 15	17	17	17	17
15 / 20	18	18	18	18
20 / 25	19	19	19	19
25 / 35	20	20	20	20
35 /	21	21	21	21
PROPORTIONAL TEST PIECE				
Gauge Length $5.65\sqrt{S_o}$	22	22	22	22
IMPACT TEST (LONGITUDINAL)				
Test Temperature	—	0°C	0°C	—40°C
Minimum Average Energy		J / kg m / ft lb	J / kg m / ft lb	J / kg m / ft lb
Width of test piece				
10 mm	—	27 / 2,8 / 20	47 / 4,8 / 35	27 / 2,8 / 20
7,5 mm	—	23 / 2,3 / 17	39 / 4,0 / 29	23 / 2,3 / 17
5 0 mm (*See* Note 9)	—	19 / 1,9 / 14	31 / 3,2 / 23	19 / 1,9 / 14

1. For Grade A, rimming steel may be accepted up to 12,5 mm (0·5 in) thick inclusive, provided that it is stated on the test certificates or shipping statements to be rimming steel and is not excluded by the purchaser's order.

2. Other deoxidation methods, except rimmed steel, may be used for Grade D in thicknesses up to and including 35 mm (1·4 in), provided that in thicknesses over 25,5 mm (1·0 in) the condition of supply for plates is either normalized or controlled rolled. In such cases, the requirements for fine grain practice and the minimum silicon and aluminium contents do not apply.

3. For Grade A in thicknesses over 12,5 mm (0·5 in), the manganese content is to be not less than 2,5 times the carbon content.

4. For Grade B, when the silicon content is 0,10 per cent or more (killed steel) the minimum manganese content may be reduced to 0,60 per cent.

5. For all grades the sum of carbon content plus 1/6 of the manganese content shall not exceed 0,40 per cent.

6. For Grade D when the thickness is 25,5 mm (1·0 in) or less, the minimum manganese content may be reduced to 0,60 per cent.

7. The total aluminium content may be determined instead of the acid soluble content. In such cases the total aluminium content is to be not less than 0,020 per cent.

8. For Grades A and B over 25,5 mm (1 in.) in thickness, the minimum yield stress is 220 N/mm.² (22,5 kg/mm², 14·3 ton/in²).

9. Where non-standard subsidiary impact test pieces are used, the minimum value may be obtained by interpolation.

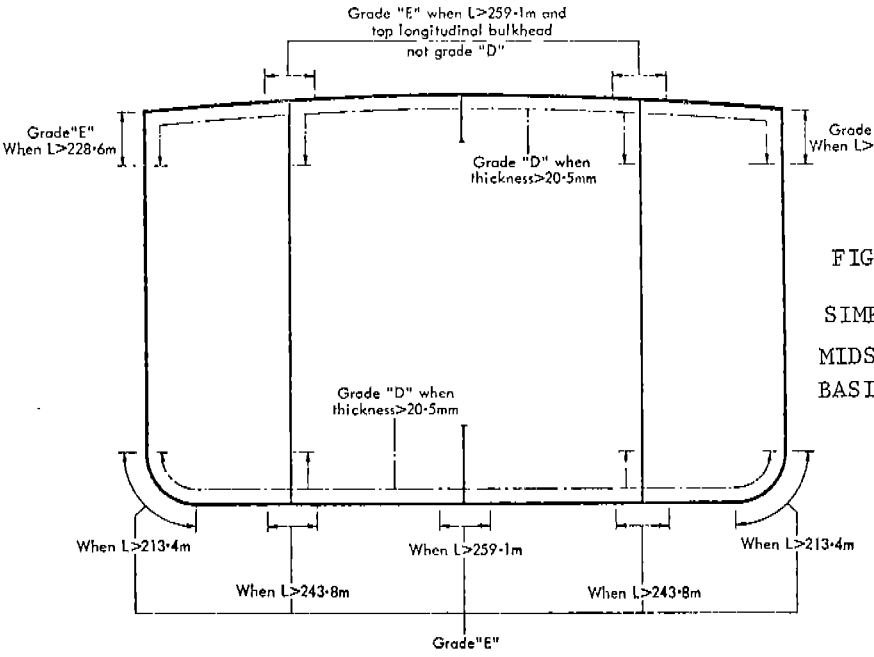

FIGURE 2.3.1.

SIMPLIFIED TANKER MIDSHIP SECTION SHOWING BASIC STEEL REQUIREMENTS

turn-of-the bilge strakes. Figure 2.3.1 shows this requirement for a typical tanker section[13].

The American Bureau of Shipping specifies the minimum width of the sheerstrake for the midship to the length of 0.4 L using the following equations. In these equations, L is the length of the vessel and b is the width of the sheerstrake.

(a) for vessels less than 120 m (395 ft) in length,

$$b = 5L + 916 \text{ mm}$$
$$\text{or } b = 0.06L + 36 \text{ in.}$$

(b) for vessels of 120 m (395 ft) or more in length but not exceeding 427 m (1400 ft) in length

$$b = 1525 \text{ mm}$$
$$\text{or } b = 60 \text{ in.}$$

The thickness of the sheerstrake is also specified in the ABS requirements.

The stress analysis of ship structures has been improved through the years, most importantly through the use of finite-element stress-analysis computer programs. Many such programs are in use and some are favored by certain design agencies over others, but general structural programs such as STRUDL, STRESS, and DAISY are suited to analyze a complete ship, a section in more detail, or a single member in great detail. The ABS is favoring DAISY as an applicable program. Obviously, the use of better stress analysis techniques and the resulting improvement in design details to reduce stress concentrations will improve the brittle fracture problem.

2.3 SURVEY OF MARINE ENGINEERS, SHIPYARDS, AND REGULATING AGENCIES

In order to determine the state of current research and practice on the problem of arresting cracks in ship hulls, a survey of domestic and foreign shipyards, design agencies, academic institutions, and regulatory agencies related to ship hull design was undertaken.

Before the survey was started, the scope of the effort was further refined in that the data were to include only commercial ship hull designs and not military ships. Both fatigue and fast-fracture arrest concepts were to be considered, but special purpose ships or materials for special applications were not to be included.

The survey asked:

(1) Do you presently design crack arrester systems for ship hull structures?

(2) Have you generated experimental data to support the effectiveness of various ship hull crack arrester devices? If so, are these data available?

(3) What design procedure is followed for fracture control in ship hulls?

As a component of the foreign survey, a search was made of the open literature to identify the most current crack arrester data along with additional agencies to be contacted. The use of the U.S. Air Force CIRC computer storage file of Slavic-language technical literature search indicated a small number of journal articles pertaining to hull crack arresters.

2.3.1 Results of Domestic Survey

Approximately 30 percent of thirty-seven U.S. companies contacted responded. Among the topics discussed with representatives of the companies were

(a) Crack arresting techniques, if any, that are being used or recommended in their work

(b) Experimental data on crack arresters, either published or unpublished

(c) Any past experiences with crack arresters.

The results indicate that very little that is new in the way of crack arresting techniques is currently being used by domestic shipbuilders and naval architects. Most respondents indicated that they are generally aware of and use the practices of employing notch-tough steels and designing to avoid stress concentrators in the hull and deck attachments. Most of those who consciously design and build crack arresters use the welded, integral strakes of notch-tough steel at the turn of the bilge and sheer-strake locations. But, over half of those responding to

the survey have also used bolted or riveted strakes to act as crack arresters. Nearly all of those responding indicated that they look upon ABS for direction in this area.

The respondents followed the ABS requirements for material strengths in the high-stress areas. Some shipbuilders indicated they used a grade or two tougher than that recommended by ABS for that particular thickness and application as an additional degree of conservativeness in design. The high-stress zone such as the turn of the bilge and the sheerstrake areas were treated by using integral strakes of welded-in tougher materials by most of the shipbuilders and agencies.

Historically, the riveted or bolted-on sheerstrake was mentioned by many respondents as a technique used in the past. However, a fairly large number of respondents (about 55 percent) indicated that on special conditions, this procedure is still used today. Nearly all of the respondents admitted to the use of careful design and review procedures to avoid stress concentrators in the deck details particularly. Also, nearly all the agencies and shipyards indicated that they used generally tough materials in the entire hull construction.

No unpublished experimental data on hull crack arresters were uncovered as a result of the survey, although most respondents were aware of the work that has been done in testing notch-tough steels for their crack-resistant properties.

2.3.2 Results of Foreign Survey

A total of 23 foreign agencies and shipyards were contacted by letter requesting information on crack arresting devices. Japan was excluded from the letter contact because Dr. K. Masubushi visited the leading shipyards, universities, and steel companies there to obtain their most current data. Of those contacted by letter, 48 percent responded in a fairly short time with information regarding the problem area of crack arresting devices. Various agencies also sent copies of their publications related to the problem area. A total of seven of these documents were received. These documents were added to the collection of material used in preparing this report. The seven documents received are Reference Numbers 17 through 23.

The foreign survey respondents were essentially unanimous in that they were using or recommending use of notch-tough steels as recommended by the regulating agencies such as Lloyd's Register and Det Norske Veritas.

One specific design in Sweden is a weak link of iron bar material welded between the hull and the heavy bilge keel. This design is intended to prevent a crack which may start in the higher stressed outer fibers of the keel from running into the hull shell. This design is shown in Figure 2.4.1.

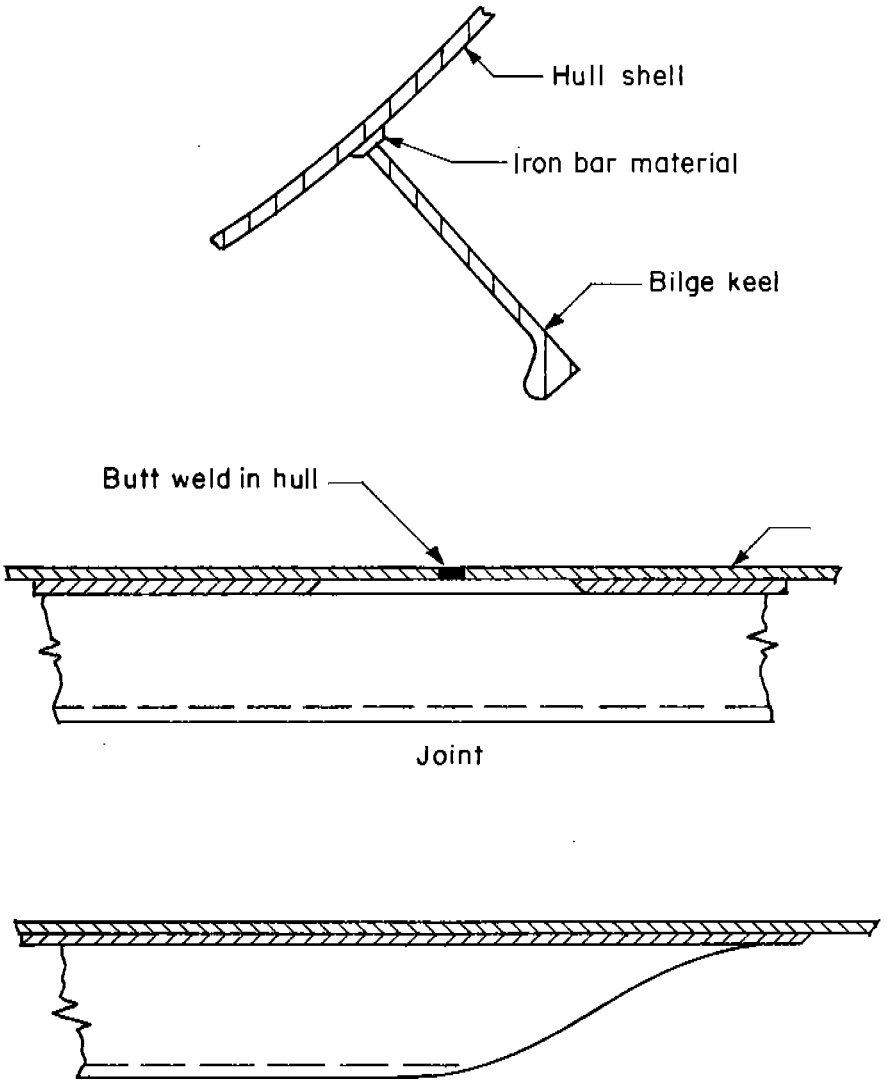

FIGURE 2.4.1. BILGE KEEL CRACK ARRESTER DESIGN (ERIKSBERGS)

Another organization in Sweden has been using the integral notch-tough steel strakes on all their ships since 1950. For strakes above the water line, they have used nothing lower than Grades E or EH steels, even though the classification society requirements may indicate that Grade D is acceptable.

As a result of the survey effort in Japan, a number of articles and papers containing experimental data and theoretical analysis were added to the data base. An analysis of the more pertinent publications has indicated that a variety of crack arresting techniques have been studied in Japan. Recently, however, with the downturn in the economy there, the shipbuilding industry no longer stimulates continued crack arrester study programs. However, the Japanese have, until recently, been more prominent in investigating new concepts for crack arresters than has anyone else in the world.

The publications from Japan are listed as Reference 6 through 11 and 14 through 16. Five types of crack arresters were examined with extensive experimental programs in that country.

The riveted seam is a crack arrester which is essentially no longer in use today because of the scarcity of riveters in the industry. Bolted strakes appear to be somewhat the modern counterpart of the riveted seam. These are used to a limited extent, as best as can be determined. (Fig. 2.2.1)

Integral crack arresters are the most common type described in the Japanese literature. This type of crack arrester uses a welded-in strake of notch-tough steel. The assumption on which this concept is based is that a crack running into a panel of tougher material will arrest if the toughness or the panel width is large enough. (Fig. 2.2.2)

The patch type of crack arrester consists of a short strap of material welded along its short ends to the ship hull. The welding shrinkage creates a compressive load in the hull material under the strap. The strap will experience a tensile load. The theory behind the idea is that a crack will not propagate through the compressive stress area under the strap provided the stress is large enough. (Fig. 2.2.3)

Stiffener-type crack arresters were also investigated in Japan. The stiffener is a perpendicular strip of steel welded along the strake direction in the hull. The stiffener on one or both sides of the base plate and running through the base plate were all examined in experiments. Calculations have shown that if the main crack passes through the stiffener, the stress distribution changes and the crack can be arrested. (Fig. 2.2.4)

The ditch-type crack arrester was also investigated. This type is made by reducing the base material thickness by machining the groove along the plate. The running crack intersects the ditch and it is assumed that the fracture mode changes at the reduced section where a shear lip is produced. The effect of the shear lip is to increase the energy dissipation mode and change the crack

propagation direction to eventually arrest the crack. (Fig. 2.2.5)

These designs are, as yet, laboratory studies. None are currently being used in shipbuilding, except for the integral type.

3.0 CONCEPTS FOR ARREST OF FAST FRACTURE

3.1 ANALYSIS OF FRACTURE ARREST

The process of crack arrest in structures can be discussed with LEFM (linear elastic fracture mechanics) concepts and parameters[24] although actual problems may require more complicated elastic-plastic treatments. The LEFM recognizes 4 forms of energy: (i) elastic strain energy, (ii) kinetic energy, (iii) work done by applied forces, and (iv) the energy dissipated by crack tip flow and fracture processes. The first 3 forms depend primarily on the crack length, the applied loads and the geometry of the body containing the crack and are calculated by solving problems in the mathematical theory of elasticity. The net change in these 3 energies per unit area of crack extension is called the energy release rate $\mathcal{G}$ and this is the driving force for crack extension.† The rate of change of the last energy form, i.e., the energy dissipated per unit area of fracture, is called the fracture energy, R, and expresses the resistance to cracking.†† The fracture energy is a material property essentially independent of the geometry and applied loads.†††

Crack-extension criteria follow from the principle of energy conservation, namely, that the energy release rate must be balanced by the fracture energy. This statement means that crack extension (growth of a stationary crack) or continued propagation of a moving crack are only possible when

$$\mathcal{G} = R \tag{3.1-3}$$

Equivalently, no crack growth is possible or, for a propagating crack, arrest must take place, when

---

† stationary crack[2] $\mathcal{G} = -\frac{dU}{dA} + \frac{dW}{dA}$ (3.1-1)

fast propagating and arresting crack[25] $\mathcal{G} = -\frac{dU}{dA} - \frac{dT}{dA} + \frac{dW}{dA}$ (3.1-2)

where U is the strain energy, T the kinetic energy, W the work performed on the structure by the surroundings, A the crack area. For the evaluation of $\mathcal{G}$ for a fast propagating or arresting crack, the terms $\frac{dU}{dA}$, $\frac{dT}{dA}$ and $\frac{dW}{dA}$ must be evaluated from fully dynamic analyses.

†† The fracture energy for the extension of a stationary crack is usually referred to as $\mathcal{G}_c$, the critical energy release rate.

††† It is, in fact, a basic postulate of LEFM that all inelastic irreversible energy dissipation processes that accompany crack extension can be included in a single material property that is possibly a function of the crack speed, but is independent of the crack length, the applied loads, and the external geometry of the body. The extent to which this is true really determines the applicability of LEFM.

$$\mathcal{G} < R \qquad (3.1\text{-}4)$$

for all values of R.† These criteria, as well as the role of strain energy, and kinetic energy are illustrated schematically in Figure 3.1.1 for the case of a crack that is propagating in a structure under fixed grip conditions.†† In this case, the strain energy release rate $-\frac{dU}{dA}$ first increases with crack extension and then decreases when the crack length, a, becomes large relative to the dimensions of the cracked member. Figure 3.1.1 shows that the criterion for the onset of fracture is satisfied when $a = a_o$. At this instant, the crack begins to extend rapidly. The crack continues to propagate until $a = a_a$, where the criterion for crack arrest is satisfied. In the initial stage (the interval AB), the strain energy release rate $-\frac{dU}{dA}$ supplies the crack driving force and imparts kinetic energy to the body (see shaded area in Figure 3.1.1). In the latter stage (the interval BC) the crack continues to propagate even though $-\frac{dU}{dA}$ is less than R by virtue of the kinetic energy recovered from the structure. During this period both the strain energy release rate and the kinetic energy release rate, $\frac{dT}{dA}$ contribute to the crack driving force.

Detailed dynamic calculations of this type are available for beamlike configurations [26]. The example shown in Figure 3.1.2a and 3.1.2b for a rectangular double-cantilever-beam (DCB) test piece under fixed grip conditions, illustrates that about 85% of the kinetic energy imparted to the specimen is returned to the crack tip under these conditions. This represents 30% of the energy spent in fracturing material and produces a disproportionate amount of crack extension because kinetic energy is only part of the driving force. At the same time, it should be noted that very little kinetic energy return is anticipated for small cracks in large bodies that approximate the crack-in-an-infinite-body idealization. [27] In other words, the contribution of the kinetic energy release rate is a variable that depends on the geometry of the structure. There is a need for dynamic analyses that define the amount of kinetic energy return in different classes of problems.

---

† Note that the condition where $\mathcal{G}$ exceeds R is not possible because it would violate the energy balance principle. The stationary crack relation, inequality (3.1-4), it might be pointed out, does not violate the energy balance. The reason is that in this case, the crack growth area corresponds to a virtual crack extension only.

†† Under fixed grip conditions $\frac{dW}{dA} = 0$, and the 3 criteria reduce to the following expressions:

1. Criterion for the Onset of Fracture $R \leq -\frac{dU}{dA}$ (3.1-5)

2. Criterion for the Continuation of Fast Fracture $R \leq -\frac{dU^D}{dA} - \frac{dT^D}{dA}$ (3.1-6)

3. Criterion for Fracture Arrest $R > -\frac{dU^D}{dA} - \frac{dT^D}{dA}$ (3.1-7)

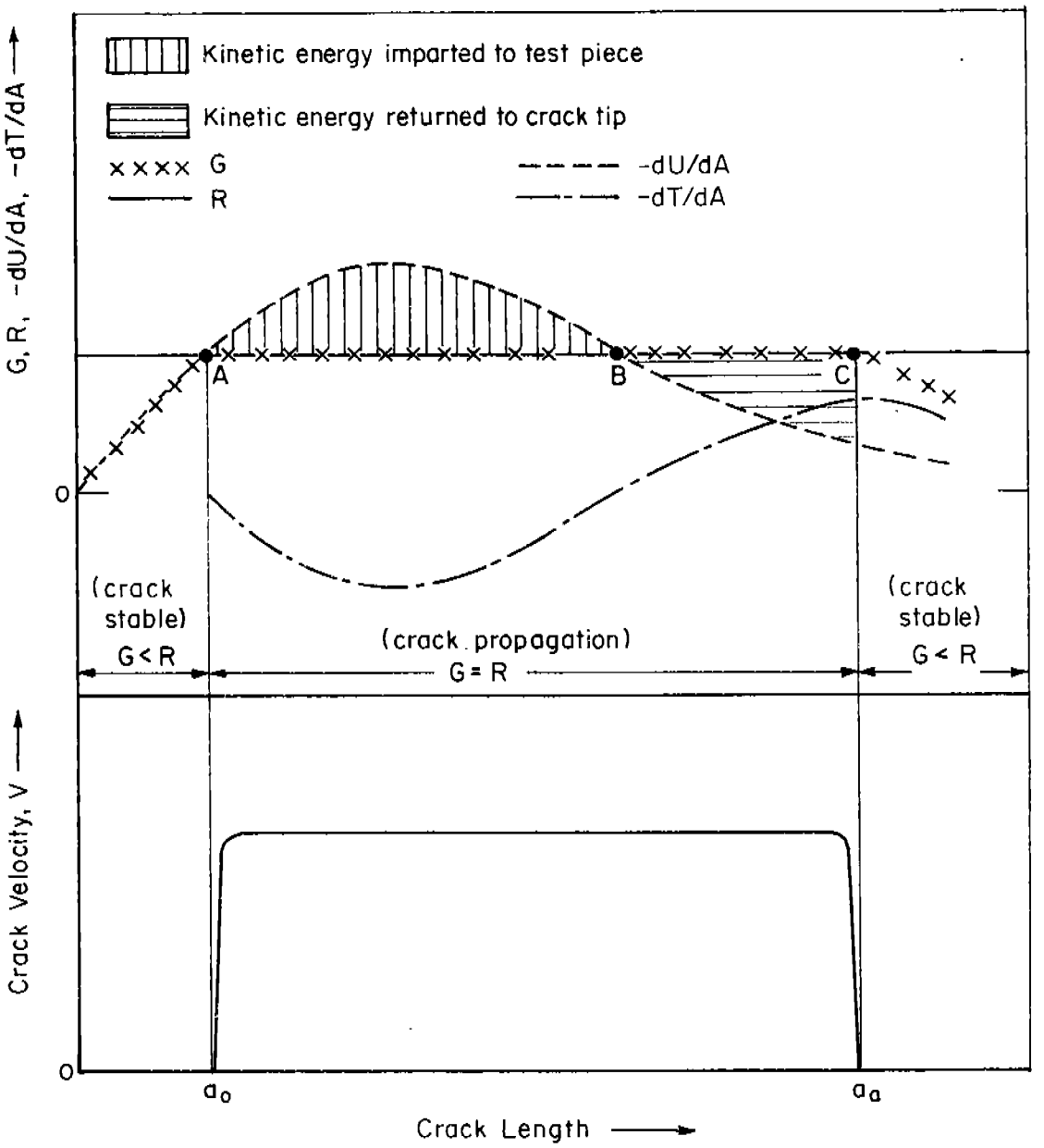

FIGURE 3.1.1.

SCHEMATIC REPRESENTATION OF THE COMPONENTS OF THE CRACK DRIVING FORCE, G, THE FRACTURE RESISTANCE R AND CRACK VELOCITY V ATTENDING THE FRACTURE OF A STRUCTURAL MEMBER UNDER FIXED GRIP CONDITIONS. The lower part of the diagram shows the velocity of a crack initially of length a_o. Cracks smaller than a_o or larger than a_a cannot grow spontaneously for the particular grip displacement represented because $\mathcal{G} < R$. Such cracks could grow slowly by fatigue (under the action of cyclic grip displacements that do not exceed the value represented) or stress corrosion.

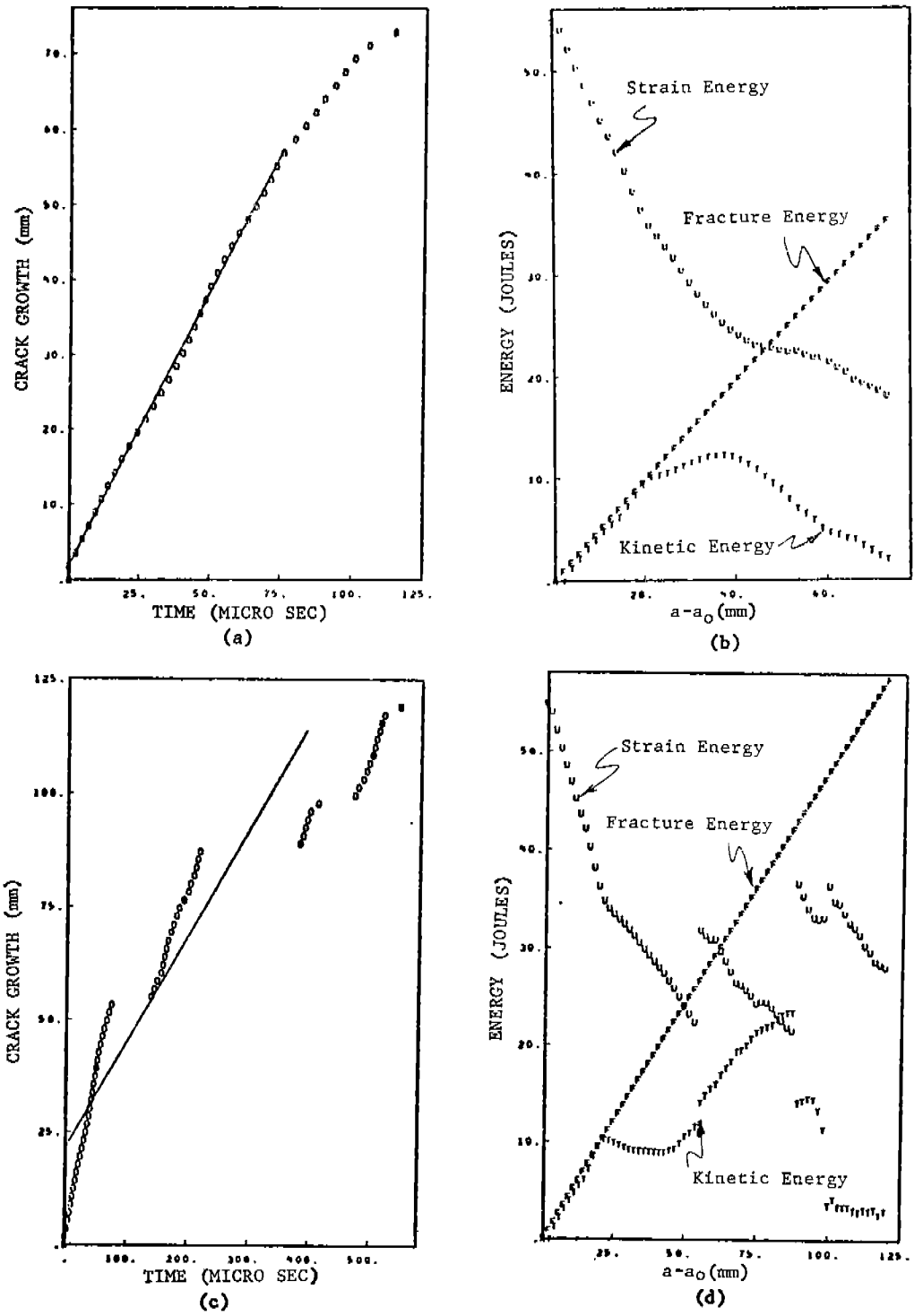

FIGURE 3.1.2.

INFLUENCE OF LOADING SYSTEM COMPLIANCE AND MASS ON CRACK PROPAGATION AND ARREST IN THE (ZERO TAPER) RECTANGULAR-DCB (a_o/h = 1.0) TEST PIECE FOR TYPE A MATERIAL RESPONSE AND $K_Q/K_{ID,min}$ = 1.5

(a) and (b) Wedge loading (W), compliance = 0
(c) and (d) Tensile loading M-2, compliance = 1.6 mm/MN, mass 12.4 kg

The mass and compliance of the loading system are also important factors which enter the problem by way of the external work term $\frac{dW}{dA}$. Figures 3.1.2a and 3.1.2b, give the results of calculations for propagation and arrest when the grips are fixed and $\frac{dW}{dA} = 0$. These may be compared with Figures 3.1.2c and 3.1.2d. for rectangular DCB-test pieces when the grips are <u>not</u> rigidly fixed, and possess the mass and compliance typical of a laboratory loading system. In this case, the external work term $\frac{dW}{dA}$ makes periodic contributions to the crack driving force causing the crack to reinitiate a number of times. The extent of propagation is nearly twice the value obtained under fixed grip conditions.

These concepts serve to distinguish between the two principle strategies for arresting a crack in a monotonic structure. Cracks can be stopped either by:

- Increasing the fracture resistance, R or
- Decreasing the crack driving force

in the path of the crack. Two strategies are illustrated in Figure 3.1.3 for a plate under essentially constant load. The strain energy term, $-\frac{dU}{dA}$, increases monotonically under these conditions (see Figure 3.1.3b). This means that the crack will not stop without an arresting device. The crack can be arrested by the first strategy of inserting a tough arrester with a high R-value in the path of the crack (Figures 3.1.3c and 3.1.3d). The second strategy is implemented by attaching a stiffener which produces a local reduction in $-\frac{dU}{dA}$ (Figures 3.1.3e and 3.1.3f). In both cases some kinetic energy return is shown schematically and will affect the performance of the arrester.

In principle, the rigorous application of these concepts to the design of crack arresters is straightforward. The energy components $\frac{dU}{dA}$, $\frac{dT}{dA}$, and $\frac{dW}{dA}$ are calculated for the structure and loading of interest. The fracture energy of the hull plate and/or arrester plate are measured in the laboratory. Together, these quantitites define the width, spacing or cross section of stiffener or energy absorbing arresters. In practice, the task is a difficult one. Methods of evaluating the energy components from dynamic analyses (see Chapter 6) are only now being developed for simple structural elements [28]. Their application to the complex hull structures will not be routine. For this reason, a number of simplified treatments of crack arrest based on static analyses have currency and these are reviewed in Sections 3.3 and 3.4 of this chapter. The evaluation of the very large R-values required of arrester materials also presents special, unresolved problems which are examined in Chapter 5.

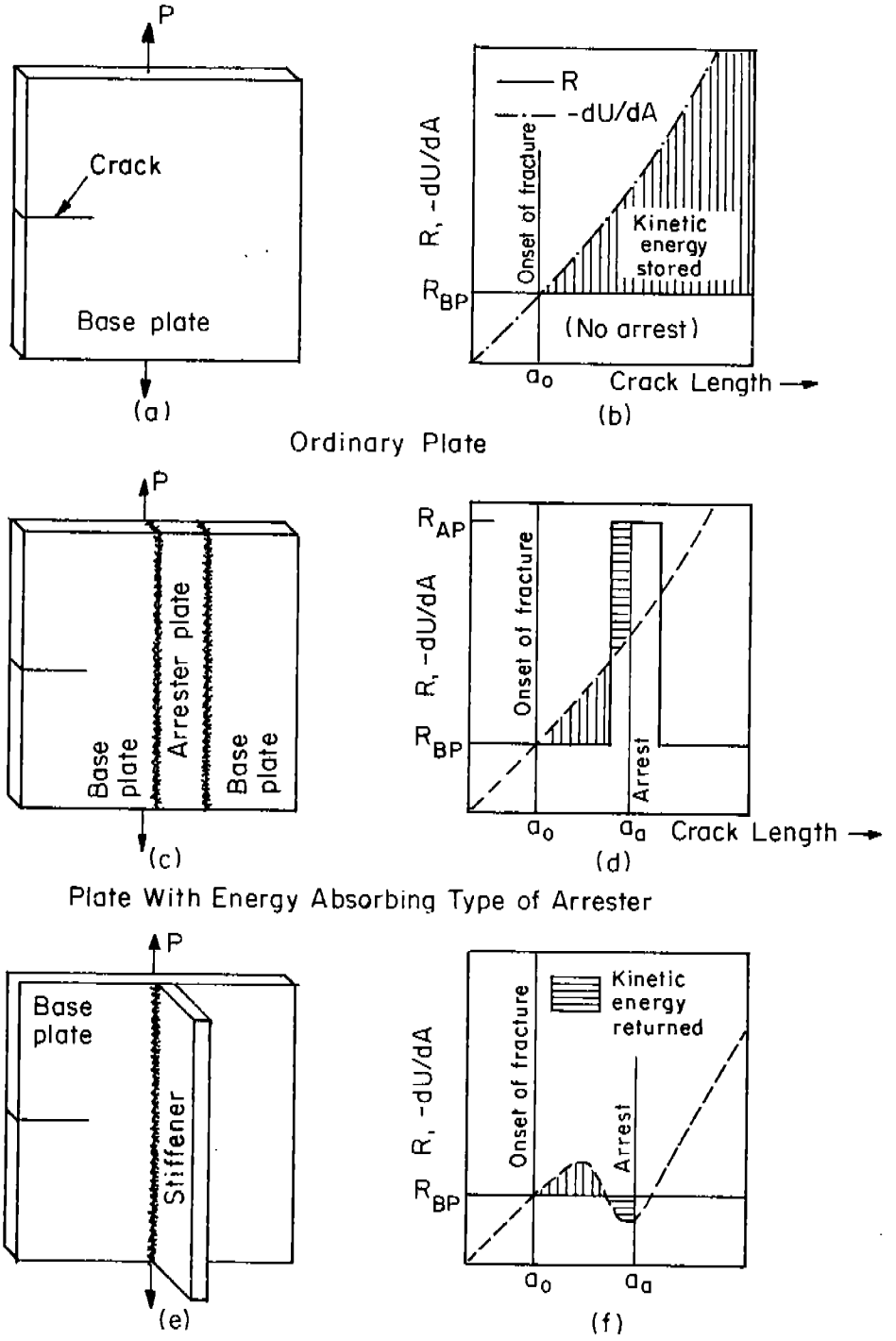

FIGURE 3.1.3

EXAMPLES OF THE PRINCIPAL STRATEGIES FOR PROMOTING CRACK ARREST: (a) ordinary plate under constant load and no arrester), (b) plate with arrester which increases fracture resistance R in the path of the crack, and (c) plate with a stiffener type of arrester which reduces the strain energy release rate in the path of the crack. The quantities R_{BP} and R_{AP} refer to the fracture energies of the base plate and arrester plates, respectively.

3.2 CRACK ARREST MATERIAL PROPERTIES

The treatment of crack arrest is further complicated by the variation of the fracture energy R with crack velocity and plate thickness. Eftis and Kraft [29] have deduced R-values from the Barton and Hall [30] wide-plate, ship-steel experiments. Their results, which reflect low-energy cleavage fractures below the nil ductility temperature (NDT), indicate that R-values first decrease with increasing velocity, display a minimum at a finite velocity, and then increase dramatically for crack velocities in excess of 600 ms. Recent results for low-energy fibrous fractures in AISI 4340 steel are reproduced in Figure 3.2.1c. Here the fracture energy increases monotonically with crack velocity. Since tough arrester materials also display the fibrous mode, it is possible that their minimum fracture energy values will also be observed at zero velocity.

Rigorous calculations of fracture arrest must take into account the variation of R with velocity and an arrest criterion based on the minimum fracture energy R_{min} (see Figure 3.2.1a):

$$\mathcal{G} < R_{min} \tag{3.2-1}$$

It therefore becomes necessary to distinguish among several different values of the fracture energy (and their equivalent fracture toughness values). Symbols and definitions of different quantities employed here and abroad are listed in Table 3.2.1. Note that the criteria for crack extension can also be expressed in terms of the stress intensity parameter K and various fracture toughness parameters as explained in the footnote to Table 3.2.1:

criterion for onset of crack extension	$K = K_c$	(3.2-2)
criterion for continuing propagation	$K = K_D$	(3.2-3)
criterion for crack arrest	$K < K_{D,min}$	(3.2-4)

The subscript I (i.e., G_{Ic}, K_{Ic}, $\mathcal{G}_{Ia}$, K_{Ia}) is introduced to distinguish energy and toughness values measured when the crack-tip plastic flow is predominantly plane strain* as opposed to so-called "plane-stress" values which reflect significant amounts of through-the-thickness deformation. The plane-strain values are independent of thickness while full shear (plane-stress) values of tough materials display a modest thickness dependence $K_c \propto t^n$, where t is the thickness and $0.25 < n < 1.0$ [33-36].

---

* According to ASTM E399, plane strain is obtained when the plate thickness $t \geq 2.5\left(\frac{K_{Ic}}{\sigma_Y}\right)^2$ where σ_Y is the yield stress. A similar expression can be expected to apply to fast running cracks provided σ_Y is interpreted as the dynamic yield stress.

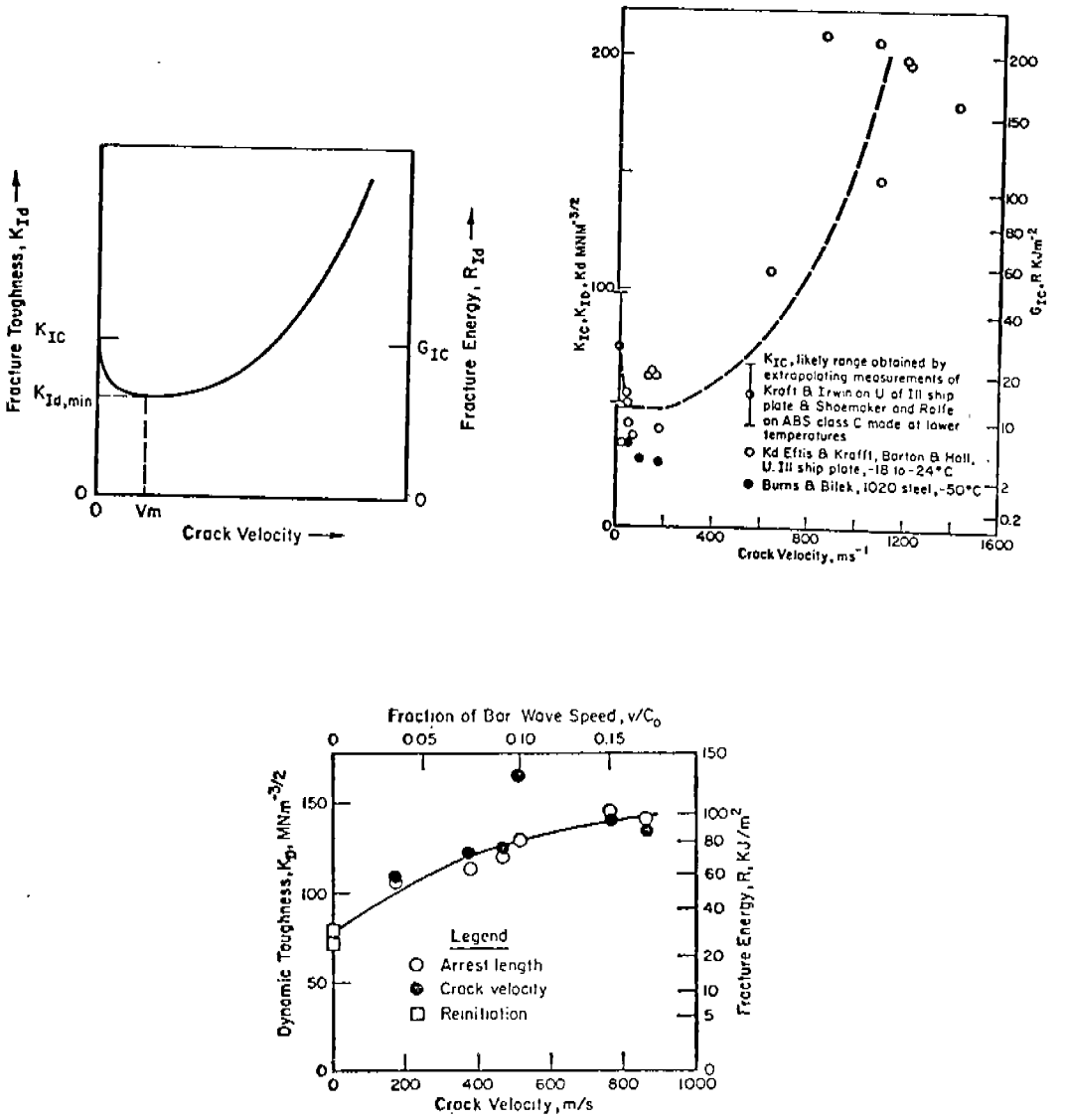

FIGURE 3.2.1. EXAMPLES OF THE CRACK VELOCITY DEPENDENCE OF THE FRACTURE RESISTANCE R AND THE CORRESPONDING PROPAGATING CRACK TOUGHNESS K_D: (a) schematic of a dependence with a minimum showing R_{min} and $K_{D,min}$, (b) results for cleavage fracture of ship plate after Eftis and Krafft [29] and Barton and Hall [30] and 1020 steel after Burns and Bilek [32], and (c) results for flat fibrous fracture of 4340 steel after Hahn, et al [31]

TABLE 3.2.1. SUMMARY OF FRACTURE ENERGY AND EQUIVALENT FRACTURE TOUGHNESS† VALUES RELATED TO THE CRACK ARREST PROBLEM

DEFINITION	FRACTURE ENERGY[(a)]	FRACTURE TOUGHNESS[(b)]
1.0 The fracture energy and toughness at the onset of unstable crack extension and for essentially zero crack velocity		
1.1 Values corresponding to slow loading rates	$\mathcal{G}_c$	K_c
1.2 Values for high loading rates	$\mathcal{G}_d$	K_d
2.0 The minimum fracture energy and toughness		
2.1 Values derived from dynamic analyses	R_{min}	$K_{D,min}$
2.2 Estimates derived from static analyses of an arrested crack	$\mathcal{G}_a$	K_a
2.3 Japanese practice for estimates from static analysis[(c)]	$\mathcal{G}_c$	K_c
3.0 The fracture energy and toughness at an arbitrary crack velocity	R_D	K_D

† The fracture energy of an extending crack (i.e. $\mathcal{G}_c$, R_{min}, R, $\mathcal{G}_a$, etc.) is related to a corresponding fracture toughness parameter (i.e., K_c, $K_{D,min}$, K_D, K_a, etc.) by the expression $K = A^{1/2}(V)[E\mathcal{G}/1-\nu^2]^{1/2}$ where $A(V)$ is a function of crack velocity that depends on C_1, C_2 and C_r and $A^{1/2}(V) = 1$ when $V=0$, $1 \leq A^{1/2}(V) \leq 1.1$ for $0 \leq V \leq 1500$ ms^{-1} for steel. [27,39]

(a) Common units: in lbs/in^2 = 1.75 J/m^2.

(b) Common units: Ksi $\sqrt{\text{in}}$ = 1.10 MN/m$^{3/2}$ = 1.10 MGr = 3.54 Kg/mm$^{3/2}$.

(c) In all but the more recent Japanese technical papers the quantities $\mathcal{G}_c$ and K_c are so defined that $\mathcal{G}_a = \pi\mathcal{G}_c$ and $K_a = \pi\sqrt{K_c}$.

The quantities $\mathcal{G}_d$ and K_d in Table 3.2.1 have been related to R_{min} and $K_{D,min}$ by Kraft and Irwin [37] and Krafft [38]. These workers propose that the crack-tip stress, strain, and strain-rate environment of a rapidly loaded stationary crack and a propagating crack, and the fracture energy in these two cases are the same provided the stress rate $\dot{K}$ and the crack velocity V are comparable:

$$\mathcal{G}_a(\dot{K}) = R(V) \tag{3.2-5}$$

A simple elastic argument suggests that the stress rates $K = 10^5$ $MNm^{-3/2}s^{-1}$ to 10^7 $MNm^{-3/2}s^{-1}$ are comparable to the crack velocities of $V = 1$ ms^{-1} to 100 ms^{-1} corresponding to R_{min}. Accordingly, the $\mathcal{G}_d$-values measured at these high rates of loading are a measure of R_{min}. Results in Figure 3.2.2 lend some support to this concept which is not well established.

3.3 THE STATIC, ARREST TOUGHNESS ($\mathcal{G}_a$, K_a) ANALYSIS

Irwin and Wells [42] and Crosley and Ripling [41,43-45] have proposed a simplified treatment of crack arrest. Their approach embodies the same basic crack arrest criterion, i.e., $\mathcal{G} < R_{min}$, but approximates the driving force for continued crack propagation with the value appropriate for a stationary crack of the same length.* The statically evaluated energy release rate at arrest, $\mathcal{G}_a$, is taken as a close approximation of R_{min}, and the criterion for crack arrest given in Equation (3.2-1) reduces to:

$$\mathcal{G}_a > \mathcal{G} = -\frac{dU}{dA} + \frac{dW}{dA} \tag{3.3-1}$$

or

$$K_a > K \tag{3.3-2}$$

where K_a and K are the corresponding stress-intensity parameters and K_a is called the arrest toughness.

According to the static arrest theory, $\mathcal{G}_a$ or K_a are geometry independent properties of material that coincide with the value of $\mathcal{G}$ or K at the point of crack arrest. This concept appears to be valid in some cases. For example, Crosley and Ripling [41] find that K_{Ia} values of reactor grade A533B steel are independent of the crack jump distance in a contoured DCB specimen (see Figure 3.3.1). They also report that cracks initiated in brittle weldments inserted in single-edge-notched (SEN) test pieces of the same material arrest at the same value of K_{Ia}. [45] Studies of various stiffener type of arresters by Yoshiki, Kanazawa and Machida [46,47] in Japan also lend support to the static-K_a approach. As shown in Figure 3.3.2, predictions of arrest based on K_a measurements (referred to as K_c in Japan) and statically calculated K values were found to be in good agreement with experiment.

---

* In other words, the kinetic energy term $-\frac{dT}{dA}$ is neglected and $-\frac{dU}{dA} + \frac{dW}{dA}$ is evaluated using static analyses.

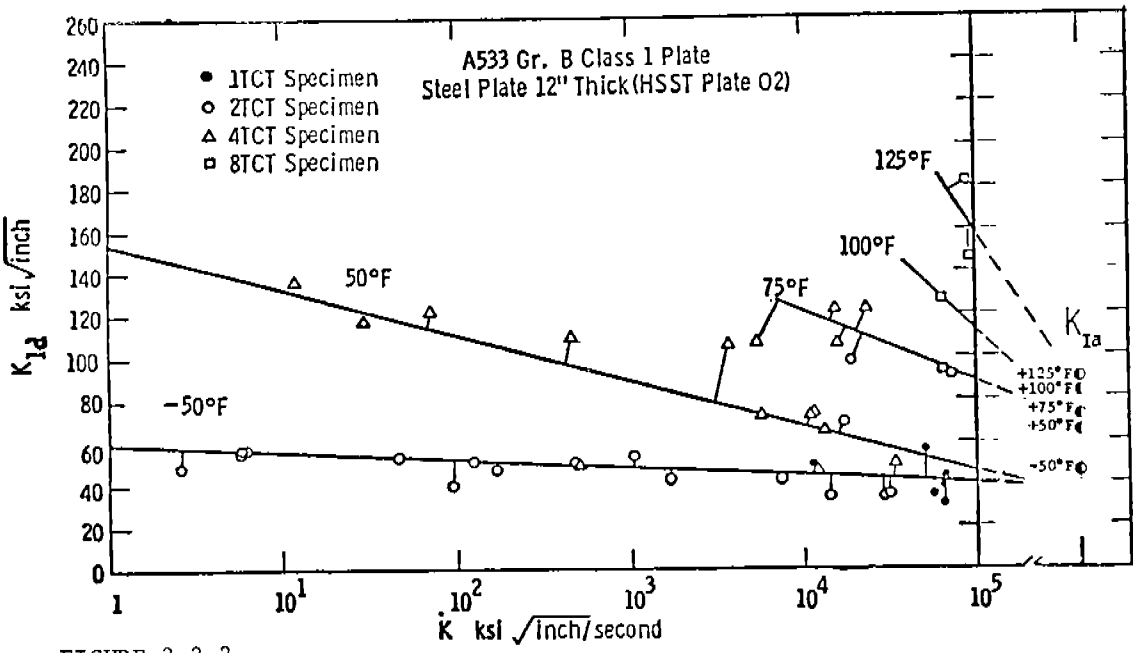

FIGURE 3.2.2

COMPARISON OF K_{Id}-MEASUREMENTS OF SHABBITS [40] WITH K_{Ia}-MEASUREMENTS BY CROSLEY AND RIPLING [41], BOTH ON A533B STEEL. The graph shows that $K_{Id}(\dot{K} \sim 5.10^5)$, obtained by extrapolation correlate to some degree with K_{Ia}-values.

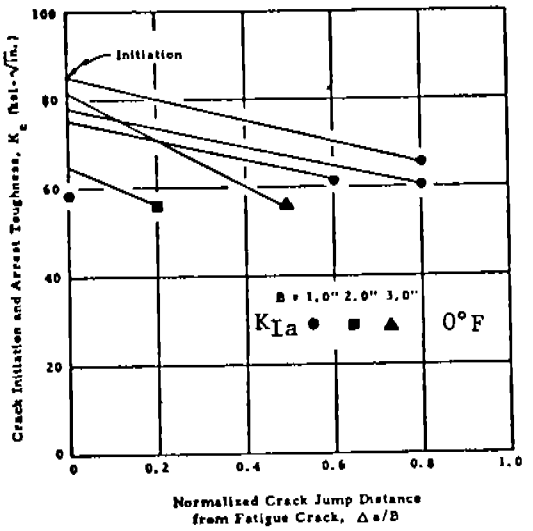

FIGURE 3.3.1. INFLUENCE OF THE CRACK JUMP DISTANCE ON THE ARREST TOUGHNESS, K_{Ia}, OF A533B STEEL AFTER CROSLEY AND RIPLING [41].

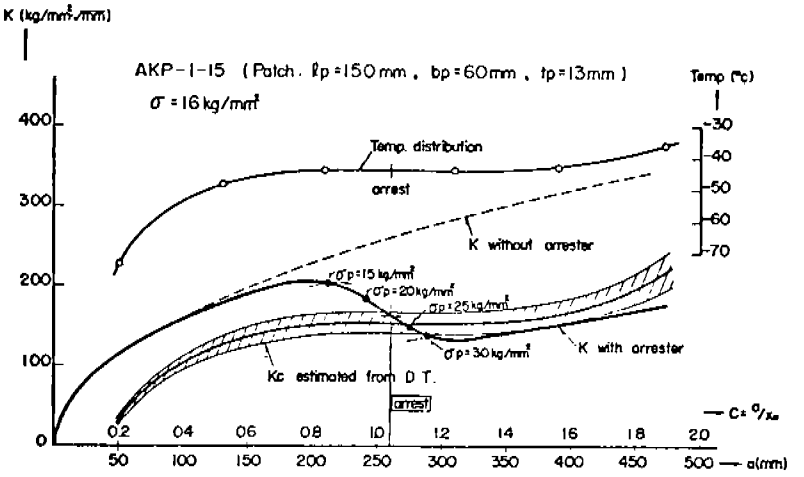

(a)

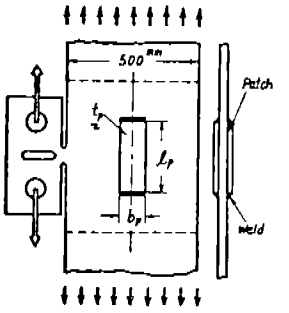

(a) Welded Patch Type

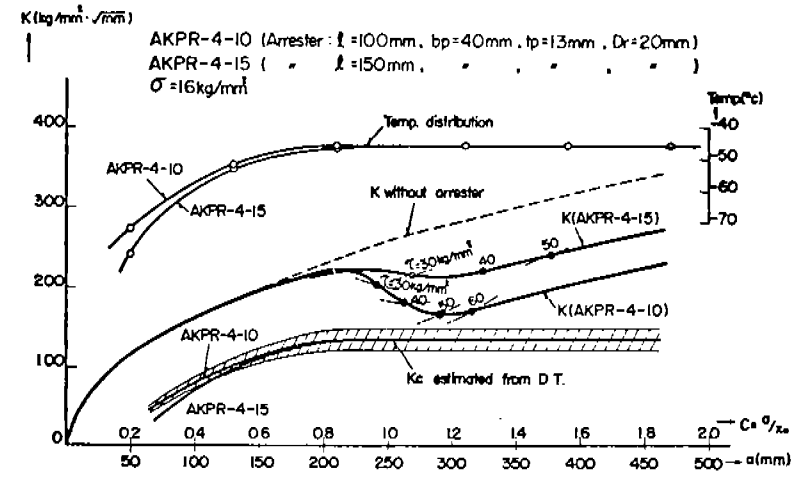

(b)

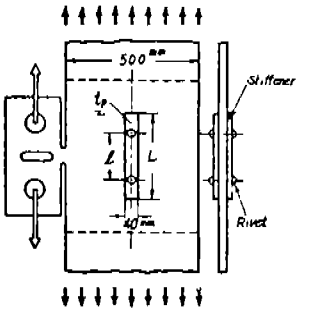

(b) Riveted Stiffener Type

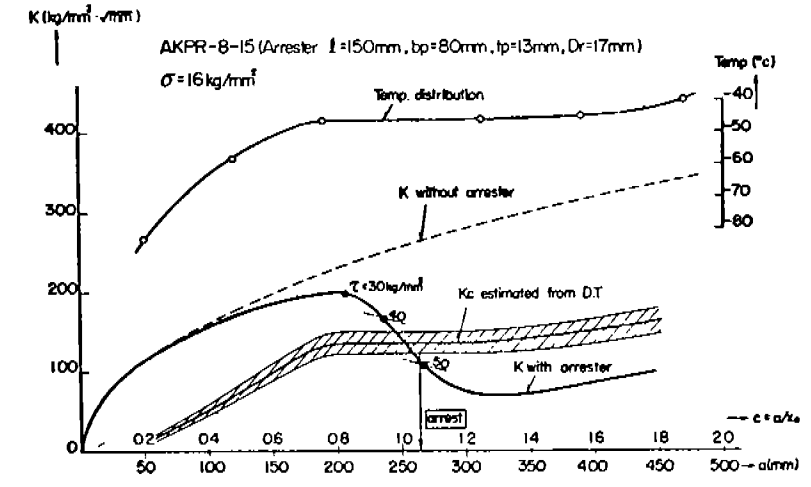

(c)

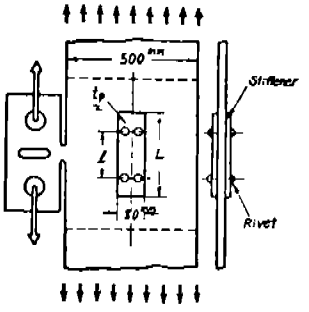

(c) Riveted Stiffener Type

FIGURE 3.3.2.

COMPARISON OF EXPERIMENTAL RESULTS FOR STIFFENER-TYPES OF CRACK ARRESTERS WITH PREDICTIONS FROM THE STATIC ANALYSIS AFTER YOSHIKI, ET AL [47] : (a) welded notch type stiffener, and (b) and (c) riveted stiffeners.

At the same time, there is a growing body of evidence showing that the static analysis of arrest is not generally valid. Dynamic calculations [26,28,48] show that by neglecting the kinetic energy term both the driving force, $\mathcal{G}$, and R_{min} are undervalued by static analysis. Results presented in Table 3.3.1, illustrated that the ratio $\frac{K_{Ia}}{K_{D,min}}$ (which should be invariant and close to unity if the static theory is valid) actually depend on the loading system and on the geometry. For this reason, the errors contained in a static analysis of arrest in a structure may or may not be compensated for by the discrepancy between $\mathcal{G}_a$ and R_{min}.

3.4 APPLICATIONS OF THE STATIC TOUGHNESS ARREST APPROACH AS USED IN JAPAN

Serious difficulties of the type described in Section 3.3 have, in fact, been encountered in the more recent analyses of large-scale ship-plate arrester model tests performed in Japan [46,7]. As shown in Figure 3.4.1, arrest was observed in the models even though the statically calculated K values were twice K_a. Japanese workers believe that the discrepancy can be traced to dynamic features attending the propagation of long cracks which invalidate the static analyses. We believe the discrepancy may also be connected with their imprecise treatment of the loading system (the $\frac{dW}{dA}$ term) and with their K_a measurements. The Japanese investigators have dealt with this problem by postulating an effective crack length and effective stress intensity.

$$a_{eff} = 0.1\ a + 190\ mm \tag{3.4-1}$$

and

$$K_{eff} = \sigma \sqrt{a_{eff}} \tag{3.4-2}$$

which contains an empirical correction designed to lower calculated K values to the K_a levels at arrest. Figure 3.4.1 illustrates that the correction is reasonably successful when applied to the experiments from which it was derived. However, the general applicability of this correction (e.g., its application to the stiffener experiments in Figure 3.3.2 which can be explained without a correction) is open to question.

3.5 FRACTURE ARREST APPROACH AS USED IN AIRCRAFT STRUCTURES

The riveted skin-stringer design of many aircraft structures is basically a crack-arrest structure. Aircraft are presently designed to arrest a two-bay crack; i.e., a crack originating at a stringer is to be arrested at the two adjacent stringers. The Air Force has recently issued MIL-A-83444, "Airplane Damage Tolerance Design Requirements", in which this arrest requirement is formalized.

TABLE 3.3.1. COMPUTATIONAL RESULTS FOR CRACK ARREST IN THE DCB SPECIMEN FOR VARIOUS DIFFERENT GEOMETRIES AND INITIAL STRESS INTENSITY FACTORS [48]

Initiation Conditions		Computational Results: Speed-Dependent Fracture Energy			Computational Results: Speed-Independent Fracture Energy		
a_o/h	K_q/K_{Ic}	a_r/h	$\bar{V}/C_o$	$K_{I\Omega}/K_{Im}$	a_r/h	$\bar{V}/C_o$	$K_{I\Omega}/K_{Im}$
1.0	1.00	1.45	.074	0.89	1.00	.0	1.00
1.0	1.25	1.75	.094	0.86	1.40	.086	0.82
1.0	1.50	1.95	.104	0.88	1.90	.149	0.64
1.0	1.75	2.05	.116	0.95	2.55	.192	0.47
1.0	2.00	2.15	.122	1.01	3.35	.203	0.35
1.0	3.00	2.60	.146	1.13	6.70	.262	0.15
1.0	4.00	2.90	.163	1.26	*	.308	*
2.0	1.00	2.90	.063	0.80	2.00	0	1.00
2.0	1.50	3.60	.097	0.83	3.50	.097	0.61
2.0	2.00	4.20	.115	0.85	5.15	.156	0.42
2.0	3.00	5.35	.138	0.84	*	.214	*
2.0	4.00	6.55	.149	0.78			
3.0	1.00	3.55	.067	1.08	3.00	0	1.00
3.0	1.50	5.60	.089	0.73	4.80	.072	0.67
3.0	2.00	6.95	.106	0.66	6.90	.124	0.47

* Crack did not arrest.

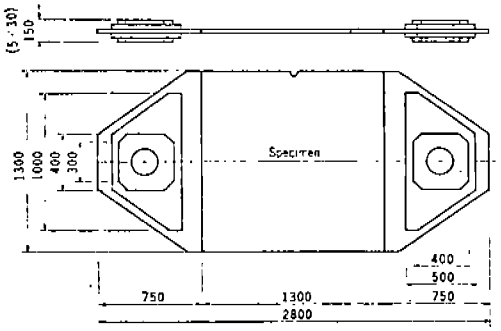

Specimen for butt welded-type crack arrester model

(a)

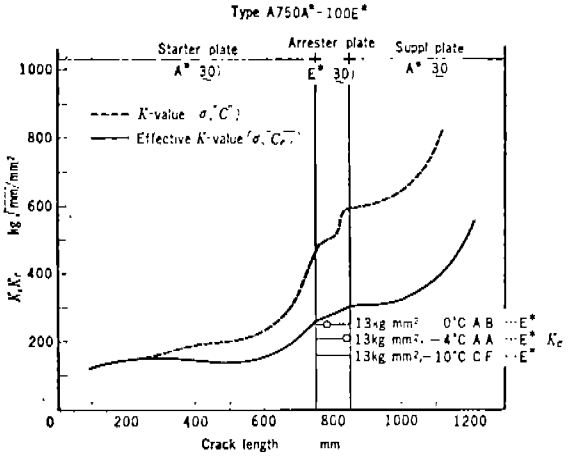

(b)

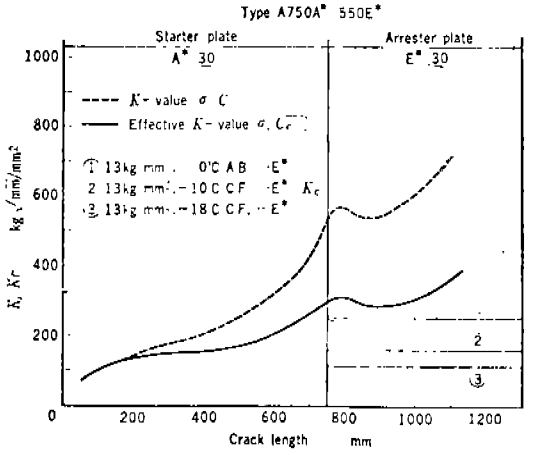

(c)

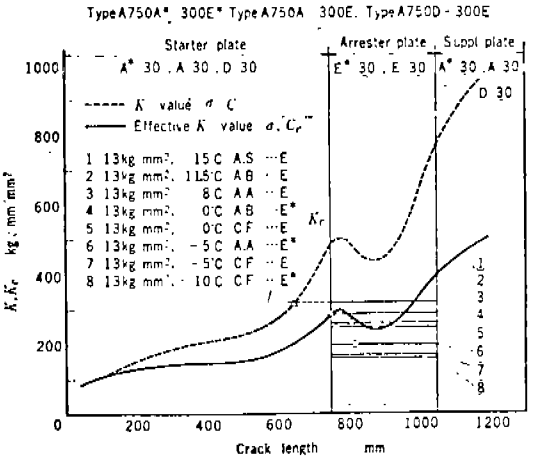

(d)

FIGURE 3.4.1. COMPARISONS OF EXPERIMENTAL RESULTS FOR LARGE, WELDED-TYPE, ENERGY ABSORBING CRACK ARRESTER MODELS WITH CALCULATIONS BASED ON THE STATIC ANALYSIS AFTER KIHARA, ET AL [7] : (a) test piece configuration, (b)-(d) results for different materials.

So far, the static analysis of arresters has proven satisfactory for aircraft structures, because (1) fast crack growth in aluminum alloys is still relatively slow (in the order of 500 ft/sec) and (2) thin aluminum plates show an increasing crack resistance as the crack extends. Nevertheless, MIL-A-83444 prescribes that a safety margin of 15 percent should be taken on the static analysis to account for possible dynamic effects.

Analysis methods for stringer-skin configurations have been developed by Romualdi, et al [49], Poe [50,51], Vlieger [52,53], and Swift and Wang [54,55]. Both finite-element methods and closed-form solutions can be used. The basic procedure is outlined in Figure 3.5.1. The stiffened panel is split into its composite parts. Load transmission takes place through the fasteners. As a result, the skin will exert forces F_1, F_2, etc., on the stringer, and the stringer will exert reaction forces F_1, F_2, etc., on the skin. This is depicted in the upper line of Figure 3.5.1.

The three cases have to be analyzed separately. Compatibility requires equal displacements in sheet and stringer at the corresponding fastener locations. These compatibility requirements deliver a set of n (n is number of fasteners) independent algebraic equations, which can be solved numerically to derive the fastener forces. According to Swift [56], 15 fasteners at either side of the crack need to be included to give a consistent result. A proper analysis includes the effects of (1) stiffener yielding and bending, (2) fastener yielding, and (3) fastener-hole deformation.

For the arrest analysis [53], consider a skin-stringer combination as in Figure 3.5.2 (top). The displacements of adjacent points in skin and stringer will be equal. Let a transverse crack develop in the skin. This will cause larger displacements in the skin, which has to be followed by the stringers. As a result, they take on load from the skin, thus decreasing the skin stress at the expense of higher stringer stress. Consequently, the displacements in the cracked skin will be smaller than in an unstiffened plate with the same size of crack. This implies that the stresses in the stiffened plate are lower and that the stress intensity is lower. The closer the crack tip is to the stringer, the larger the load-sharing effect.

If the stress intensity for a central crack in an unstiffened plate is $K = \sigma\sqrt{\pi a}$, then the stress intensity for the stiffened plate is $K = \beta\sigma\sqrt{\pi a}$. The reduction factor, β, becomes smaller when the crack approaches the stringer. Since the stringers take load from the skin, their stress will increase from σ to $L\sigma$, where L increases when the crack approaches the stringer. Obviously, $0 \leq \beta \leq 1$ and $L \geq 1$. Their values depend upon stiffening ratio, fastener stiffness, and crack size. For a qualitative discussion, it may suffice to let β and L vary as in Figure 3.5.2.

Now the arrest diagram for a simple panel with two stringers and a central crack can be constructed. Fast crack extension in an unstiffened plate will take place at a stress given by $\sigma_c = K_c/\sqrt{\pi a}$, represented by the lower line in Figure 3.5.3. For the stiffened panel, the stress for fast crack growth can be calculated as $\sigma_c = K_c/\beta\sqrt{\pi a}$. Knowing β from the static analysis, σ_c can

be calculated. It varies with crack size as shown in Figure 3.5.3. Since β decreases if the crack approaches the stringer, the curve turns upwards for crack sizes in the order of the stringer spacing.

The possibility of fastener failure and stringer failure should be considered also. Here, only stringer failure will be discussed. The stringer will fail when its stress reaches the ultimate tensile stress, σ_{uts} of the stringer material. As the stringer stress is $L\sigma$, where σ is the nominal stress in the panel away from the crack, stringer failure will occur at σ_{sf} given by $L\sigma_{sf} = \sigma_{uts}$. Using L as depicted in Figure 3.5.2, the panel stress at which stringer failure occurs is given in Figure 3.5.3.

Now consider a crack of size a_1. At a stress σ_1 fast crack growth occurs (point A). It will run to point B where it is arrested (because K will be lower than K_c again). Further increase of the stress will cause the crack to propagate in a stable manner to C, where again fast fracture would occur at a stress $\bar{\sigma}$. If the crack size is a_2, a stress σ_2 is required for fast crack growth. Arrest will not occur because $\sigma_2 > \bar{\sigma}$.

It has been outlined that β and L depend upon stiffening ratio. This implies that the diagram of Figure 3.5.3 is not unique. It shows the case where plate failure is the critical event. In other cases, stringer failure may be critical; this is so when the stringers are relatively small in section as compared to the bay sectional area. This is depicted in Figure 3.5.4. A crack of size a becomes unstable at a stress σ_3. It will run to point D where the stringer will fail. Hence, it will not be arrested. The highest stress for arrest, $\bar{\sigma}$, is now determined by point E as shown.

Many large panel experimental data are available to show the adequacy of the analysis procedure for aircraft structures. Some test data by Vlieger [52,53] are shown in Figure 3.5.4. The test data confirm the predicted behavior. In case of a short crack fracture, instability occurs at a stress too high for crack arrest at the stringer. Longer initial cracks showed some slow crack growth and then sudden fast crack growth. Crack arrest occurred at the stringer, after which the panel could be loaded to $\bar{\sigma}$ (horizontal level) where final failure occurred.

3.6 DYNAMIC ANALYSIS OF CRACK PROPAGATION AND CRACK ARREST

The problem of arresting a rapidly propagating crack is of great concern in several different kinds of engineering structures. These have in common the feature that unchecked unstable crack growth would have catastrophic consequences. They include aircraft (as discussed in the preceding section), nuclear pressure vessels, bridges, and gas transmission pipelines, in addition to ship hulls.

There is currently no universally accepted theoretically-based design approach to ensure crack arrest. A static approach, or, what amounts to the same thing, the "arrest toughness" or K_{Ia} approach, is almost universally employed. This approach is based on the idea that crack arrest is just the reverse of crack-growth initiation. However, there is a body of experimental results

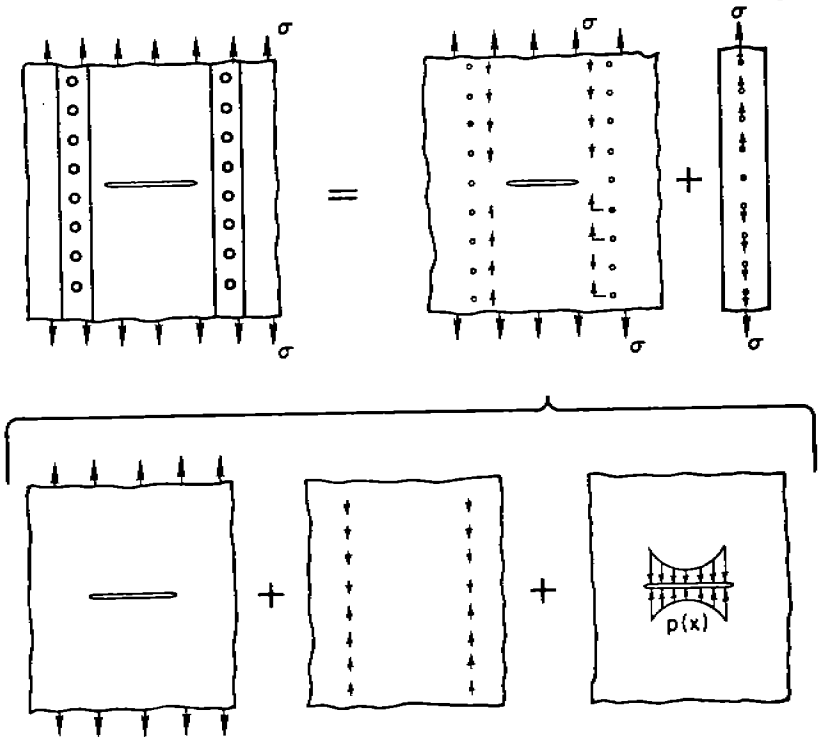

FIGURE 3.5.1. ANALYSIS OF STIFFENED PANEL

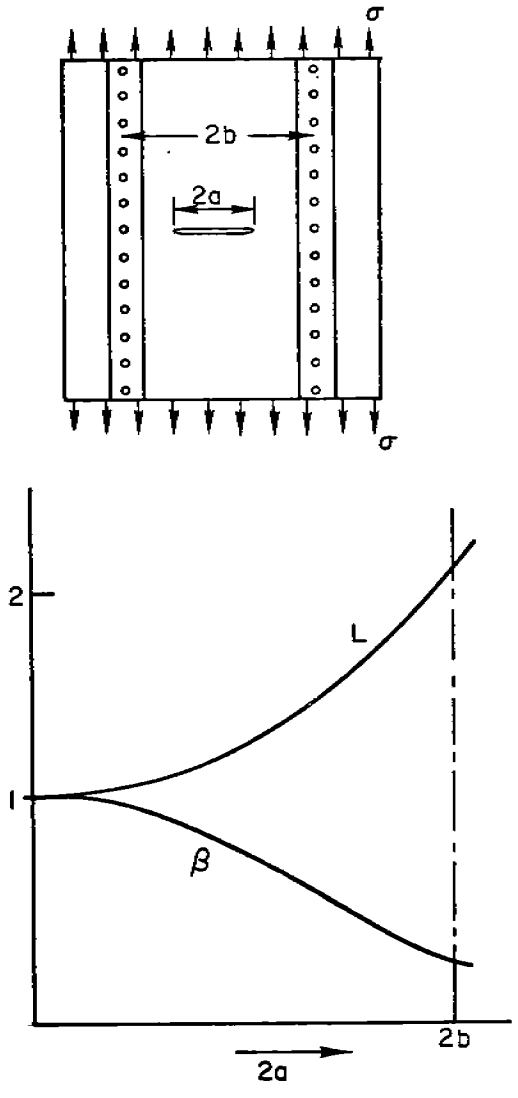

FIGURE 3.5.2. SKIN STRESS REDUCTION AND STRINGER LOAD CONCENTRATION

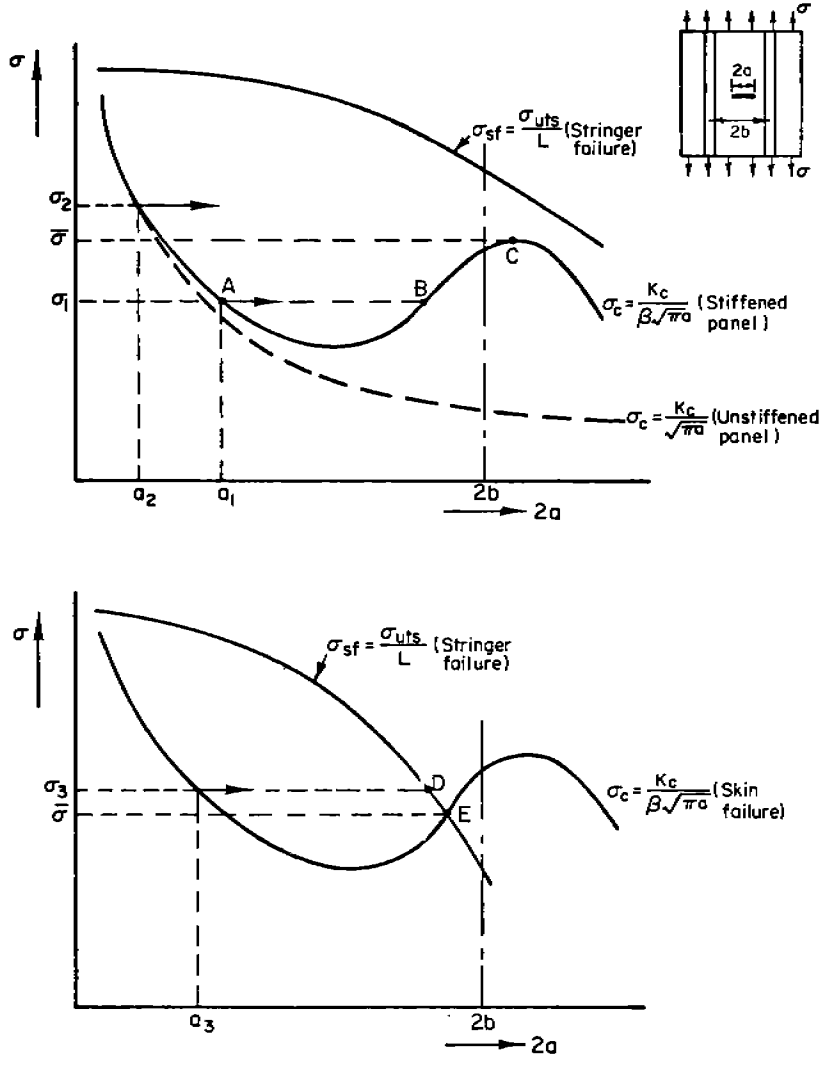

FIGURE 3.5.3. ARREST DIAGRAM FOR STRINGER CRITICAL CASE

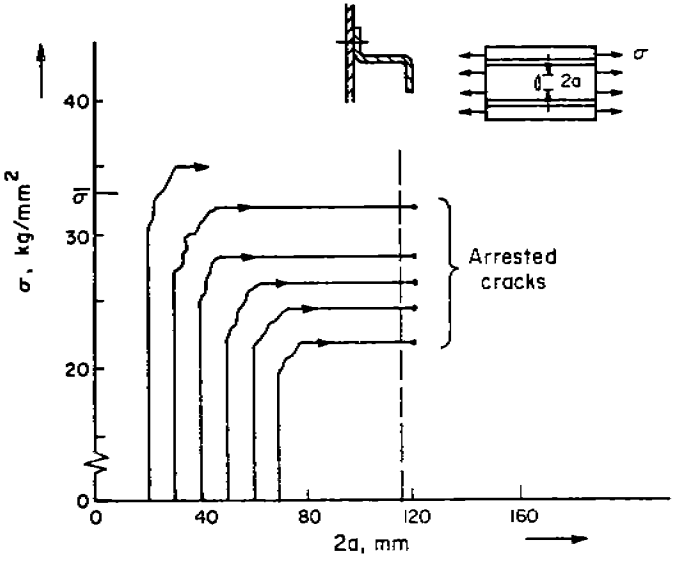

FIGURE 3.5.4. ARREST DATA BY VLIEGER FOR ALUMINUM ALLOY PANELS WITH Z-STIFFENERS

together with a rigorous energy-based method of analysis that has shown that crack arrest is a dynamic process that must be treated within the context of a dynamic fracture-mechanics theory. This work, originated at Battelle with prior Ship Structure Committee support [57] and continued on behalf of other agencies [58-67], includes several generalizations of the static approach. These include

- A kinetic energy contribution
- Inertia effects
- Dependence of fracture toughness on crack speed.

The primary purpose of this section of the report is to demonstrate that statically based analyses can dangerously overestimate the capacity of a structure to arrest a rapidly propagating crack. It will further be shown that even analyses taking full account of the essential aspects of dynamic fracture mechanics can still be inadequate for predicting crack arrest when other vital features of the problem are neglected. In particular, the otherwise admirable analyses of Freund [68,69] cannot cope with stress waves reflected back to the propagating crack tip from the specimen boundaries. This feature is not only important for experimental work carried out using small laboratory size test specimens, but would also be important in analyzing crack arrest devices.

Large-scale numerical computations are beyond the scope of the work reported here. This precludes complete analyses of the various candidate arrester systems. Nevertheless, it is important to have some quantitative evidence on the dynamic amplification of the crack driving force. This must be done in order to convincingly demonstrate the fact that static analyses of crack arrest can significantly overestimate the capability of a system to arrest a rapidly propagating crack. To accomplish this, some calculations were made with an existing computer model that was developed on an earlier Ship Structure Committee program to analyze crack propagation and crack arrest in the double cantilever beam (DCB) test specimen [57]. While hardly representative of most engineering structures, the DCB specimen geometry does lend itself to performing dynamic crack propagation-arrest analyses. Such analyses currently cannot be made for actual structures without performing large-system numerical computations. Hence, for the purposes of this report, the existing DCB analysis model was a natural vehicle, if not the only possible one, to demonstrate the differences between static and fully dynamic fracture mechanics concepts to evaluate crack arrester systems.

In this section of the report, the governing equations for the DCB specimen dynamic analysis procedure are first outlined. Next, a brief description of the alternative approaches is given where it is shown that, for crack arrest predictions, the conventional quasi-static approaches can be represented within the confines of a "quasi-dynamic" approach. Finally, some sample calculations are performed to contrast the quasi-dynamic and fully dynamic predictions for crack propagation and arrest in DCB specimens. This will set the stage for the analyses reported in Section 6 on the various types of ship-hull crack arresters.

3.6.1 Governing Equations for Dynamic Crack Propagation in the DCB Test Specimen

The starting point for the derivation of the equations governing dynamic crack propagation in the DCB specimen are the equations of the theory of elasticity with inertia terms included. Because the peculiar "beam-like" geometry of this specimen can be exploited, only four equations need to be explicity considered. These are the two equations for motion along the length of the beam (the x direction) and two Hooke's law equations. The two equations of motion are given by

$$\frac{\partial \sigma_x}{\partial x} + \frac{\partial \tau_{xy}}{\partial y} + \frac{\partial \tau_{xz}}{\partial z} = \rho \frac{\partial^2 u_x}{\partial t^2} \qquad (3.6\text{-}1)$$

and

$$\frac{\partial \tau_{xz}}{\partial x} + \frac{\partial \tau_{yz}}{\partial y} + \frac{\partial \sigma_z}{\partial z} = \rho \frac{\partial^2 u_z}{\partial t^2} \quad . \qquad (3.6\text{-}2)$$

The two constitutive or Hooke's law equations that enter into the analysis are given by

$$E \frac{\partial u_x}{\partial x} = \sigma_x - \nu(\sigma_y + \sigma_z) \qquad (3.6\text{-}2)$$

and

$$\frac{\partial u_x}{\partial z} + \frac{\partial u_z}{\partial x} = \frac{\tau_{xz}}{G} \quad . \qquad (3.6\text{-}4)$$

In the above equations, E, G, ν and ρ denote Young's modulus, the shear modulus, Poisson's ratio, and the density, respectively; u_x and u_z are displacement components; $\sigma_x, \sigma_y, \sigma_z, \tau_{xy}, \tau_{xz}, \tau_{yz}$ are stress components; and t denotes time.

Problems in which two-dimensional spatial variations and time variations both enter are difficult and, generally speaking, inappropriate to treat in a preliminary phase of an investigaton. The simplification that can be introduced to make the mathematical analysis more manageable is made by introducing cross-sectionally averaged dependent variables into the analysis. If A = A(x) is the area of the DCB specimen cross section at any axial position x, then these new variables can be obtained formally as follows. The deflection w = w(x) is

$$w = \frac{1}{A} \int_A \int u_z \, dydz \quad . \tag{3.6-5}$$

The rotation $\Psi = \Psi(x)$ is

$$\Psi = - \frac{1}{I} \int_A \int z u_x \, dydz \quad . \tag{3.6-6}$$

The shearing force $S = S(x)$ is

$$S = \int_A \int \tau_{xz} \, dydz \quad . \tag{3.6-7}$$

The bending moment $M = M(x)$ is

$$M = \int_A \int z\sigma_x \, dydz \quad . \tag{3.6-8}$$

By Operating on Equations (3.6-1) through (3.6-4) by $\int_A \int dydz$ and using Equations (3.6-5) through (3.6-8), after some manipulation, the equations of motion for the DCB specimen in terms of the cross-sectionally averaged variables are found to be

$$\frac{\partial S}{\partial x} - k_e w = \rho A \frac{\partial^2 w}{\partial t^2} \tag{3.6-9}$$

$$\frac{\partial M}{\partial x} + k_r \Psi - S = = \rho I \frac{\partial^2 \Psi}{\partial t^2} \tag{3.6-10}$$

$$- EI \frac{\partial \Psi}{\partial x} = M \tag{3.6-11}$$

$$\frac{\partial w}{\partial x} - \Psi = \frac{S}{\kappa GA} \tag{3.6-12}$$

where I is the moment of inertia, k_e and k_r, respectively, represent the extensional force and bending transmitted across the crack plane, and κ is a constant which depends on the shape of the cross section and on Poisson's ratio. Of course, $k_e = k_r = 0$ where the specimen is cracked, but are functions of the specimen geometry and elastic properties otherwise.

Now considering that A and I are functions of x and eliminating M and S from Equations (3.6-9) through (3.6-12), it is found that

$$\frac{\partial}{\partial x}\left\{\kappa GA\left[\frac{\partial w}{\partial x} - \Psi\right]\right\} - k_e w = \rho A \frac{\partial^2 w}{\partial t^2} \qquad (3.6\text{-}13)$$

and

$$\frac{\partial}{\partial x}\left\{EI \frac{\partial \Psi}{\partial x}\right\} - k_r \Psi + \kappa GA\left\{\frac{\partial w}{\partial x} - \Psi\right\} = \rho I \frac{\partial^2 \Psi}{\partial t^2} \quad . \qquad (3.6\text{-}14)$$

specializing to a rectangular cross section allows the following relations to be introduced

$$A = bh$$

$$I = \frac{1}{12} bh^3$$

$$\kappa GA = \frac{1}{3} Ebh$$

$$k_e = \frac{2Eb}{h}$$

$$k_r = \frac{1}{6} Ebh$$

where h = h(x) is the half-height of the specimen, b = b(x) is the specimen thickness, and, as above, E = E(x) is the elastic modulus. Substituting the above relations into Equations (3.6-13) through (3.6-14) and introducing the Heaviside step function H to delineate the position of the crack tip (i.e., x = a), the equations of motion for a rectangular DCB specimen whose geometry and elastic properties vary continuously along its axis are found to be

$$\frac{\partial}{\partial x}\left\{\frac{Ebh}{3}\left[\frac{\partial w}{\partial x}-\Psi\right]\right\}-\frac{2Eb}{h}H(x-a)w=\rho bh\frac{\partial^2 w}{\partial t^2}-\sum_{j=1}^{p}\delta F_j\,(x-X_j) \qquad (3.6\text{-}15)$$

and

$$\frac{\partial}{\partial x}\left\{\frac{Ebh^3}{12}\frac{\partial\Psi}{\partial x}\right\}+\frac{Ebh}{3}\left\{\frac{\partial w}{\partial x}-\Psi\right\}-\frac{Ebh}{6}H(x-a)\Psi=\frac{\rho bh^3}{12}\frac{\partial^2\Psi}{\partial t^2}\,. \qquad (3.6\text{-}16)$$

In Equation (3.6-15), terms typified by $F_j\,\delta(x-X_j)$, where δ is a Dirac delta function, are inserted to represent an external force (per unit length) exerted at the point $x = X_j$. This makes it possible to treat the effect of stiffener-type arrest devices, for example. Note the forces are taken to be positive in the direction of positive w.

The situation of most interest here is that in which E, h, and b are all constants. Equations (3.6-15) and (3.6-16) can then be written as

$$\frac{\partial^2 w}{\partial x^2}-\frac{\partial\Psi}{\partial x}+\frac{6}{h^2}H(x-a)\,w=\frac{3}{C_o^2}\frac{\partial^2 w}{\partial t^2}-\frac{3}{Ebh}\sum_{j=1}^{p}F_j\delta(x-X_j) \qquad (3.6\text{-}17)$$

and

$$\frac{\partial^2\Psi}{\partial x^2}+\frac{4}{h^2}\left[\frac{\partial w}{\partial x}-\Psi\right]-\frac{2}{h^2}H(x-a)\Psi=\frac{1}{C_o^2}\frac{\partial^2\Psi}{\partial t^2}\,, \qquad (3.6\text{-}18)$$

where $C_o^2 = E/\rho$ is the bar wave speed (C_o = 5000 M/sec in steel). It can be seen that the characteristic wave speeds are C_o and $C_o/\sqrt{3}$, the latter being a result

of the choice of Poisson's ratio of $\nu = 0.27$ in this work. This enters the equations of motion via the parameter κ. In particular, it is found that $\kappa GA = Ebh/3$.

Expressions for the strain energy and the kinetic energy of the system can be obtained in terms of the variables introduced above. Omitting the details, the resulting expression for the strain energy U is

$$U = \int_0^L \left\{ EI \left(\frac{\partial \psi}{x}\right)^2 + \kappa GA \left(\frac{\partial w}{\partial x} - \psi\right)^2 + F\psi^2 + H(x-a) \left[k_e w^2 + k_r \psi^2\right] \right\} dx \qquad (3.6\text{-}19)$$

while the kinetic energy T is

$$T = \int_0^L \left\{ \rho A \left(\frac{\partial w}{\partial t}\right)^2 + \rho I \left(\frac{\partial \psi}{\partial t}\right)^2 \right\} dx \quad , \qquad (3.6\text{-}20)$$

where L is the overall length of the specimen.

The most important use of the strain and kinetic energy expressions is in determining the crack driving force. This is done through the definition of the dynamic energy release rate $\mathcal{J}$ in terms of an energy balance for the system. This is given by

$$\mathcal{J} = \frac{1}{b} \left\{ \frac{dW}{da} - \frac{dU}{da} - \frac{dT}{da} \right\} \quad , \qquad (3.6\text{-}21)$$

where W is the work done by external loadings. By substituting Equations (3.6-19) and (3.6-20) into (3.6-21), it is found that $\mathcal{J}$ can be given a "crack tip" interpretation. This is

$$\mathcal{J} = \frac{2E}{h} \left\{ w^2 + \frac{h^2}{12} \psi^2 \right\}_{x=a(t)} \quad , \qquad (3.6\text{-}22)$$

where, it should be emphasized, the bracketed quantity is to be evaluated at the axial position representing the current crack tip. This is not only a much more convenient way in which to compute $\mathcal{J}$, i.e., in comparison to Equation (3.6-12), but is also more physically satisfying as well.

The condition under which crack propagation can occur is that a balance exists between the energy "released" from the structure as the crack extends by an increment and the energy absorption requirement of the material that is associated with that growth increment. A quantitative statement of the energy balance for crack propagation is

$$\mathcal{J}(a,t) = R(\dot{a}) \quad , \qquad (3.6\text{-}23)$$

where the dynamic energy-release rate (or crack-driving force) $\mathcal{G}$, as can be seen from Equation (3.6-22), is a function of crack-tip position and time while the energy dissipation rate $\mathcal{R}$ is a material property that can at most be a function of crack speed. Note that the units of $\mathcal{G}$ and $\mathcal{R}$ are energy per unit area of crack advance.

Figure 3.6.1 illustrates how the dynamic crack-propagation criterion given by Equation (3.6-23) is implemented. In Figure 3.6.1(a), the hypothetical crack speed is calculated on the basis that, if an increment of crack growth were to occur at some time following the last previous growth increment, the actual speed would be in inverse proportion to the time. For a specified energy-dissipation rate $\mathcal{R}$ that is a function of crack speed, the crack tip's energy requirement is then known once the hypothetical speed is determined. This is shown as the decreasing curve in Figure 3.6.1(b). A typical computational result for the crack-driving force, as obtained from Equation (3.6-22), is also shown. Where these two curves intersect crack growth occurs (i.e., where $\mathcal{G} = \mathcal{R}$). Note that this kind of calculation can be performed for any specific kind of $\mathcal{R} = \mathcal{R}(\dot{a})$ dependence including the simplest: $\mathcal{R} = \mathcal{G}_c$ = constant.

3.6.2 General Approaches to Crack Propagation and Crack Arrest

The arrest of a rapidly propagating crack in a structure under load can be considered on several different levels of complexity. Starting from the simplest (and least accurate) and continuing with more complicated (but more accurate) approaches, the various types can be classified as either

- Completely static
- Quasi-static
- Quasi-dynamic
- Fully dynamic.

The primary distinction that differentiates between static and dynamic approaches is that inertia terms and the contribution of kinetic enery to the crack-driving force are excluded in the former but not the latter. Physically, this means that static theories are limited to situations where (1) the crack propagates slowly and (2) changes its speed only gradually. As the extensive work done at Battelle and other institutions has shown, the arrest of rapid crack propagation tends to occur rather abruptly. This alone indicates that statically based treatments must be applied to crack arrest with due caution. Quantitative results reinforcing this idea can be produced too, as shown in the next section of this report.

The distinction between the two dynamic analysis procedures lies in the particular specialization that is involved for simplification. The quasi-dynamic treatments referred to above are those obtained by considering the structure to be an infinite elastic medium. Hence, in these approaches, the effect of stress waves reflected back to the propagating crack tip from the boundaries of the structure and/or from internal load points and discontinuities (e.g., welded-on stiffners) must be neglected. These effects can be taken into account in a fully dynamic analysis, albeit at the expense of specializing the structural

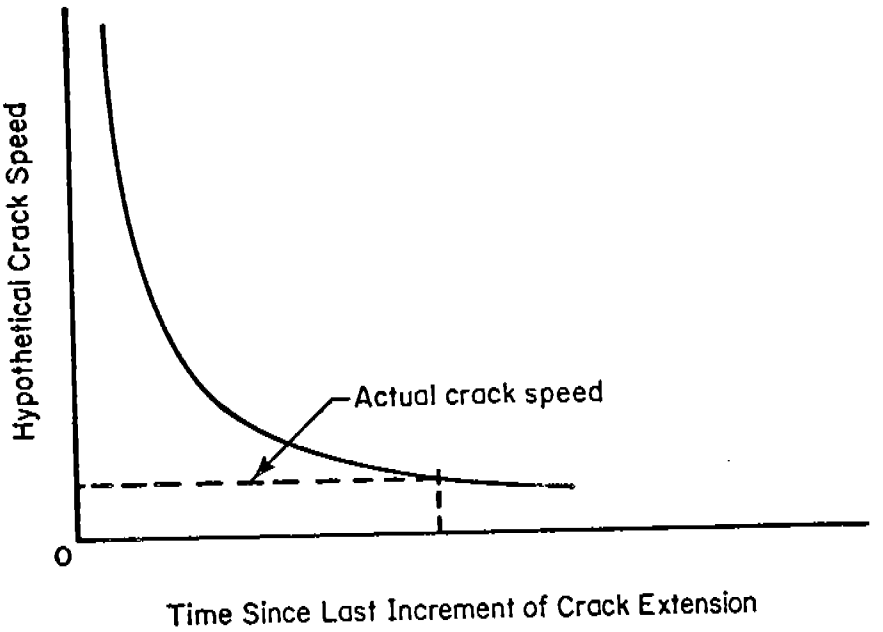

(a) Hypothetical crack speed.

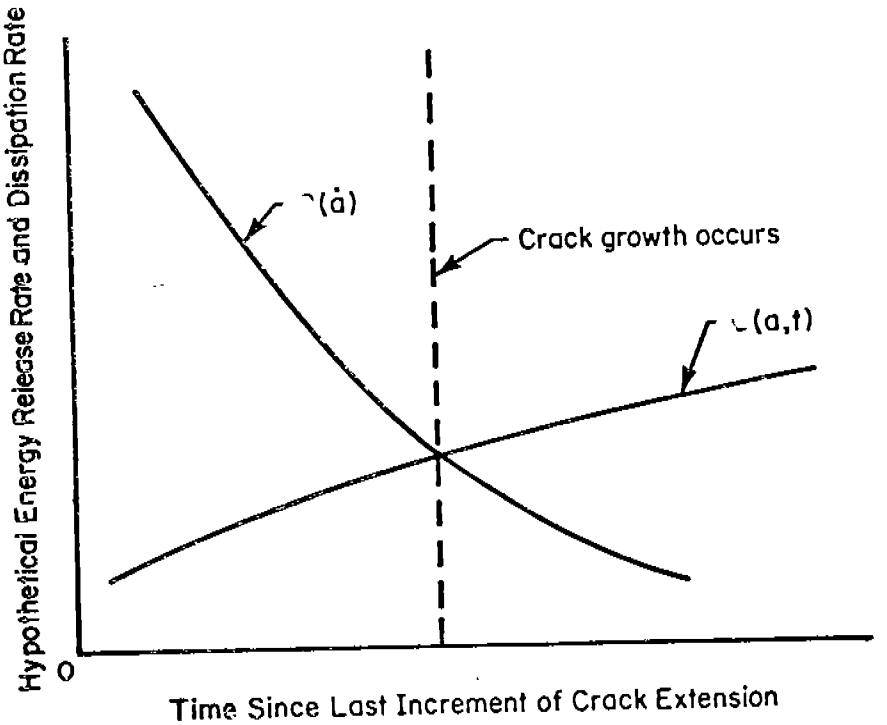

(b) Corresponding energies.

FIGURE 3.6.1 GRAPHICAL ILLUSTRATION OF DYNAMIC CRACK PROPAGATION CRITERION FOR SPEED-DEPENDENT MATERIALS

geometry under consideration (e.g., as in the DCB analysis described above). Nevertheless, in considering crack arrester systems, a fully dynamic analysis procedure is obviously called for, at least in the preliminary stages of the analysis.

It is a fact that the arrest point determined from either a static, a quasi-static, and quasi-dynamic treatments will always be closely related and, in some cases, will be exactly the same. Consequently, for the purposes of this report, it will suffice to describe the most accurate of these (the quasi-dynamic) with a view towards contrasting its crack arrest predictions with those of a fully dynamic calculation.

A very elegant analyses of the propagation of a semi-infinite crack in an infinite medium is that given by Freund.[27,68,69] Using a Laplace transform in conjunction with the Wiener-Hopf Technique, Freund has solved the equations of motion for a half-plane crack propagating in an unbounded medium for a fairly unrestricted class of crack motion. A key result of the analysis relates the dynamic stress intensity factor K, a function of crack length a, and speed $\dot{a}$, to the product of the static intensity factor K_s and a universal function of crack speed $k(\dot{a})$ according to

$$K(a,\dot{a}) = k(\dot{a})\, K_s(a) \quad . \tag{3.6-24}$$

The geometry-independent function k, which must be computed numerically, decreases monotonically from unity at zero crack speed to zero at the Rayleigh velocity C_R.

A second key result obtained by Freund is one that relates the dynamic energy-release rate to the dynamic stress-intensity factor. For plane-strain conditions, this is

$$\mathcal{G}(a,\dot{a}) = \frac{1-\nu^2}{E}\, A(\dot{a})\, K^2(a,\dot{a}) \tag{3.6-25}$$

where A is a geometry independent, monotonically increasing function which is unity at zero speed and becomes unbounded at the Rayleigh speed.

It is of some importance to recognize that Equation (3.6-25), although derived for an infinite medium, is generally valid, i.e., the relation is geometry independent. This has been proven by Nilsson.[51] As a result, it is possible to use the idea of dynamic fracture toughness $K_D = K_D(\dot{a})$ interchangeably with an intrinsic material energy-dissipation rate. That is, from Equation 3.6-25), one can write

$$R(\dot{a}) = \frac{1-\nu^2}{E}\, A(\dot{a})\, K_D^2(\dot{a}) \tag{3.6-26}$$

and use either Equation (3.6-24) or the relation

$$K(a,\dot{a}) = K_D(\dot{a}) \tag{3.6-27}$$

as the crack propagation criterion. In either case, it is found that the quasi-dynamic equation of motion for the crack tip is given by

$$K_s^2(a) = \frac{K_{ID}^2(\dot{a})}{g(\dot{a})} \quad , \tag{3.6-28}$$

where $g = AK^2$ is also a universal function of crack speed. The function $g = g(\dot{a})$ can be interpreted as the ratio of the dynamic to the static energy release rates.

In order to apply Equation (3.6-28) to investigate crack arrest, an explicit relation for the function $g(\dot{a})$ is needed. In Freund's analysis, a numerical integration was used to determine this function. However, it can be shown that the function $g = g(\dot{a})$ is more than adequately expressed by the simple relation

$$g(\dot{a}) = 1 - \frac{\dot{a}}{C_R} \quad . \tag{3.6-29}$$

Hence, substituting Equation (3.6-29) into Equation (3.6-28) and rendering the resulting equation dimensionless by introducing the material constant K_{IC}, the equation of motion for the crack tip becomes

$$\frac{K_s(a)}{K_{IC}} = \frac{K_{ID}(\dot{a})}{K_{IC}} \left[1 - \frac{\dot{a}}{C_R}\right]^{-1/2} \tag{3.6-30}$$

The next step is to introduce the relation for K_s for the DCB specimen. Equation (3.6-30) can then be solved iteratively for the crack speed as a function of crack length. By numerically integrating these results, the crack length can be obtained as a function of time.

As a final point, Equation (3.6-30) can be used to show that the crack-arrest point predicted with the quasi-dynamic theory is equivalent to those obtained from the completely statically based approaches. Consider a material having a dynamic fracture toughness that exhibits a minimum value K_{DM}, at some finite crack speed $\dot{a}_M$; nb, the case $a_M = 0$ and $K_{DM} = K_{IC}$ is not precluded. A propagating crack will arrest when (and only when) Equation (3.6-27) can no longer be satisfied. Using the static theory, this occurs at a crack length a_r such that

$$K_s(a_r) = K_D(\dot{a}_M) = K_{DM} \quad .$$

Now, from Equation (3.6-30), this condition means that the crack will arrest when

$$K_s(a_r) = K_{ID}(\dot{a}_M)\left[1 - \frac{\dot{a}_M}{C_R}\right]^{1/2} ,$$

or when

$$K_s(a_r) \propto K_{DM} ,$$

where the constant of proportionality is a material property. Note that the value of this constant will be simply equal to unity when $K_D = K_{IC}$. Hence, in these cases, the arrest point given by either the static or the quasi-dynamic approaches will be exactly the same.

3.6.3 Comparison of Crack Arrest Predictions Made by Static Fracture Mechanics with Those of Dynamic Fracture Mechanics

Crack propagation experiments in the DCB test specimen can be made for either of two general kinds of loading conditions: wedge loading and pull-rod loading. For the first set of conditions, crack growth is initiated from a blunt crack by slowly forcing the load pins apart. In this case, essentially no external work is done on the specimen as the crack propagates. For the second set of conditions, crack growth is initiated from a sharp crack by pulling the load pins apart with elastic rods. This system does involve work done on the specimen while the crack is running. Either set of conditions can be analyzed. However, because for a substantial period of time after the initiation of growth, there is no difference between the two cases, the more economical wedge load conditions have been used in the analyses reported here.

In order to use Equation (3.6-30) to obtain a prediction of crack arrest, the appropriate static stress-intensity factor expression for the geometry and load under consideration must be supplied. For the DCB specimen with wedge loading, Kanninen[66] has shown that

$$K = \sqrt{3Eh^3\lambda^2\delta}\left[\lambda a\left(\frac{\operatorname{Sinh}^2\lambda c + \sin^2\lambda c}{\operatorname{Sinh}^2\lambda c - \sin^2\lambda c}\right) + \left(\frac{\operatorname{Sinh}\lambda c\,\operatorname{Cosh}\lambda c - \sin\lambda c\cos\lambda c}{\operatorname{Sinh}^2\lambda c - \sin^2\lambda c}\right)\right]\cdot$$
$$\cdot\left[2\lambda^3 a^3 + 6\lambda^2 a^2\left(\frac{\operatorname{Sinh}\lambda c\,\operatorname{Cosh}\lambda c + \sin\lambda c\cos\lambda c}{\operatorname{Sinh}^2\lambda c - \sin^2\lambda c}\right)\right. \qquad (3.6\text{-}31)$$
$$\left. + 6\lambda a\left(\frac{\operatorname{Sinh}^2\lambda c + \sin^2\lambda c}{\operatorname{Sinh}^2\lambda c - \sin^2\lambda c}\right) + 3\left(\frac{\operatorname{Sinh}\lambda c\,\operatorname{Cosh}\lambda c - \sin\lambda c\cos\lambda c}{\operatorname{Sinh}^2\lambda c - \sin^2\lambda c}\right)\right]^{-1} ,$$

where $c = L-a$ is the uncracked ligament length, 2δ is the pin displacement, and $\lambda = 1.565/h$.

Aside from the specimen and arrester dimensions and mechanical properties, the test parameter which governs crack propagation in the DCB specimen under wedge loading is K_q, the stress-intensity factor acting at the time of crack-growth initiation.[1] Note that because of the initial blunting of the crack tip, it is possible to have $K_q > K_{IC}$. High values of K_q mean that large amounts of energy can be stored in the specimen initially and, hence, rapid crack propagation can be achieved. Another feature of the wedge-loaded DCB results is that cracks generally propagate at an essentially constant speed. This is useful in the analysis of arrester devices because the speed of the crack as it approaches the arrester can be readily identified.

One additional feature makes the wedge-loaded DCB an even more suitable device for the preliminary examination of crack arrester devices. This is due to the fact that it is a more efficient supplier of kinetic energy to the crack tip than is an actual structure. This makes the predictions made for a given arrester system conservative in that it will under estimate the ability of the device to arrest a crack in an actual structure. Looked at in another way, evaluations of arrester systems using a laboratory test specimen configuration such as the DCB specimen will automatically include a factor of safety.

The particular geometry chosen to perform the computation contrasting the dynamic and static crack arrest approaches is shown in Figure 3.6.2. An initial set of computations was made for a "standard" specimen without an arrest section. The specific dimensions for the geometry shown in Figure 3.6.2 are as follows:*

$$a_o = 50 \text{ mm}$$
$$h = 50 \text{ mm}$$
$$e = 25 \text{ mm}$$
$$b = 25 \text{ mm}$$
$$L = 300 \text{ mm}.$$

Wedge loading was assumed which means that the pin displacement at the onset of motion and its minimum displacement thereafter (nb, the pins are free to rise above the wedge while the crack is in motion and, in fact, they do) are fixed by the specified value of K_q, cf, Equation (3.6-31). A constant crack speed-independent value of K_D was taken to facilitate comparison with the static theory in these computations. As pointed out above, this then means that the arrest point given by the quasi-dynamic theory exactly coincides with the completely static and quasi-static approaches.

Two example computational results are shown in Figure 3.6.3(a) and (b). These are for K_q values of 2.0 K_{IC} and 3.0K_{IC} ($G_q/G_c = 4.0$ and 9.0), respectively. It can be clearly seen that the prediction of the crack arrest

---

* In addition, load pins 100 mm in length and 25 mm in diameter were considered. The specimen material was taken to be steel with $E = 0.20865 \text{ MN/min}^2$.

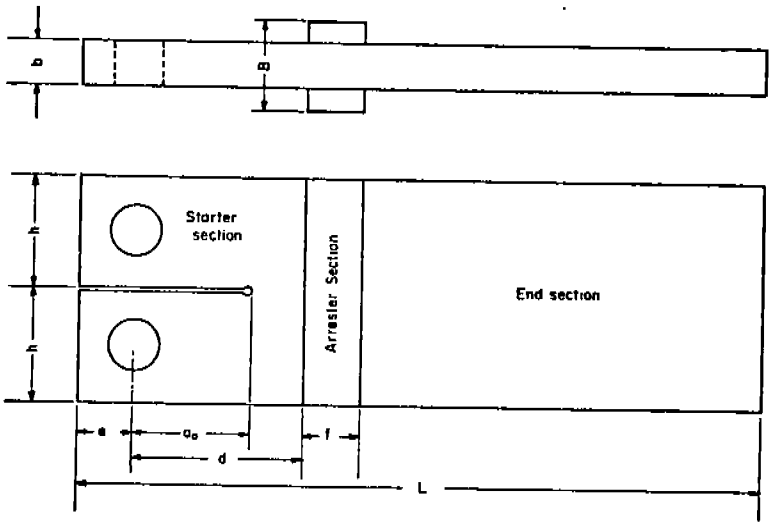

FIGURE 3.6.2. DCB SPECIMEN GEOMETRY FOR ARRESTER CALCULATIONS

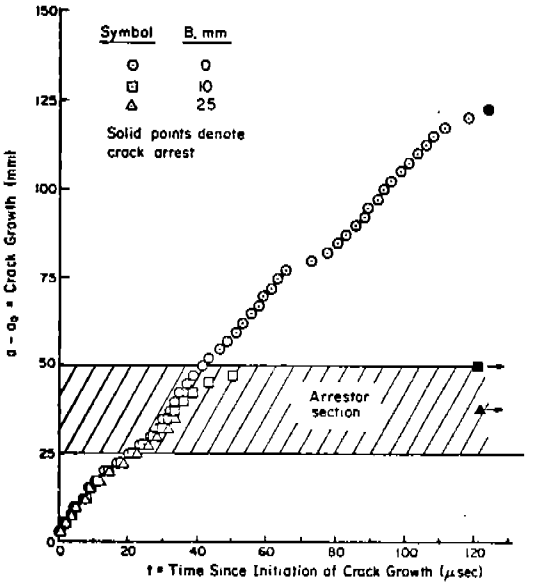

FIGURE 3.6.3.(a). CRACK PROPAGATION COMPUTATIONS FOR A DCB SPECIMEN WITH AN INTERMITTANTLY ATTACHED STIFFENER CRACK ARRESTER FOR K_q/K_{IC} = 2.0

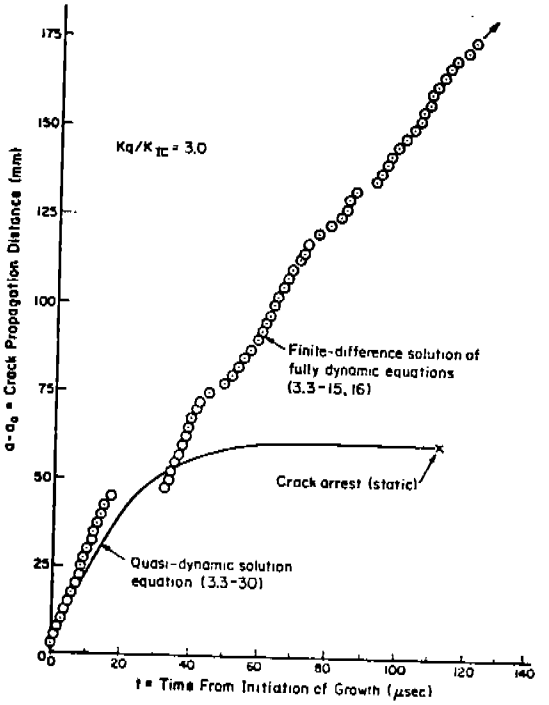

FIGURE 3.6.3.(b). COMPARISON OF CRACK PROPAGATION PREDICTIONS FROM FULLY DYNAMIC ANALYSIS WITH QUASI-DYNAMIC ANALYSIS FOR A STANDARD DCB SPECIMEN WITH $K_D = K_{IC}$

point is a very considerable underestimate--the fully dynamic theory always predicts that the crack would propagate well beyond the crack arrest point determined by a static approach. In fact, the static theory would always predict crack arrest within the DCB specimen under wedge loading conditions. This can be seen from Equation (3.6-31) which shows that $K \to 0$ as $a \to L$. However, many experiments in which the crack completely penetrates the specimen without arresting under wedge loading conditions have been performed. This fact further distinguishes between the static and the fully dynamic analysis procedures. The latter does not suffer from this limitation, as can be seen in the computation shown in Figure 3.6.3(b) where the crack did not arrest.

The comparative arrest point predictions made with the fully dynamic and the static approaches for the standard DCB test specimen are summarized in Figure 3.6.4. It is again clear that the static theory gives a possibly dangerous overestimate of the capacity of a structure to arrest a crack. This reemphasizes the conclusion stated above that the investigation of systems designed to arrest a rapidly propagating crack must be conducted within the framework of a fully dynamic crack-propagation theory.

The physical reason for the inadequacy of the static and quasi-dynamic approaches to predicting crack arrest can be seen in Figure 3.6.5. This figure shows the distribution of the energy contained in the test specimen during the run-arrest process for the calculation shown in Figure 3.6.3(a). Because no external work is supplied to the specimen with wedge-loading conditions, as the fracture energy is removed (at a constant rate due to the assumption that $K_D = K_{IC}$), the total energy to be partitioned into strain energy and kinetic energy steadily diminishes. It can be seen that while the strain energy generally decreases (as in the static situation), the kinetic energy initially increases, reaches a maximum, then decreases almost to zero.

Comparison with the results shown in Figure 3.6.3(a) reveals that the statically calculated arrest point is reached at about the same point that the kinetic energy reaches a maximum in the fully dynamic calculation. This indicates that it is the return of kinetic energy to the crack tip that is the primary source of difference between the static and fully dynamic approaches.* The average rate of change of the kinetic energy being greater (negatively) than the strain energy after the maximum has been reached further reveals that the kinetic energy actually provides the greater contribution to the crack driving force, cf, Equation (3.6-21).

The practical conclusion that can be drawn from these calculations is the following. When a crack arrester system is to be used in a ship hull or any other engineering structure, the dynamic amplification of the crack driving force is an important consideration in the design. This increase is primarily due to the return of kinetic energy to the crack tip and, in turn, this is a function of the geometry of the structure. One practical way of accounting for this effect that could be used in the engineering design process is by the concept of a "dynamic amplification factor", a multiplicative geometry-dependent factor which could be incorporated into an otherwise completely static fracture-mechanic analysis.

---

* The dynamic and static strain energies will also contribute to a difference but this is apparently less important.

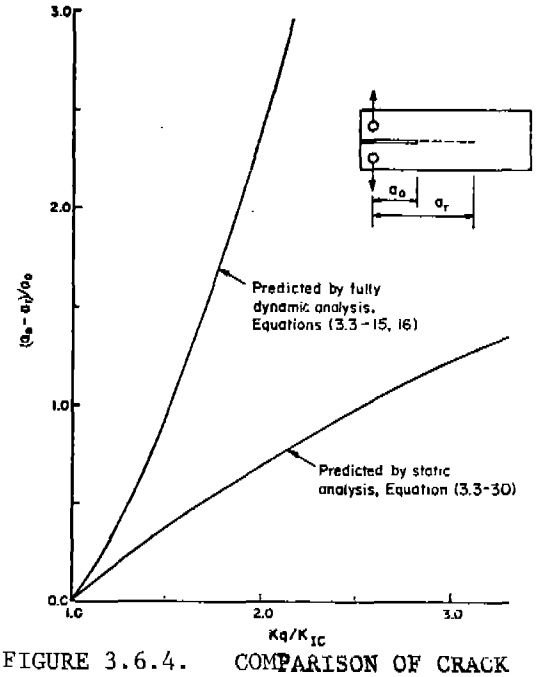

FIGURE 3.6.4. COMPARISON OF CRACK ARREST POINT IN A DCB TEST SPECIMEN WITH STATIC AND WITH FULLY DYNAMIC ANALYSIS

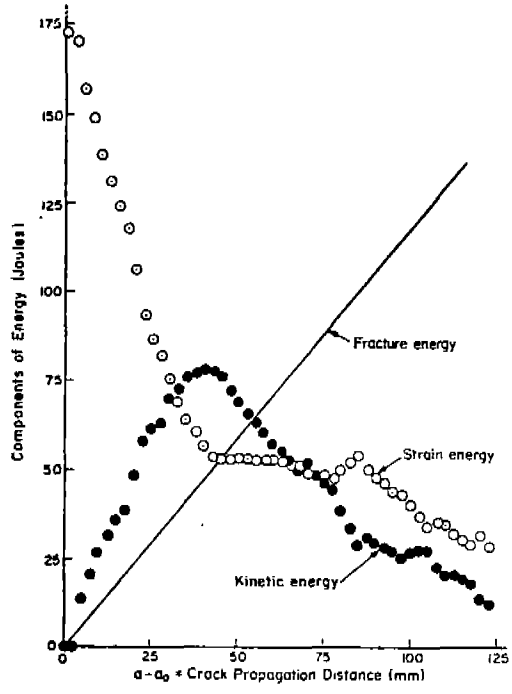

FIGURE 3.6.5. DISTRIBUTION OF ENERGY DURING RAPID CRACK PROPAGATION IN A DCB TEST SPECIMEN FOR K_q/K_{IC} = 2.0 AND $K_D = K_{IC}$

Very large monolithic structures will return no kinetic energy and, hence, will have a dynamic amplification factor of unity. The DCB test specimen is a highly efficient utilizer of kinetic energy and, consequently, will have a relatively high dynamic amplification factor, e.g., approximately two. A structure like a ship hull might be expected to have a value close to unity, but this cannot be established without further work. It might be anticipated that the manner in which the arrester is attached to the base plate may have a large effect on the dynamic amplification factor, perhaps as much as the structural configuration itself.

Finally, for comparison with the calculations reported in Section 6, the results given in Figures 3.6.6 and 3.6.7 are of interest. In Figure 3.6.6 are shown the average crack speeds calculated for crack propagation in the standard DCB specimen without arrester as a function of the stress-intensity factor at the initiation of crack growth. [The difference between the average speed during the initial phase of growth and the average speed over the entire event can best be seen in Figure 3.6.3(b)]. These can be viewed as input to the problem found by the designer of a crack arrester system. The results shown in Figure 3.6.7 typify the kind of information that is available to him in doing his job, albeit for a wedge-loaded DCB specimen. That is, given an anticipated crack speed or, equivalently, a K_q value, Figure 3.6.7 provides an obvious way of estimating the toughness required of an integral "high-toughness" strip crack arrester using a static approach. Some example calculations showing how this process would be performed, together with further illustrations illustrating the over optimism of the results given in Figure 3.6.7, are given in Section 6 of this report.

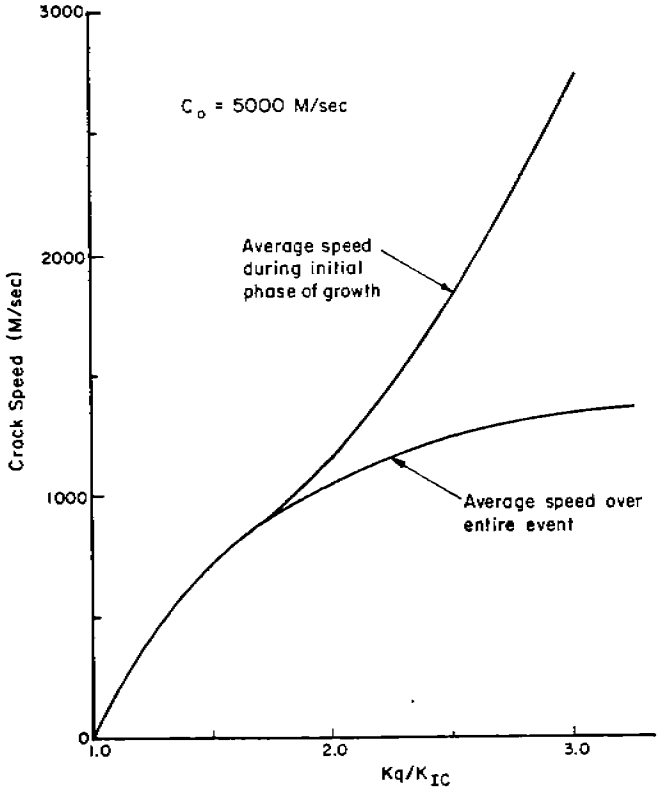

FIGURE 3.6.6. CRACK SPEEDS IN THE DCB TEST SPECIMEN CALCULATED BY A FULLY DYNAMIC ANALYSIS AS A FUNCTION OF THE STRESS INTENSITY AT INITIATION OF GROWTH

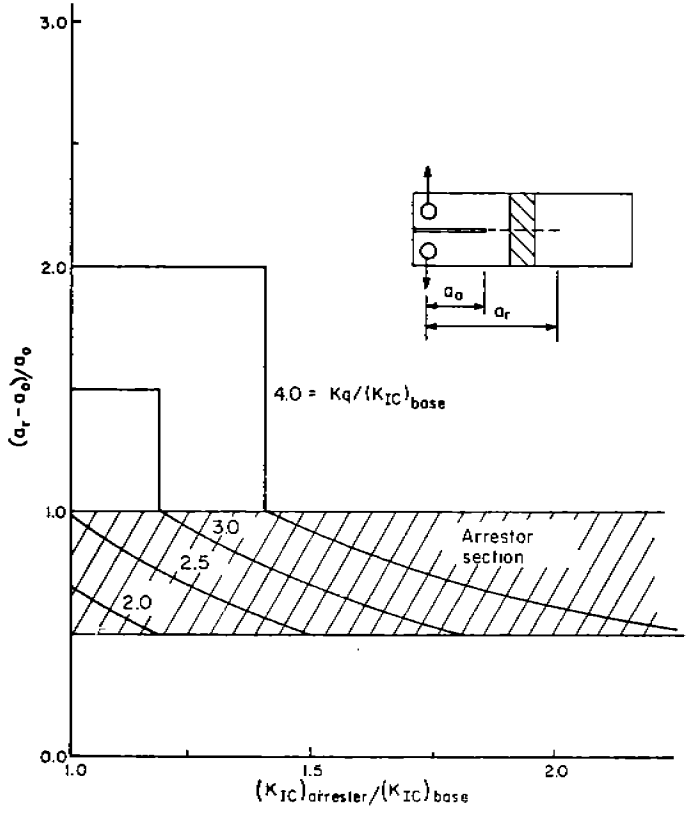

FIGURE 3.6.7. CALCULATED CRACK ARREST POINT IN DCB SPECIMENS WITH HIGH-TOUGHNESS ARRESTER USING A STATIC ANALYSIS

4.0 FATIGUE-CRACK PROPAGATION

4.1 INTRODUCTION

This section is concerned with fatigue-crack growth in ship hulls and with the effect of crack arresters on crack growth. In order to facilitate the discussion, the concepts of crack-growth analysis and stress-history effects will be briefly discussed first. Thereafter, the procedure for analysis of service cracks will be considered. Finally, fail-safe design practice and arrester efficiency will be discussed.

Fatigue-crack-growth analysis of damage-tolerant structures has to deal with both prearrest and postarrest behavior. In the prearrest period, the crack may grow from a small initial flaw to a size that causes fast unstable crack propagation. This period is of interest if attempts are made to prevent cracks from reaching a critical size by means of periodic inspections. If unstable crack growth and arrest occurs, the postarrest behavior is of interest. The long arrested crack will extend by subsequent cyclic loads. It should not grow to a size that would again cause fast fracture during a relatively short postarrest period required to complete the voyage and dock the ship for repair of the arrested partial failure. Both prearrest and postarrest crack growth will be considered in this section.

4.2 CONCEPTS OF CRACK GROWTH ANALYSIS

The concept of crack-growth analysis is now well known. Its application to ship structures has been the subject of a recent study of the Ship Structure Committee [70]. Therefore, the basic concept will be discussed only briefly here.

Fatigue-crack growth is governed by the range of the stress-intensity factor (ΔK) during a cycle. Generally, the rate of crack propagation can be expressed as

$$\frac{da}{dN} = f(\Delta K, R) \quad , \tag{4.2-1}$$

where a is the crack size, N is the cycle number, and R is the ratio between the minimum and maximum stress in a cycle. Many forms have been proposed [71,72,73] for Equation (4.2-1). For the purpose of the present discussion, it is sufficient to use the simple relationship

$$\frac{da}{dN} = C\Delta K^n \tag{4.2-2}$$

which is applicable to many steels for a limited [71] range of ΔK, with n on the order of 3, and R = 0 (i.e., the minimum stress in each cycle is zero).

The crack-growth properties of a material can be determined by using a simple specimen for which a K-solution is known. Center-cracked specimens are often used, for which

$$\Delta K = \Delta \sigma \sqrt{\pi a} \qquad (4.2\text{-}3)$$

if the crack is small compared to the specimen [72] size. In this equation, $\Delta\sigma$ is the range of the nominal stress in a cycle. The specimen is subjected to cyclic loading and crack growth is recorded. The increment of crack growth per cycle provides the crack-growth rate da/dN which can then be plotted as a function of ΔK. According to Equation (4.2-2), the result will be a straight line on double-log paper.

The prediction of crack growth in a structure then requires a calculation of the stress-intensity factor for the given structural geometry with a crack at the critical location. Using this stress intensity, the crack-growth rate can be determined from the da/dN-ΔK plot. An integration over a range of crack sizes provides the crack-growth curve, i.e., crack size as a function of the number of cycles.

4.3 STRESS-HISTORY EFFECTS

The analysis of the growth of service cracks is complicated by a number of factors. The most prominent of these is the service stress history. Ship hull stresses vary randomly as a function of payload distribution and weather. For a crack-growth analysis, the service load history may be described by its root mean squares (rms) value, its power spectrum, or its excedance spectrum.

If crack-growth calculations have to be based on the rms value, random-load crack-growth data have to be available. This is usually not the case. If the analysis is based on the spectrum, some stress history has to be assumed and the crack-growth integration as described in the previous section is to be based on the stresses in the assumed history. Computer routines for such an analysis are available, especially in the aerospace industry.

In some materials, the occurrence of high-stress cycles has a drastic effect on crack growth during subsequent cycling at lower amplitudes [74,75,76] During a high-stress cycle, a relatively large plastic zone develops at the crack tip. Due to its permanent stretch, the material in this zone does not fit normally in its elastic surrounds after unloading. As a result, it will be under a compressive residual stress. This means that the general stress level at the crack tip region is lowered, so that subsequent crack growth is slowed down. This effect is called retardation. It is illustrated in Figure (4.3.1).

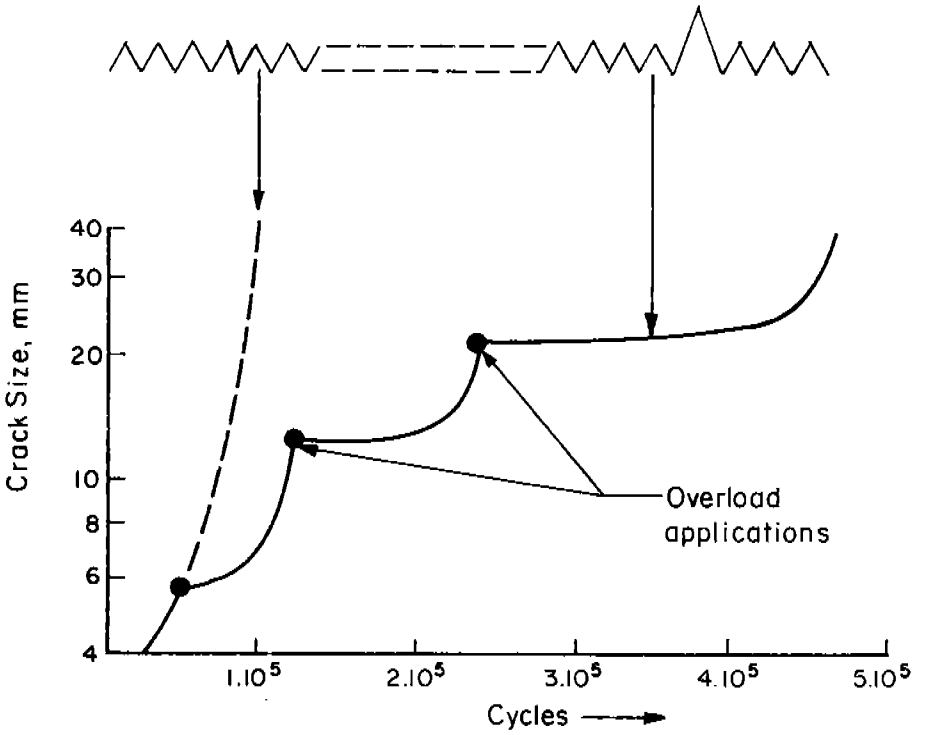

FIGURE 4.3.1. RETARDATION OF FATIGUE CRACK GROWTH DUE TO OVERLOADS

Models have been developed [77,14] to account for the retardation behavior in the crack-growth integration procedure. At present, no information is available on whether retardation is a significant factor in ship steels subjected to a ship-stress spectrum. Therefore, a crack-growth analysis would conservatively neglect retardation. However, it is worth exploring whether the beneficial effect of retardation can be counted on in ship hull cracking. Since retardation is usually more pronounced in higher strength materials, it would become of special importance for modern high-strength ship steels.

4.4 ANALYSIS OF SERVICE CRACKS

The prediction of crack growth in service requires the following steps:

- Analysis of the structure and structural details to define critical locations
- Stress analysis of the structural details to determine the stress-intensity factor for a crack at the critical location
- Establishment of service stress history at the location of the crack
- Determination of material crack-growth properties, taking into account the different crack-growth rates in weld material and heat-affected zone if relevant to the crack problem under consideration
- Integration of crack growth, either cycle-by-cycle, or blocks of cycles for a small increment of crack growth.

Each of these steps was discussed in some detail in the previous paragraphs. Only the stress analysis to arrive at the stress-intensity solution will be briefly considered in the following paragraphs.

A reliable stress-intensity solution is even more important for fatigue analysis than for residual strength analysis, because fatigue-crack-growth rates vary with the third or fourth power of ΔK. Not only nominal stresses are of importance, but also local stresses due to stress concentrations and residual stresses.

The nominal stress can be obtained from a global-stress analysis or finite-element analysis. These can be applied to a finite-element analysis of a structural detail containing the crack to include local stress concentrations, e.g., in weld fillets and cutouts. Although techniques exist to include residual stresses, the complexity of the problem may make a detailed analysis prohibitive. (Residual stresses at the crack tip due to high-stress cycles would be automatically accounted for in the crack-growth integration procedures if a retardation model is used.)

Proper modeling of structural details is more important if the critical crack size is small. In that case, most of the useful crack-growth life is spent while the crack is still influenced by the stress concentration at its initiation site. Careful detail design will be aimed at reducing stress concentrations. This has the advantage that (1) the growth of small cracks will be slower and (2) the critical crack size will be larger. It implies that a significant part of the useful crack-growth life is spent while the crack tip is well away from the initial stress raiser.

From the point of view of safety, large critical crack sizes are preferable because there is a better chance of timely crack detection. In that case, the time spent in the small crack region is of less interest. Since only the growth of relatively large cracks has to be considered, the modeling of the initial stress raiser and of the residual stresses become less critical.

4.5 FAIL-SAFE CONCEPTS

Safety requires that a structure can still withstand an appreciable load under the presence of cracks or failed parts. It also requires that

- Either the damage can be detected before it reaches a dangerous size
- Or that damage growth is so slow that it never reaches a dangerous size through the specified life
- Or the structure is provided with means to arrest a crack when the damage has reached the critical size that causes unstable growth. Sufficient remaining crack-growth life should then provide some time for corrective action.

In each case, fatigue-crack growth is of importance. Consider the crack-growth curve in Figure 4.5.1. Suppose the structure contains an initial defect of the size a_i. If the crack were not to grow critical within a lifetime, the maximum life of the structure would be t_L. In order to calculate this life, the growth of small cracks would have to be considered involving the difficulties discussed in the previous section.

If the inital defect size happended to be a^* instead of a_i (Figure 4.5.1), the life to critical would be much shorter. In view of this risk, a large safety factor would have to be taken on t_L, or, more realistically, one can provide for crack arresters that would limit the risk of a critical crack.

Stretching this idea further, one might entirely rely upon crack arresters and not be concerned about the point in time they might become effective. However, an unstable crack might still cause considerable damage. It would be advantageous if a crack could be detected and repaired before it grows to a critical size. This would require

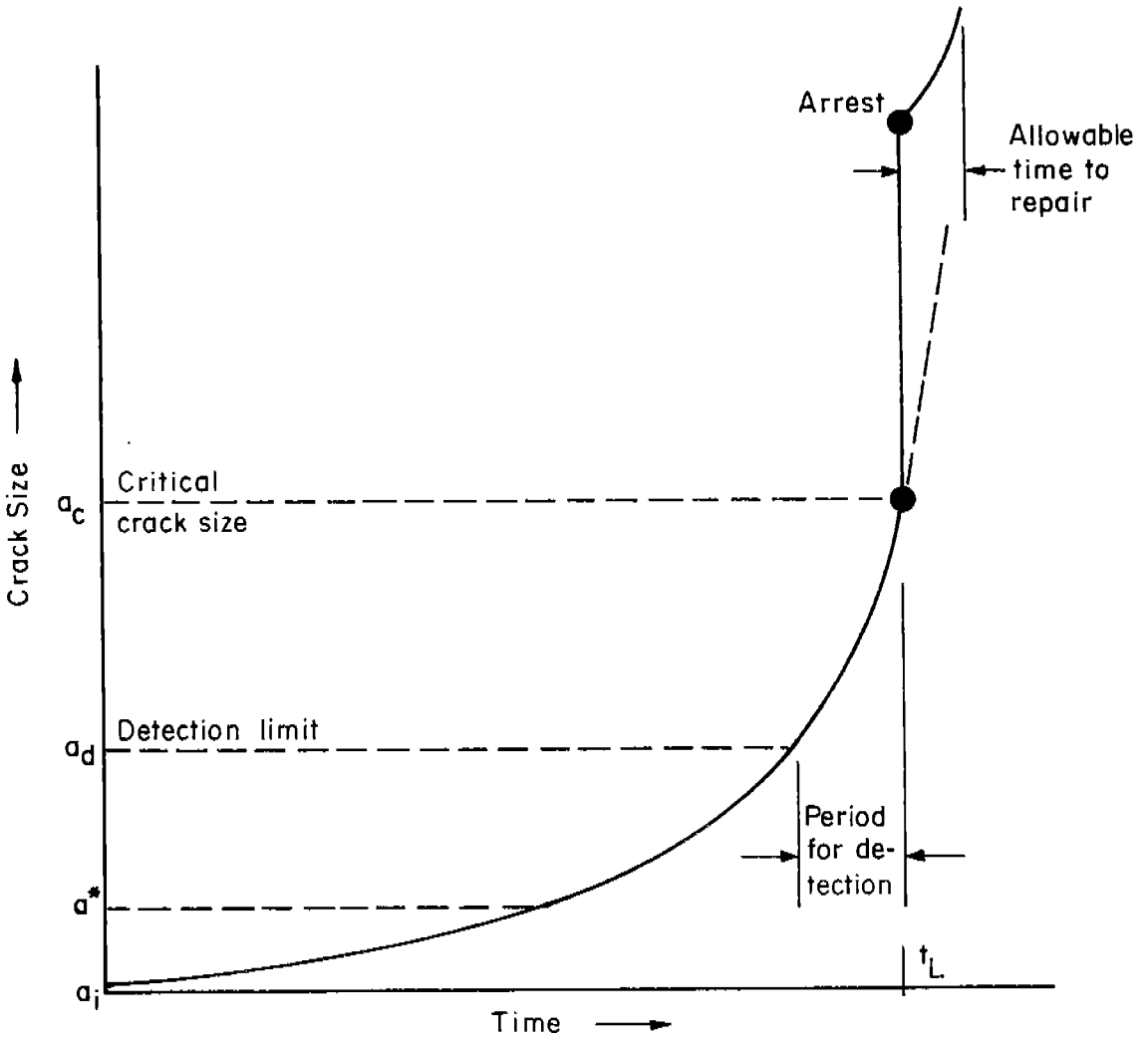

FIGURE 4.5.1. CRACK GROWTH AND FAIL-SAFETY

- Periodic inspection which may not always be feasible
- Easily detectable cracks; i.e., large critical crack size and a long period for detection
- Scheduling of inspections on the basis of a calculated crack-growth curve in the region a_d to a_c (Figure 4.5.1).

If the critical crack size is large and crack growth is slow, the detection limit a_d may be rather large. This would imply that inspection requirements could be less stringent. Also, crack-growth calculations would be less difficult because cracks in the range a_d-a_c would be large enough not to be affected too much anymore by the stress concentration at the initiation site.

In the case fast crack growth and arrest do occur the rate of crack growth after arrest is of interest for the safety during the rest of the voyage until docking for repair. Since a postarrest crack will be large, fatigue-crack-growth rates may be high. This asks for rather accurate information on postarrest behavior.

In order to obtain an appreciation of the time involved in crack propagation, a simple and rough estimate was made of a crack-growth curve for a ship hull. A through crack in a deck is assumed at a location not directly affected by other structural members. Two stress spectra were considered,[10] one for the Wolverine State and the other for the Minnesota. Figure 4.5.2 shows the spectra together with the stepped approximation used for the crack-growth analysis.

Since reliable crack-growth data for ship steel were not available, the $da/dN - \Delta K$ relation was assumed as in Figure 4.5.3. The spectrum was divided in blocks of 0.1 year and crack growth was calculated for 0.2-inch crack increments for the small crack region and 1-inch increments for the large crack region. No retardation was considered. The results are shown in Figure 4.5.4.

It turned out that crack growth was largely determined by the low-stress cycles. This is the reason why crack growth for the Minnesota spectrum is slower than for the Wolverine State spectrum, since the latter contains many more low-amplitude cycles.

A typical value for the toughness at low temperature would be[8] 60 ksi $\sqrt{\text{in.}}$. Taking 20 psi as the highest stress in the spectrum, the critical crack size would be $2a = 2 \cdot 60^2/\pi \cdot 20^2 \approx 5.7$ in. If the detectable crack size were 3 inches, the period for crack detection would be 3 years for the Minnesota and 0.5 years for the Wolverine State. These times are long enough to conclude that a fail-safe approach based on crack growth may be feasible.

4.6 CRACK ARRESTERS AND FATIGUE

Despite the increasing amount of literature on crack arresters in ship hulls, no information was available on the interaction of fatigue cracks with

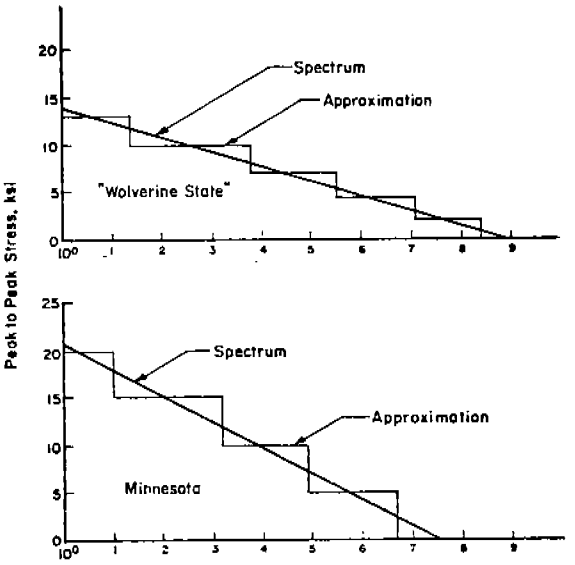

FIGURE 4.5.2. STRESS EXCEEDANCE SPECTRA FOR TWO SHIPS, EACH FOR 20 YEARS EXPERIENCE

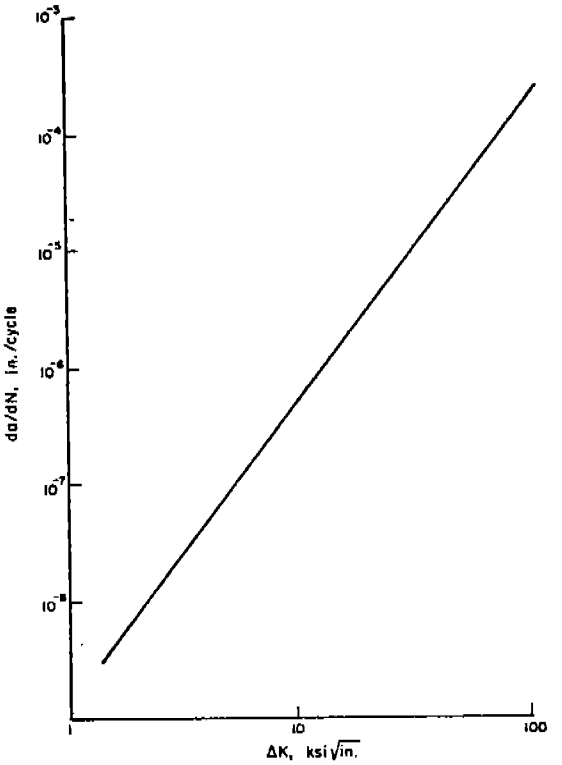

FIGURE 4.5.3. ASSUMED CRACK RATE PROPERTIES FOR CRACK-GROWTH CURVES IN FIGURE 4.5.2

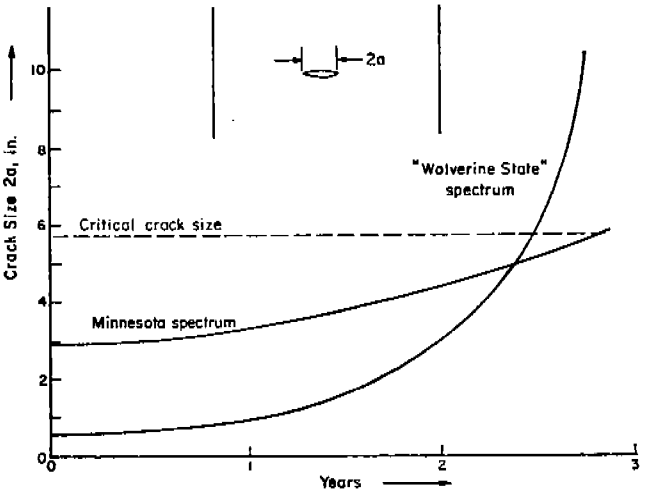

FIGURE 4.5.4. HYPOTHETICAL CRACK GROWTH CURVES CALCULATED IN THE BASIS OF TWO SHIP SPECTRA

crack arresters. Therefore, this discussion will be based on analysis and data for aircraft materials and aircraft structures. Only some general observations will be made with regards to ship structures.

Arrester configurations conceived so far can be categorized as

(1) arresters that decrease the stress intensity

(2) arresters that increase the toughness.

In both cases, a fast growing crack is fully arrested because the crack-driving force falls below the critical value (with or without dynamic effect considered). A fatigue crack approaching an arrester of these types will not be arrested. It will merely slow down. If the arrester is a patch or a stringer, the K-reduction may be quite large. Fatigue-crack-growth rates will be much lower, because they vary with the third or fourth power of ΔK. If the arrester is a high-toughness insert and has fatigue-crack-growth properties better than the primary structure, there will be a deceleration. Since the various kinds of steels do not show largely different fatigue-crack behavior, the slow-down will likely be less effective than for the arresters of Type 1.

The stress-intensity factor reduction for a crack arrester can be calculated. The da/dn-ΔK diagram then shows the reduction in crack-growth rate. Rate prediction on this basis has been found well in agreement with experimental data for aircraft stiffened panel structures. As an example, consider the results of Poe [51] given in Figures 4.6.1 and 4.6.2.

Figure 4.6.1 shows the prediction and the test data for a panel with riveted stringers. The crack-growth rate is plotted as a function of crack size. The dashed lines show what the growth rates would be in the absence of stringers. The solid lines show the prediction for the stiffened panel. If the crack tip is close to the stringer, the reduction in the stress-intensity factor is the largest (which would cause a fast running crack to arrest there). As a consequence, the largest reduction of fatigue-crack growth rates also occurs in this region. Also shown in Figure 4.6.1 is the integrated crack-growth curve (right scale) which clearly reflects the results of the deceleration of growth.

Figure 4.6.2 presents similar results for an integrally stiffened panel. The reduction in stress intensity is much less in this case, so the stiffeners are less effective. In addition, the fatigue crack can directly penetrate the stiffener which further reduces its effect.

It appears that crack arresters can have a significant influence on fatigue-crack growth. However, it is questionable whether this is always effective for ships. Crack arresters in ship hulls will be relatively wide spaced. This means that there is more chance that fatigue cracks will develop at locations remote from the arrester than close to the arrester. Only if they develop in a region close to an arrester can they benefit from the K-reduction. In the case of welded arresters, the fatigue crack will penetrate the arrester thus reducing its efficiency. If the arrester is far away, the crack will reach a critical size before it comes into the vicinity of the arrester and can benefit

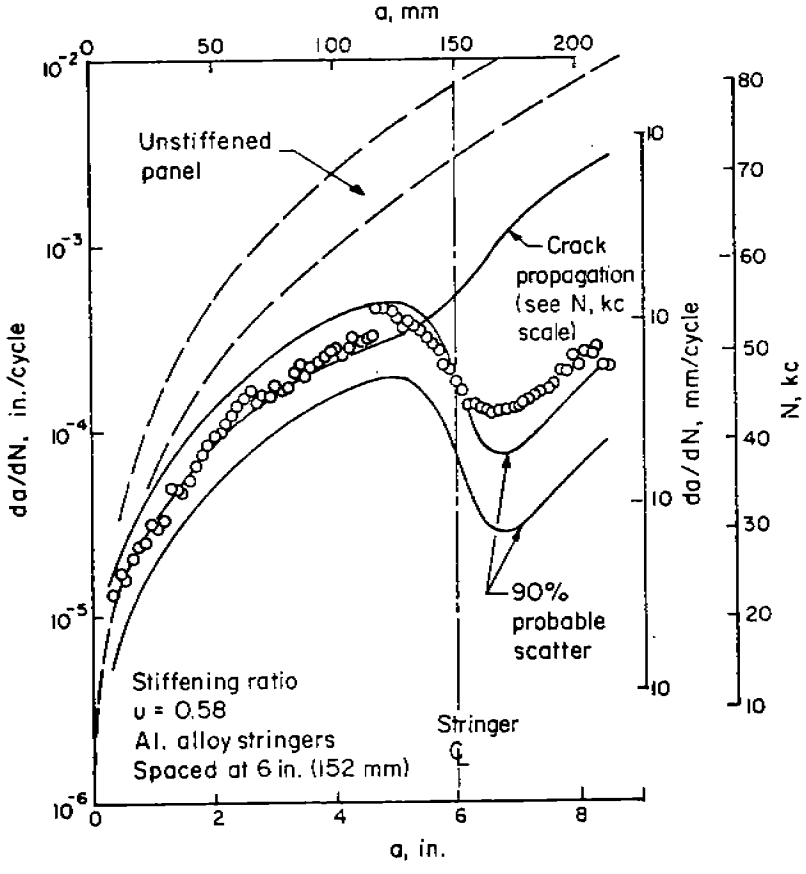

FIGURE 4.6.1. FATIGUE CRACK GROWTH IN STIFFENED PANEL ACCORDING TO POE[51]

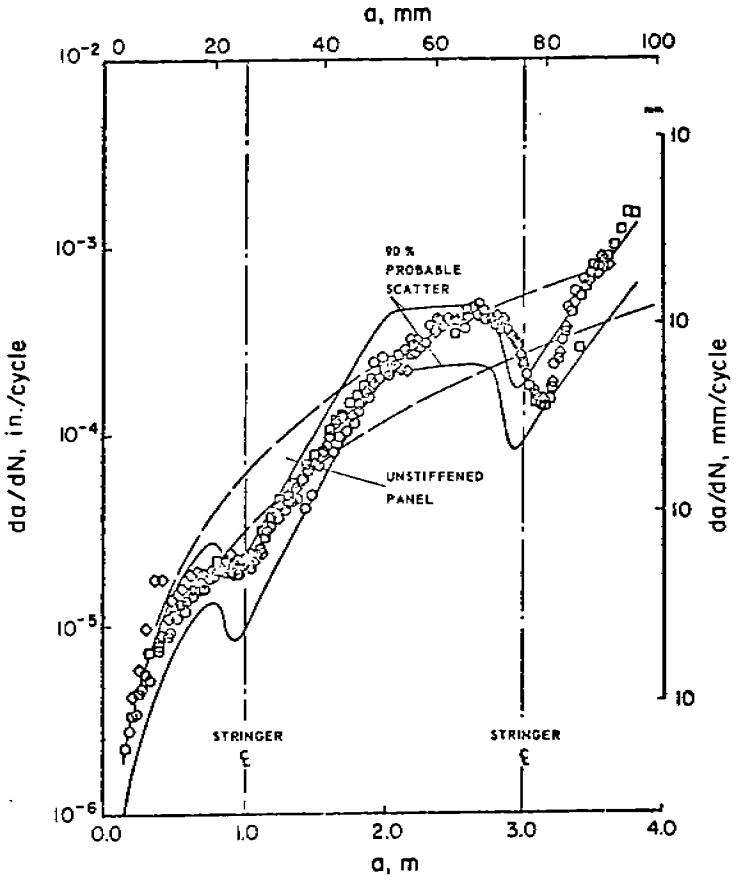

FIGURE 4.6.2. FATIGUE CRACK PROPAGATION IN INTEGRALLY STIFFENED PANEL ACCORDING TO POE[51]

from the K-reduction. In the case of welded arresters, the fatigue crack will penetrate the arrester thus reducing its efficiency. If the arrester is far away, the crack will reach a critical size before it comes into the vicinity of the arrester and can benefit from it. In the example in the previous section, the critical crack size was on the order of 6 inches.

The significance of arresters for fatigue-crack growth is most likely in the postarrest behavior. After instability and arrest, the arrester may be effective to sufficiently decrease growth rates to allow completion of the voyage until repair. In that case, the tough material insert will not largely reduce fatigue-crack-propagation rates. However, in the case of riveted arrester strips the postarrest fatigue crack would fully benefit from the growth rate reductions shown in Figure 4.6.1.

As pointed out in Section 3.5, the reduction of the stresses in the hull would occur at the expense of high stresses in the arrester strip. These stresses may be so high that the arrester strip has only a very short fatigue life. If it would fail by fatigue, it would cause immediate fast fracture of the hull, because it would no longer act as an arrester. Therefore, a complete analysis of postarrest behavior should include fatigue analysis of the arrester strip. It is recommended that complete prearrest and postarrest analyses be made of some realistic structures with arresters, to obtain definitive information of these matters and to evaluate the feasibility of arrester systems from the point of view of fatigue and fatigue-crack propagation.

5.0 CHARACTERIZATION OF ARRESTER MATERIALS

The design of in-plane, energy-absorbing arresters, specifically--the selection of optimum arrester width, thickness, spacing and material combinations--requires the measurement of the fracture energy or toughness values of candidate materials. In this section, estimates are made of the minimum toughness levels required of steels for this class of arrester. Generally, the toughness levels are found to be high, and at or near the upper shelf. Some of the problems associated with measuring large fracture toughness values are described, along with possible ways to overcome these problems. The arrester toughness requirements recommended by Rolfe, et al.[5], in terms of dynamic tear (DTE) energy are compared with estimated minimum K_D requirements. Finally, currently available toughness data for ship steels are compared with estimated requirements for arresters.

5.1 ESTIMATE OF K_D (OR K_c) FOR ARRESTER MATERIALS

It is instructive to make a rough estimate of the toughness levels that are required of in-plane arresters. This is most easily done for the case of a plate that is large relative to a propagating centrally located crack bounded by two arresters of the same thickness as the base plate, as shown in Figure 5.1.1. The calculation can presently be made only for assumed values of φ, the fraction of the kinetic energy imparted to the structure that is returned to the crack tip prior to arrest. However, two-dimensional, finite difference dynamic analyses have recently been developed[28] and could be used in the future to evaluate and solve more complex problems.

Combinations of the minimum values of fracture energy R_{AP}, fracture toughness $K_{D,AP}$, and the width W of the arrester plate which will stop the largest crack accommodated by the arrester spacing 2S are given by the following expressions which are derived in Appendix A.

$$W = S\sqrt{\varphi} \tag{5.1}$$

$$R_{AP,minimum} = \frac{\sigma^2 \pi S}{E}\left(1 + \sqrt{\varphi}\right) \tag{5.2}$$

$$K_{D,minimum} = \sigma\sqrt{\pi S}\left(1 + \sqrt{\varphi}\right)^{1/2} \tag{5.3}$$

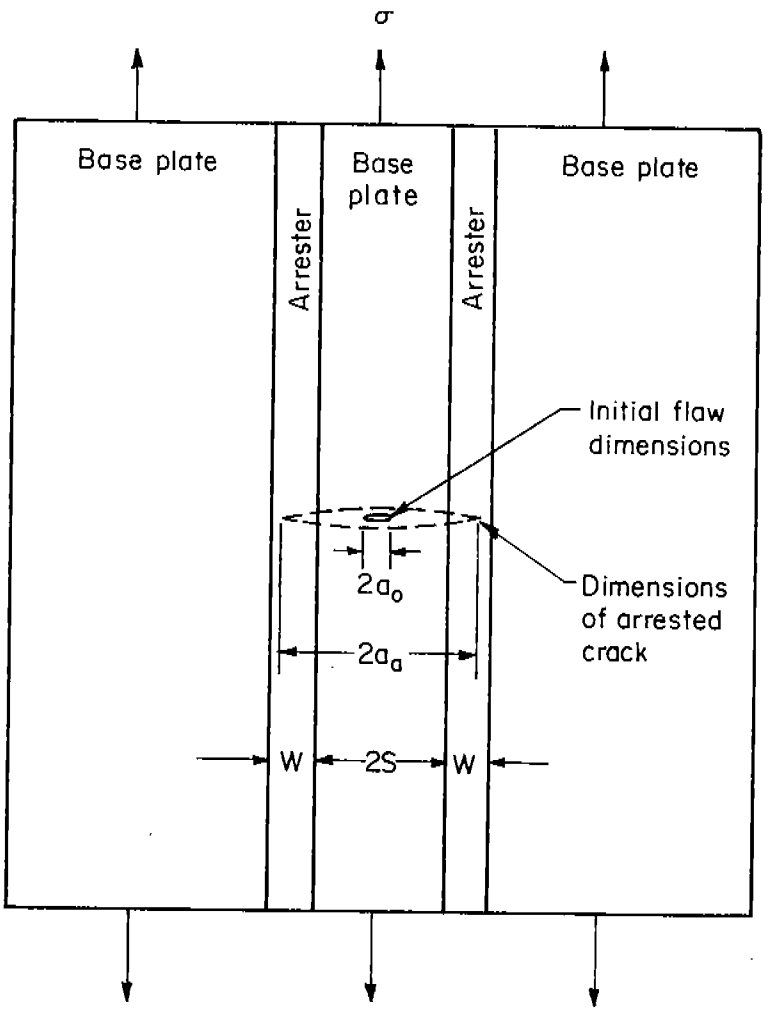

FIGURE 5.1.1. SCHEMATIC REPRESENTATION OF A LARGE, UNIFORMLY STRESSED PLATE WITH TWO WELDED-IN, IN-PLANE, CRACK ARRESTERS OF THE SAME THICKNESS AS THE BASE PLATE

Arresters with fracture energy or toughness values smaller than the minimum values will not stop a crack irrespective of their width. Equation (5.1) indicates that very narrow arresters are adequate when there is little or no kinetic energy return. However, even then the arrester must be wide enough to contain the most heavily deformed part of the crack tip plastic zone ($\sim$ 1-5 cm in radius). Residual stresses and low-toughness values in the region of the HAZ as well as the integrity of the welds will also place lower bounds on the arrester width.

Estimates of the minimum arrester plate toughness values for different spacings and three assumed levels of kinetic energy return derived from the above equation are given in Figure 5.1.2. The toughness requirements increase with the fraction of kinetic energy returned. The requirements derived by Kihara, et al.[6] from their large-scale arrester model test (see Figure 5.3.1) are also included. These are based on static analyses corrected for dynamic effects by way of the empirical, effective-crack-length-correction discussed in Section 3.3. Since the effective crack length is smaller than the true crack length at arrest, the Kihara requirements are even less conservative than the ones derived here for 0% kinetic energy return. Although both sets of estimates make provisions for dynamic effects, the estimates are only accurate for the specific geometry and loading conditions for which they were derived†. For other configurations and loading conditions they represent rough guidelines to the toughness levels required of in-plane arresters.

It is evident from Figure 5.1.2 that the toughness requirements for in-plane arresters can be quite high. For example, if $\sigma = 150$ MN/m^2 and $2S = 6$ meters, and $\varphi = 0.5$, then $K_{D_{min}}$ is about 600 MNm$^{-3/2}$. Lower applied stresses and closer spacing of arresters could reduce this requirement. Probably, the lowest reasonable value of toughness to arrest a running crack in a ship hull, assuming requirements intermediate between those of Kihara and the ones given here for $\varphi = 0.5$, $\sigma = 100$ MN/m^2 and $2S = 3$m, appears to be $K_D = 200$ MNm$^{-3/2}$. This estimate is for an arrester of the same thickness as the base plate. The same arresting capability could be achieved with a toughness level as low as $K_D = 140$ MNm$^{-3/2}$ by fashioning a double-thick sandwich consisting of 2 arrester plates each as thick as the base plate. These levels of toughness are only obtained well above the transition temperature where the fracture is accompanied by appreciable plastic flow.

† The Kihara, et al, requirements reflect the test piece dimensions and the compliance, mass and other features of the loading system used in the large-scale tests. The present calculations are approximately valid for plate dimensions that are large compared to the crack.

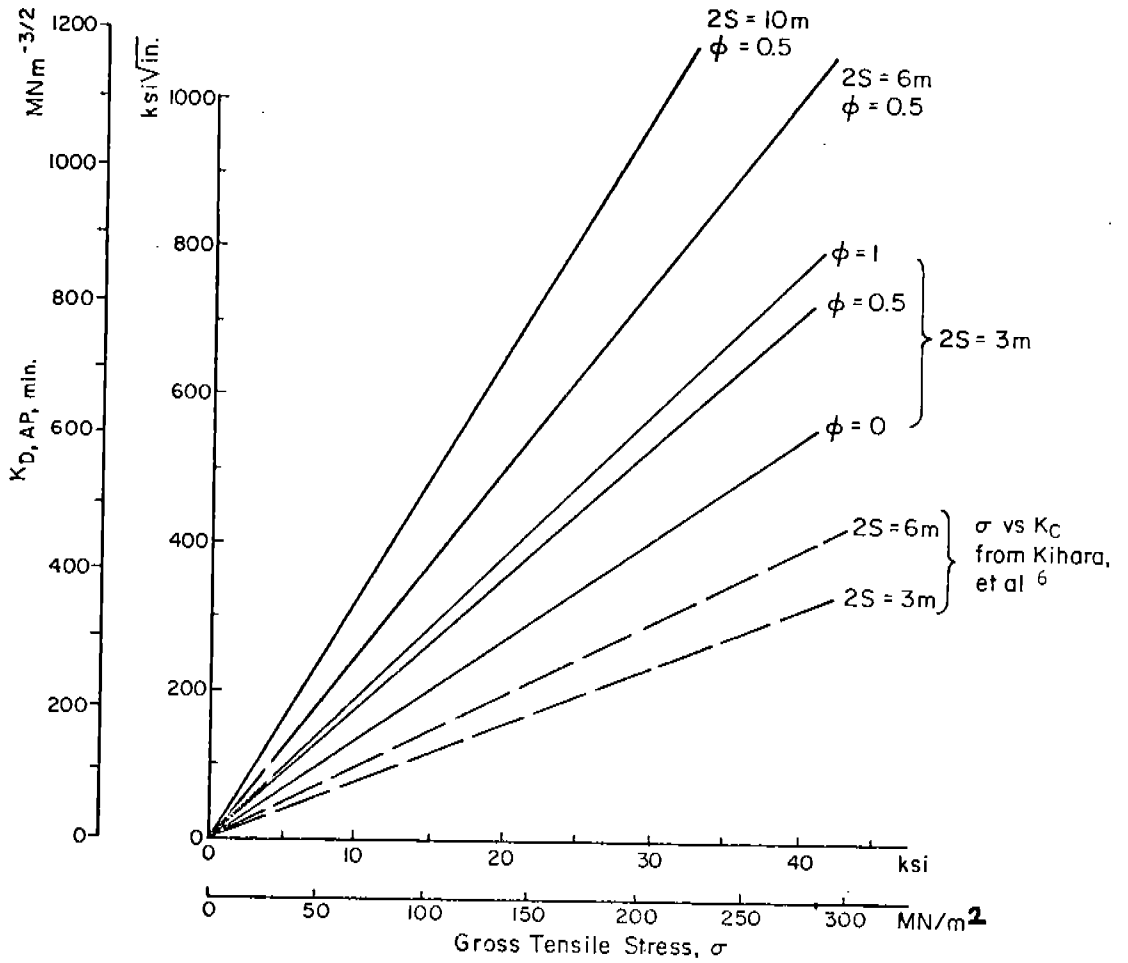

FIGURE 5.1.2. ESTIMATED MINIMUM K_D REQUIREMENTS FOR ARRESTER STEELS BASED ON EQUATION (5.3)

Figure 5.1.2 also reveals the consequences of employing higher strength steels in ship construction. If the yield strength of the steel is doubled, it is likely that both the operating stresses and the minimum K_D requirement will be doubled for a particular arrester spacing. Whereas for ordinary strength arrester steels (σ_y = 275 MN/m^2) $K_{D,min}$ should be about 200-400 MN$^{-3/2}$, the requirement for higher strength steels (σ_y = 550 to 700 MN/m^2) should be a $K_{D,min}$ about 400 to 1000 MNm$^{-3/2}$. These high-toughness values are difficult to realize in practice because of the general trend toward decreasing upper shelf toughness with increasing yield strength levels. As noted above, a multiple thickness sandwich of arrester plates can raise the crack stopping capabilities of arresting devices in these cases.

5.2 MEASURING K_D VALUES OF TOUGH-ARRESTER STEELS

From considerations described in Section 5.1 it appears that the minimum required K_D values for arrester steels of ordinary strength (275 MN/m^2 yield strength) are in the range from 200 to 400 MNm$^{-3/2}$, depending on arrester spacing and service stresses. Doubling of the yield strength (and the service stresses) will double these minimum K_D requirements.

Certain problems exist in the measurement of such high levels of fracture toughness. The most highly developed methods for measuring fracture toughness are applicable to fractures in which plasticity is limited--for example, fractures that occur under plane-strain conditions or under plane-stress conditions in which the plastic zone size is small relative to specimen dimensions and crack length (see ASTM-E-399-74). Because of the limited plasticity, these fractures can be analyzed by the methods of linear elastic fracture mechanics (LEFM) to obtain plane-strain fracture-toughness parameters such as K_{Ic}, K_{Id}, K_{ID} and K_{Ia}, and their plane-stress counterparts with the I removed from the subscript. The limited fracture plasticity that is necessary for successful applicationof LEFM methods is the very antithesis of the desired behavior of arrester steels, where large plastic zones and significant shear lips are essential to proper performance. Accordingly, problems arise in attempting to use LEFM methods for measuring fracture-toughness parameters of tough materials.

In the following paragraphs, several methods for measuring or approximating K_D values for tough steels by the methods of fracture mechanics are described.

5.2.1 Approximating K_D Values with K_c, K_{Ic}, or J_{Ic} Measurements

As noted in Section 3.2, $K_{D,min}$ may coincide with K_c (the K_c-value at zero velocity) for tough steels since these fracture with the

fibrous mode. In this case, static measurements of K_c can serve as a conservative estimate of K_D. The K_c-values can, in turn, be related to the plane-strain K_{Ic}:

$$K_c = C_1 K_{Ic} \tag{5.4}$$

where $1 < C_1 < 2$ [34,35,36]. This means that K_{Ic}-values could also serve as a lower bound measure of K_D or as a way of estimating K_c provided the factor C_1, is known. In practice, the plate size and thickness requirements for measuring K_c and K_{Ic} values for materials with $\frac{K_c}{\sigma_y} \gtrsim 0.2\text{m}^{1/2}$ are prohibitive. For example, for a steel with a yield strength $\sigma_Y = 275\ \text{MNm}^{-2}$ and $K_c = 300\ \text{MNm}^{-3/2}$, the width of a center-cracked panel adequate to measure K_c is about 3m, and the thickness required to measure K_{Ic} is about 1 m. More recent J_{Ic} techniques offer the possibility of reducing the thickness requirement by an order of magnitude. [78] Consequently, J_{Ic} measurements may offer one practical route to the evaluation of K_D or R values of high-toughness ship plate for arresters.

5.2.2 Approximating K_D From Crack-Opening Displacement

Robinson and Tetelman [79] have shown that K_{Ic} can be calculated from measurement of the crack-tip opening displacement (COD) at the onset of unstable fracture in relatively small specimens, using the following relationship:

$$K_{Ic} = \left[\frac{\sigma_y \cdot E \cdot \text{COD}}{1-\nu^2}\right]^{1/2} \tag{5.5}$$

Methods for measuring COD are described in British Standards DD19:1972. Use of such COD techniques would then permit K_D to be approximated by way of Equation (5.4).

The possibility exists also of applying COD methods to dynamic tests. Here, actual COD measurements are difficult but Robinson and Tetelman have shown that COD values can be approximated reasonably well from measurement of notch-root-contraction (NRC) on the fractured test piece.

5.2.3 Direct Measurement of K_{ID} or K_D With Battelle Duplex Double-Cantilever-Beam Test

A test has been developed at Battelle specifically to measure the ability of various steels to arrest a rapidly propagating fracture. By making appropriate measurements during the test and by applying a dynamic analysis to the results, the LEFM parameters K_{ID} or K_D can be obtained directly from the test. To date, the test has employed a relatively small test piece to measure K_{ID} values for steels of moderate toughness. The test piece is basically a double-cantilever-beam (DCB) specimen that has been modified by attaching a high-strength/low-toughness "starter section" to the "test section" by means of an electron beam weld. It is further modified by introducing face-grooves along the fracture path. This arrangement, pictured in Figure 5.2.1 and referred to as a duplex DCB specimen, makes it possible to initiate a rapidly propagating crack at virtually any temperature, even above the transition temperature of the test plate. When the propagating crack penetrates the test section, energy is absorbed in the fracture process. If the test section has sufficient toughness, the crack will eventually arrest. Analysis of the data by the methods described in Section 3.0 permits calculation of K_{ID}.

There are several reasons why valid K_{ID} data can be obtained from relatively small duplex DCB specimens of moderately tough steels. First, the high-strength/low-toughness starter section reduces the plane-strain thickness requirements drastically. Second, the grooves along the fracture path develop constraints similar to those associated with increased plate thickness. Third, the propagating crack produces a very high strain rate at the crack tip, which causes the effective yield strength to be raised (perhaps twice the static yield strength) and the plastic zone size to be reduced.

Figure 5.5.2 shows measured values of K_{ID} obtained from duplex DCB specimens for several grades of ship steel tested near the nilductility temperature. The behavior of these steels is interesting from several standpoints. The toughness of each of the four steels is seen to be strongly dependent on crack velocity, being greatest at small velocities. Nonetheless, K_{ID} for a propagating crack exceeds K_{Id}, the energy associated with crack initiation by impact. There is some thought that the minimum in the K_{ID}-versus-velocity curve (if a minimum exists) may approximate the K_{Id} values but this remains to be demonstrated.

In principle, the duplex DCB test can be used also to obtain valid K_D data by eliminating the side grooves. However, for the specimen dimensions currently employed to measure K_{ID}, removal of the side grooves would introduce several problems, particularly for high-toughness steels. The amount of strain energy that can be stored in the arms of the test piece is not sufficient to drive the crack into

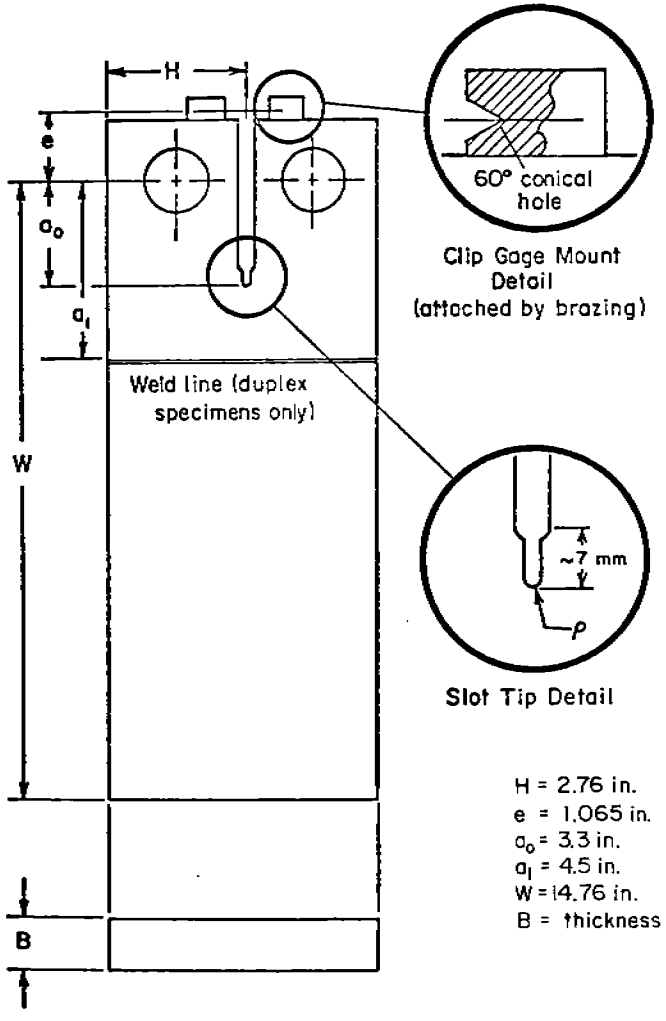

FIGURE 5.2.1. DCB-TEST PIECE CONFIGURATION; SIDE GROOVES ARE NOT SHOWN

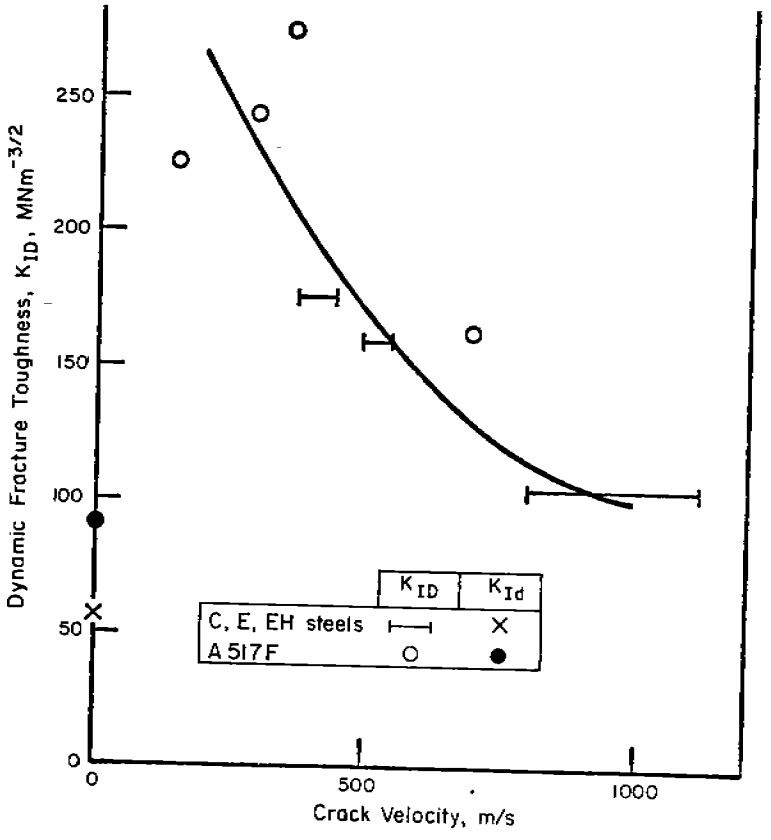

FIGURE 5.2.2. RELATION BETWEEN CRACK VELOCITY AND DYNAMIC TOUGHNESS FOR STEELS TESTED NEAR NDT.[62] Initiation Data from References 80 and 81

the tough test section for any appreciable distance, thus making analysis of the results difficult. With existing specimen dimensions and procedures, the estimated upper limit of toughness measurements is about 250 $MNm^{-3/2}$. Also, the plastic zone radius may approach or exceed the arm height of the specimen. Finally, cracks propagating into the tough test section frequently branch in the absence of side grooves; this also makes analysis of the results difficult.

The Battelle duplex DCB test is well-suited to the study of arrester behavior, both because the test section is struck with a fast-moving crack and because the test has been the subject of extensive dynamic analysis (see Section 3.0). It will require two major modifications, however, if it is to be used for measuring K_D of very tough arrester steels. First, its fracture-toughness capacity must be increased substantially above the present limit of about 250 $MNm^{-3/2}$. This may require increasing the specimen size to permit storage of greater quantities of energy in the arms. Second, the tendency of the crack to branch must be overcome. It is believed that this can be accomplished by machine loading (in place of wedge loading) in combination with a modified grip design.

5.3 CORRELATION OF LEFM PARAMETERS WITH DYNAMIC TEAR ENERGY (DTE)

Another avenue for evaluating large fracture-toughness values is to measure the total energy absorbed in the fracture of a notched bend specimen in the dynamic tear (DT) test. The energy to fracture the specimen is provided by a pendulum whose velocity just prior to impact is approximately 5 to 10 m/s. The total energy absorbed in the process of breaking the specimen, termed the dynamic tear energy (DTE), is observed directly by noting the height of the pendulum swing after fracture. The DTE divided by A, the cross-sectional area of the test piece, is a measure of the fracture energy, R

$$R = \frac{1}{\beta} \cdot \frac{DTE}{A} \tag{5.6}$$

where $\beta = 1$ when the energy losses in the impact test remote from the crack tip are zero and $\beta > 1$ when significant energy losses occur. The corresponding fracture toughness, K_D can be expressed as

$$K_D = \sqrt{RE} \tag{5.7}$$

or

$$DTE = \frac{\beta K_D^2 A}{E} \tag{5.8}$$

Figure 5.3.1 shows the relationship between DTE and K_D as expressed in Equation (5.8) for β-values of 1 and 3. Also shown are the results of experiments in which both fracture-toughness parameters and DTE were measured. For steels, the DTE versus K_{Ic} plots indicate that $\beta \approx 10$ for the 1-inch DT test and $\beta \approx 5$ for the 5/8-inch DT test. Limited DTE versus K_{ID} data suggest that β is only about 1.4, but additional data are required to confirm this.

The experimental observation that β is greater than 1.0 confirms the assumption generally made about the DT test, namely, that the energy losses remote from the crack tip in an impact test are of a significant magnitude and can in some cases overshadow the actual fracture-propagation energy. Included in these losses are crack-initiation energy, energy associated with plastic deformation at the loading points and at the specimen boundaries as the crack approaches the far side of the test bar, and the kinetic energy of the fractured specimen.

The experimental data are too meager to permit estimation of a reliable β value for use in Equation (5.8). Furthermore, the few data that do exist are at the low-toughness end of the range, rather than in the high-toughness region of interest in arrester steels. Nonetheless, for the purposes of this discussion, a β-value of 3 will be assumed reasonable for estimating the 5/8-inch DTE requirements for arrester steels from estimates of K_D requirements made in Section 5.1:

STRENGTH LEVEL	ESTIMATED K_D FOR ARRESTERS, $MNm^{-3/2}$	5/8-INCH DTE CORRESPONDING TO K_D FOR β=3, ft-lbs
Ordinary Strength (275 MN/m^2)	200 to 400	200 to 800
High Strength (550 MN/m^2)	400 to 1000	800 to 5000

The cross-hatched region of Figure 5.3.1 shows the range of 5/8-inch DTE-values exhibited by ordinary-strength ship steels at the upper shelf loads. The estimated values required of arresters thus appear to be attainable for ordinary-strength steels but not for high-strength steels.

5.4 ROLFE'S PROPOSED REQUIREMENTS FOR ARRESTER TOUGHNESS

Rolfe, et al, [5] have developed a number of quantitative fracture control guidelines for ship steels of various yield strength levels, ranging from 275 to 690 MN/m^2. The guidelines differ for different regions of a ship, being most severe for crack-arrester regions, intermediate in severity for main-stress regions, and least severe for secondary-stress regions.

To estimate satisfactory levels of fracture toughness for various regions of the ship, Rolfe employed fracture-mechanics concepts. For example, in the main-stress regions, a satisfactory level of toughness is estimated to

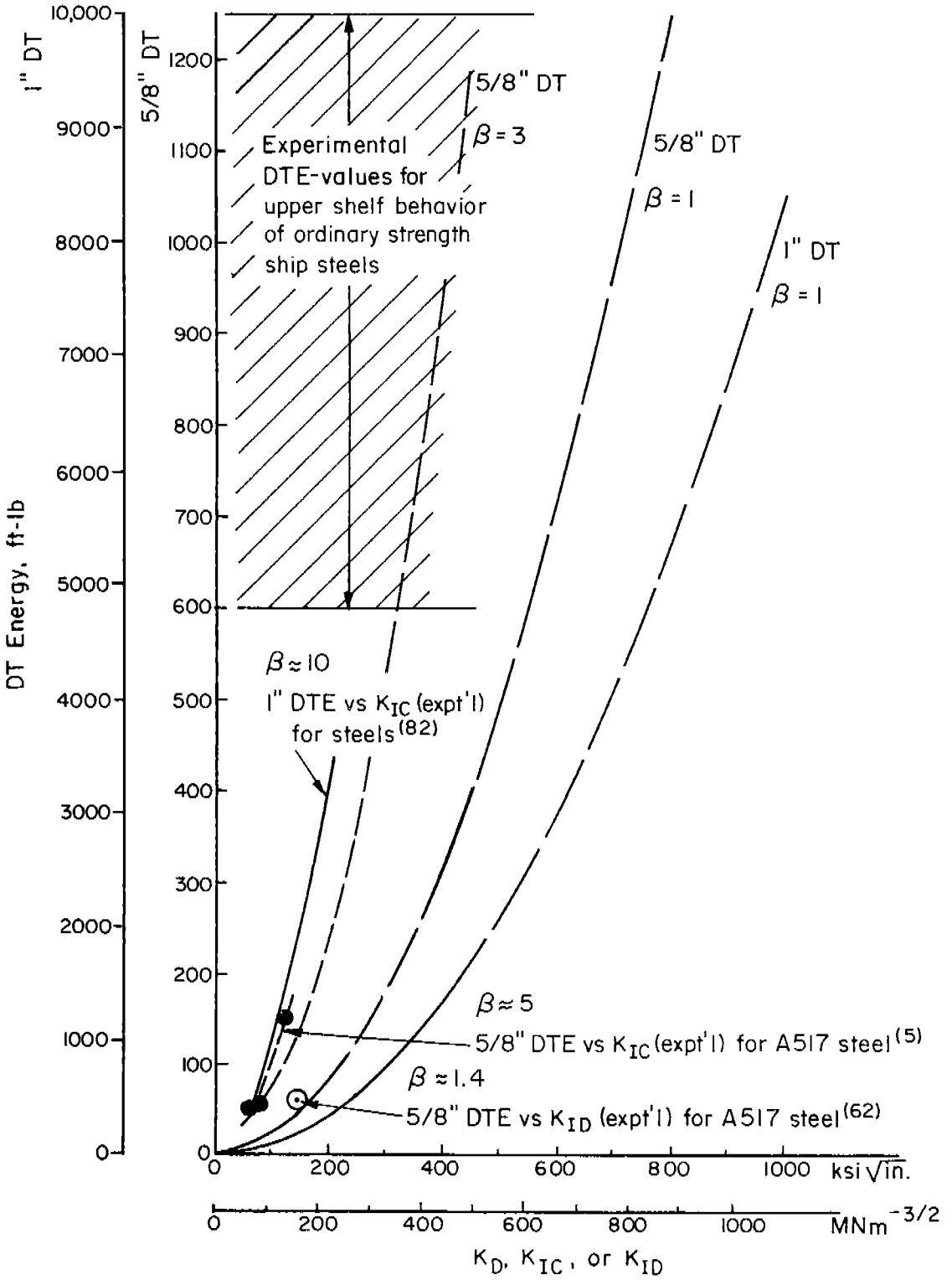

FIGURE 5.3.1. CALCULATED AND OBSERVED RELATIONSHIPS BETWEEN DYNAMIC TEAR ENERGY AND FRACTURE TOUGHNESS

be a K_{Id}/σ_{yd} ratio of $0.14m^{1/2}$ at $0^{\circ}C$ (the assumed minimum service temperature), where K_{Id} is the critical material toughness under impact loading and σ_{yd} is the yield strength under the same loading. This ratio provides an index of material toughness that is proportional to the critical crack size for unstable rupture. A ratio of $0.14m^{1/2}$ represents a toughness level above the limits of dynamic plane-strain behavior and cannot be measured directly by current fracture-mechanics tests. However, through several approximations and assumptions, Rolfe concludes that this level of toughness can be achieved by specifying that the steel satisfy two requirements:

(1) The nil-ductility-temperature must be $-18^{\circ}C$ or less.

(2) The dynamic tear (DT) energy measured at RT on a 5/8-inch specimen must equal or exceed specified values, ranging from 250 to 500 ft-lbs for steels ranging in yield strength from 275 to 550 MN/m^2.

Rolfe's estimates for toughness requirements for arrester materials are arrived at somewhat more arbitrarily than those for main-stress regions. He assumes that, to be effective, crack arresters must exhibit a plastic level of performance under dynamic loading at $0^{\circ}C$. Thus, they should exhibit DT energy values considerably greater than those for steels used in main-stress regions. For 275 MN/m^2 yield-strength steels, increasing the toughness requirements by a factor of 4 was assumed by Rolfe to be realistic. This results in a required 5/8-inch DT value at $0^{\circ}C$ of 600 ft-lb. Adjusting this requirement for steels of higher strength would indicate that for a yield strength of 690 MN/m^2, the required DT value at $0^{\circ}C$ would be 1200 ft-lb. According to Rolfe, this value is unrealistically high, based on experience with high-strength steels that should be satisfactory as crack arresters. Accordingly, the proposed DT value for 690 MN/m^2 steel is arbitrarily reduced from 1200 to 800 ft-lb. Required DT values for steels having yield strengths between 275 and 690 MN/m^2 are proportioned between 600 and 800 ft-lb.

The DT energy requirements for arrester steels proposed by Rolfe can be compared with those estimated in Section 5.3:

TYPE OF STEEL	MINIMUM TOUGHNESS REQUIREMENTS FOR ARRESTERS FROM SECTION 5.3		ROLFE PROPOSED REQUIREMENTS FOR ARRESTERS	
	K_D, $MNm^{-3/2}$	5/8-INCH DTE, ft-lb	5/8-INCH DTE, ft-lb	Corresponding K_D assuming $\beta=3$, $MNm^{-3/2}$
Ordinary Strength (275 MN/m^2)	200 to 400	200 to 800	600	350
High Strength (550 MN/m^2)	400 to 1000	800 to 5000	735	380

At ordinary strengths, Rolfe's proposed requirements are seen to be within the range of those estimated in Section 5.3. The range of values shown in the estimates from Section 5.3 for ordinary-strength steels is based on stress levels ranging from 100 to 150 MN/m^2 and arrester spacings of from 3 to 6 meters. Rolfe's proposed values, on the other hand, do not take these factors into account. Thus, the agreement for the two approaches is about as good as could be expected.

At high-strength levels, a major disagreement exists between Rolfe's proposed requirements and those estimated in Section 5.3. Rolfe proposes only modest increases in DTE (and the corresponding value of K_D) as the yield strength doubles, while the estimate of Section 5.3 suggests that K_D should be doubled and DTE quadrupled.

5.5 DATA FOR SHIP STEELS

Hawthorne and Loss [83] have characterized the DT properties of ordinary strength shipbuilding steels, employing 1-inch DT specimens*. They found that a majority of the ordinary strength hull grades cannot meet the Rolfe 5/8-inch DT requirement of 600 ft-lb at 0°C (4200 ft-lb 1-inch DT energy) for arresters. Their data show that only some of the ABS Grade E and CS plates tested in this study were able to meet these requirements. Of six plates of normalized Grades C and D steel, only one satisfied the Rolfe arrester requirement. None of the steels tested was able to meet the most demanding of the DTE requirements estimated in Section 5.3.

The problem in meeting the suggested DTE requirements for arresters stems primarily from the fact that the transition temperatures of the ABS steels are too high. Each of the grades tested by Hawthorne and Loss exhibited upper shelf 5/8-inch DTE values of 700 to 1400 ft-lbs (1-inch DTE of 5000 to 10,000 ft-lbs). However, at 0°C, most of the steels were within or below the transition region and the DTE values were correspondingly less. Heat-treated grades of steel generally exhibit lower transition temperatures and hence are more likely to meet the suggested DTE requirements than are annealed or hot-rolled steels. Rolfe, et al [5] have shown that heat treated ASTM 537A steel at a yield strength of 380 MN/m^2 has a 5/8-inch DTE value of 800 ft-lbs at 0°C. Accordingly, for ordinary-strength ship steels, it appears possible to achieve the estimated required toughness levels for crack arresters if special attention is given to heat treatment to achieve low transition temperatures.

For higher strength ship steels, DTE data are sparse. Work in progress at Southwest Research Institute on SSC Project SR-224 will provide DTE data on steels whose yield strength ranges from 345 to 690 MN/m^2. Even though only limited information is available in this strength range, it appears certain that the high-strength grades will experience greater difficulty in reaching the estimated toughness requirements than do the ordinary-strength grades. As

---

* Correlations between the 5/8-inch DT test and the 1-inch DT test revealed a ratio of about 1:7 for the respective DT energies.

strength increases, estimated arrester requirements go up and DTE shelf levels go down. Thus, there is probably a strength level above which it becomes necessary to employ multiple thickness sandwiches of arrester plates in place of a single-thickness in-plane crack arrester.

5.6 IMPLICATIONS FOR ARRESTER DESIGN

From the estimates made in the foregoing sections, it appears that only one or two of the ordinary-strength grades of ship steels currently available will be useful as arresters to stop large propagating cracks and these perhaps only marginally. This is clouded by uncertainty, however, both because of problems inherent in measuring the high-toughness values required of arrester steels and because of incomplete analyses of ship structures. Accordingly, to design arresters effectively, it will be important that good analyses are available both for the test methods employed to evaluate the arrester steels and for the various types of ship structure that might employ arresters.

The estimates made here suggest also that the toughness requirements for arresters increase dramatically with strength level, assuming a corresponding increase in operating stresses. Since shelf-level toughness of steels decreases with increasing strength, it is likely that there is some cut-off strength level above which single-thickness in-plane arresters will be ineffective and multiple thickness sandwiches of arrester plates will be required.

6.0 CRITICAL COMPARISON OF CURRENT AND PROPOSED CRACK ARRESTER CONCEPTS

The preceding sections of this report contain detailed descriptions of actual and proposed crack arrester systems for controlling fracture in ship hulls and other engineering structures. As a result of this intensive survey, it is possible to categorize the arrester systems having potential for application to ship hulls. A suggested categorization is given in Table 6.1.1.

It can readily be seen that the proposed categorization given in Table 6.1.1 is in accord with the energy-balance approach to crack propagation where crack arrest occurs when (and only when) the crack-driving force for the system, $\mathcal{G}$, is no longer equal to the material's fracture resistance. In terms of energy-based quantities, this idea can be expressed as

$$G < R_{min} \quad , \tag{6-1}$$

where R_{min} denotes the minimum value of a crack-speed-dependent fracture-energy requirement. Equivalently, the crack arrest idea can be expressed in terms of the dynamic stress-intensity factor K and the minimum dynamic fracture-toughness $K_{D,min}$ as

$$K < K_{D,min} \quad . \tag{6-2}$$

Thus, a Class I arrester system is one in which the primary aim is to <u>increase</u> $\mathcal{R}$ (or $K_{D,min}$), a Class II arrester is one that primarily decreases $\mathcal{G}$ (or K), while a Class III arrester is one in which both an increase in $\mathcal{R}$ and a decrease in $\mathcal{G}$ occurs simultaneously. From an analysis point of view, Class I is the simplest to treat; Class III is the most difficult.

One constraint that has been imposed on the critical comparison of crack arrester systems in this report is that the scope of this program precludes any experimental work or any large-system computations. Yet, on the basis of the results exhibited in Section 3, dynamic analyses appear to be required to properly evaluate the candidate systems. This points to the desirability of making the evaluations within the framework of a relatively simple physical situation where the various effects can be properly taken into account. On this basis, the DCB test specimen has been selected for the purpose of this report.

Figure 6.1.1 shows a set of hypothetical experiments in which various kinds of crack arrester systems are to be tested. The analysis of each event can be made by a relatively straightforward modification of the DCB dynamic analysis presented in Section 3.6.2. Omitting the mathematical details, the extensions required to treat each of the cases shown in Figure 6.1.1 are as follows:

(A) High-toughness insert--consider that the material in the arrest section obeys a different $K_D = K_D(\dot{a})$ relation than that of the base material.

TABLE 6.1.1. CRACK ARRESTER SYSTEMS FOR SHIP HULLS

Class	General Description	Key Properties	Examples
I	Arrester systems that present the propagating crack with a higher fracture energy requirement without at the same time introducing any appreciable change in structure stiffness.	Fracture toughnesses of base plate and arrester material.	(1) High-toughness integral insert (2) Continuously bonded stiffeners (3) Increased plate thickness
II	Arrester systems that decrease the crack driving force by imposition of some mechanical agency in the anticipated crack path thus changing the stiffness of the structure.	Elastic modulus, area and strength of base plate and arrester material	(1) Intermittently attached stiffeners (2) Pretensioned cables (3) Residual compressive stress
III	Arrester systems that direct or divert the crack from a potentially detrimental path and/or change the fracture mode of the propagating crack by simultaneously changing both the crack driving force and the fracture dissipation energy.	Fracture toughness of of base plate and arrester material (if any); modulus, area, and strength of the structural components.	(1) Riveted plates (2) Ditch-type arrester (3) Welds

(B) Integral stiffener--introduce a change in stiffness due to a locally increased thickness of an arrest section and increase the fracture area accordingly.

(C) Intermittently attached stiffener--include the restraining effect of stiffener by increasing the spring stiffnesses k_e and k_r in the arrest section.

(D) Constant-tension cables--introduce compressive forces into the equations of motion at positions corresponding to the cable locations.

Note that in Cases (C) and (D), one important parameter of the arrester system--the stiffener spacing or the cable length--can be introduced, but not varied. That is, these lengths must be related to the specimen height dimension h. However, this should not be important here because only qualitative comparisons of the various systems are sought.

Computational results typifying the analysis of crack arrester systems using the DCB specimen are given and discussed in the following. These computations were made for three different types of arrester systems positioned such that a rapidly moving crack must pass through it soon after being initiated. The basic dimensions of the DCB specimen are as given in Section 3.6.3. The arrester section dimensions are given by d = 75 mm and f = 25 mm for the inserted strip and intermittently bonded devices, cf. Figure 3.6.2. For the constant tension system, the force is taken at the position x = 75 mm.

The integral stiffener, Type (B), will be similar to Type (A) or Type (C), depending on whether the stiffener does or does not fracture. Consequently, there are three distinct arrester types that need to be considered. Note that, for convenience, a speed-independent dynamic fracture toughness was used in all of the following calculations, i.e., $K_D = K_{IC}$.

Calculations on the high-toughness inserted strip crack arrester, Type (A) in Figure 6.1.1, are shown in Figure 6.1.2. The ratio of the fracture toughness of the arrester strip relative to the base material was systematically varied to determine the effect on the crack arrest point. Figure 6.1.2(a) shows the crack length predictions as a function of time for the case where $K_q = 2.0\ K_{IC}$. Figure 6.1.2(b) shows the predictions of the arrest point as a function of the relative fracture-toughness levels of the arrester and the base material. It can be seen by comparison of Figure 6.1.2(b) with Figure 3.6.7 that the static theory badly overestimates the effectiveness of the arrester device. Other differences with the static theory can also be seen. For example, in the static approximation, if the crack does not stop in the arrester section, the arrester has no effect on it. The dynamic calculations shown in Figure 6.1.2 reveal that this is not the case, however. The energy dissipated in the arrester always diminishes the crack-driving force to some extent, causing arrest before it would normally have occurred even when it takes place beyond the arrester section.

Calculations on the intermittently attached stiffener crack arrester device, Type (C) in Figure 6.1.1, are shown in Figure 6.1.3. Figure 6.1.3(a) shows the crack length versus time calculations for the case where $K_q = 2.0\ K_{IC}$

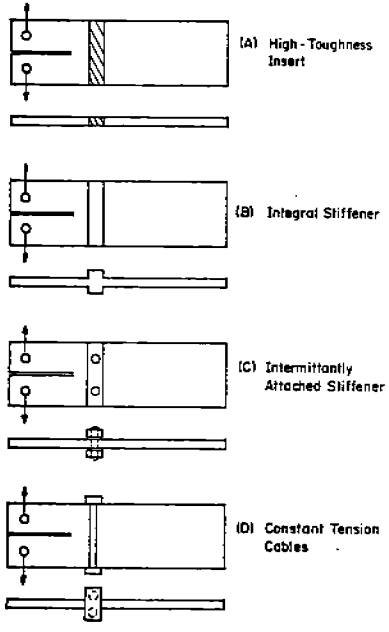

FIGURE 6.1.1. CRACK ARRESTER SYSTEMS TESTED WITH THE DCB SPECIMEN

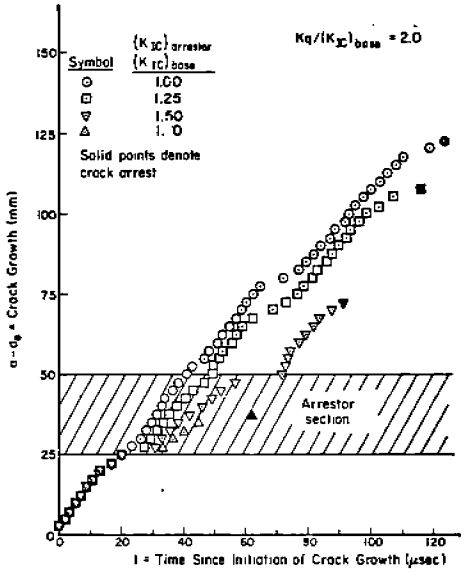

FIGURE 6.1.2.(a). CRACK PROPAGATION COMPUTATIONS FOR A DCB SPECIMEN WITH A HIGH-TOUGHNESS ARRESTER SECTION USING A DYNAMIC ANALYSIS

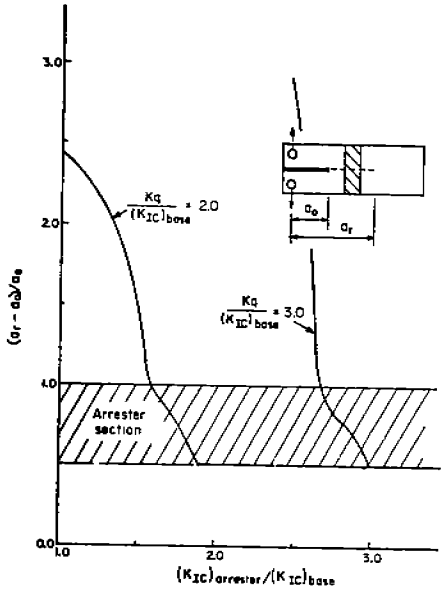

FIGURE 6.1.2(b). CALCULATED CRACK ARREST POINT IN A DCB SPECIMEN WITH A HIGH-TOUGHNESS ARRESTER SECTION USING A DYNAMIC ANALYSIS

while Figure 6.1.3(b) shows the crack arrest point as a function of the relative width of the stiffener and the base plate. Note that the elastic modulus of the stiffener was taken to be the same as that of the base plate (i.e., E = 20,6850 N/mm^2 for steel) and the width of the stiffener was fixed at 25 mm. Hence, the only arrester dimension varied was the stiffener thickness.

It can be seen from Figure 6.1.3(b) that, just as for the high-toughness insert, the arrester has an effect on the eventual arrest point even when the crack passes through it. The mechanism differs, however, as the amount of fracture energy is not changed by this kind of arrester. Instead, the mechanical restraint on the crack-tip region, particularly as the crack passes abreast of it, reduces the crack-driving force. In terms of the classification given in Table 6-1, the high-toughness strip is a member of Class I. The intermittently attached stiffener is a member of Class II.

Calculations on the constant-force (e.g., pretensioned cable) crack arrester system, Type (D) in Figure 6.1.1, are given in Figure 6.1.4. Crack-propagation-time calculations for $K_q = 2.0\ K_{IC}$ are given in Figure 6.1.4(a). The relative crack-arrest points as a function of the compressive force exerted by the device on the specimen are shown in Figure 6.1.4(b).

It can be seen that the same general effects are exhibited for the constant-force device as were evident in the results shown for the intermittently attached stiffener. This should not be entirely unexpected as this case is also a member of Class II. In fact, it can be viewed as the special limiting case of an elastic-perfectly plastic stiffener that has completely yielded. Another physical interpretation of this kind of arrester representation is in terms of a compressive residual stress field in the path of the moving crack.

The results shown for the various crack arresters in Figures 6.1.2, 6.1.3, and 6.1.4 can be used to emphasize a very essential point. This is that there can be no absolute measure of the effectiveness of a crack arrester system. The reason is that whether or not a crack is arrested by a given device depends on a great many key factors in actual applications. The most important of these variables are

- The geometry of the structure in which the arrester is installed and its specific location in the structure
- The loads acting on the structure, both at the time of crack growth initiation and while the crack is running
- The speed, direction, and length of the crack as it reaches the vicinity of the arrester.

The environment, particularly the temperature, as it affects the relative strength and toughness levels of the arrester and the base material will also play a key role.

It is a design problem to determine the most severe conditions to be expected in any application and proceed accordingly. But, any such conditions will be specific to a given application and will not be general enough to serve

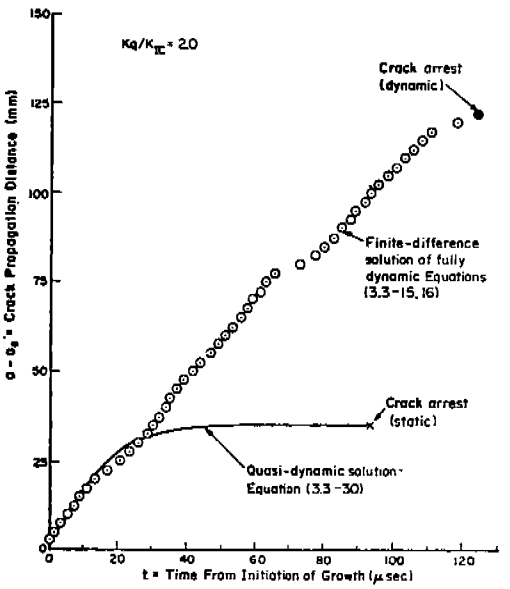

FIGURE 6.1.3(a). COMPARISON OF CRACK ARREST POINTS PREDICTED BY A FULLY DYNAMIC ANALYSIS WITH THAT OF A QUASI-DYNAMIC ANALYSIS FOR A STANDARD DCB SPECIMEN WITH $K_D = K_{IC}$

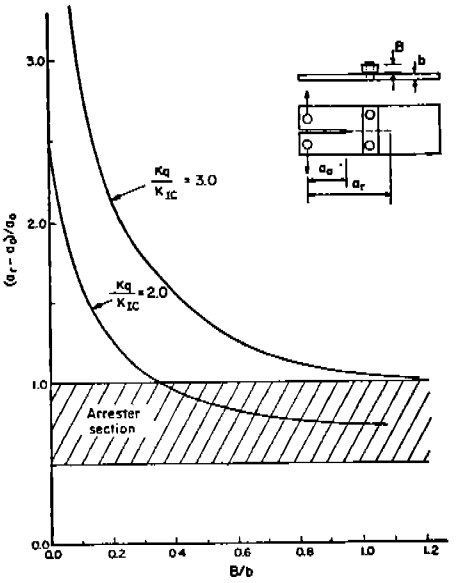

FIGURE 6.1.3(b). CALCULATED CRACK ARREST POINT IN A DCB SPECIMEN WITH AN INTERMITTANTLY-ATTACHED STIFFENER CRACK ARRESTER AS A FUNCTION OF THE STIFFENER THICKNESS

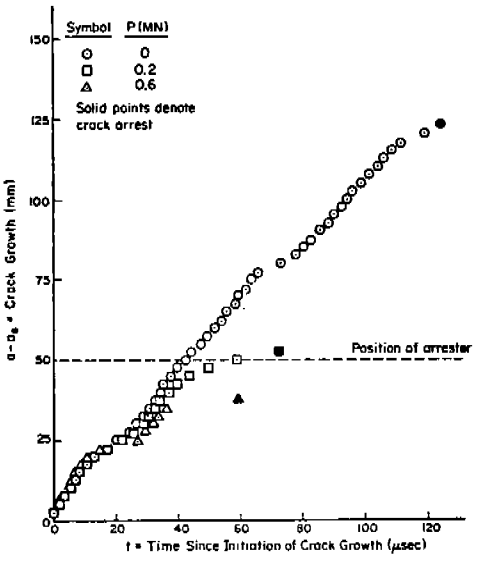

FIGURE 6.1.4(a). CRACK PROPAGATION COMPUTATIONS FOR A DCB SPECIMEN WITH A CONSTANT-TENSION CRACK ARRESTER DEVICE FOR $K_q/K_{IC} = 2.0$

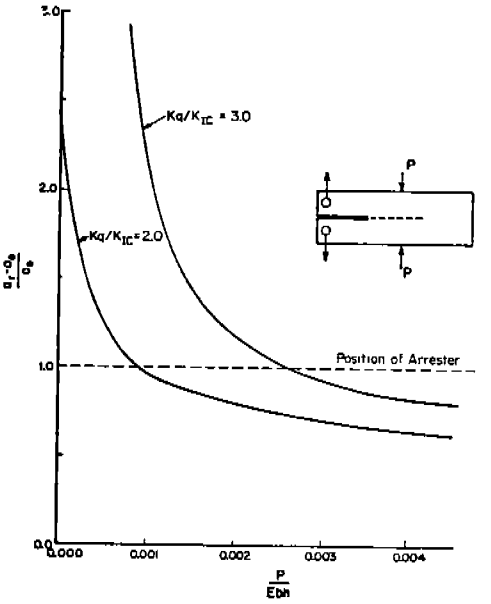

FIGURE 6.1.4(b). CALCULATED CRACK ARREST POINT IN A DCB SPECIMEN WITH A CONSTANT-TENSION CRACK ARRESTER DEVICE AS A FUNCTION OF THE FORCE APPLIED TO THE SPECIMEN

as a basis for the absolute evaluation of crack arrester systems. Hence, the evaluation must be a relative evaluation. By a relative evaluation, it is specifically meant that the effectiveness of various designs (and of the effect of various parameters within the individual designs) can only be considered within the context of an arbitrary situation. The wedge-loaded DCB specimen used in this work presents a special kind of crack-propagation event to the arrester. This event may or may not be representative of any real engineering structure. Moreover, the specific "boundary conditions" selected for the evaluation must also be arbitrary and, therefore, will preclude an absolute ranking.

Perhaps the most important point that can be made in connection with the evaluation of crack arrester systems is the following. Material property limitations aside, there is no upper limit that can be put on the effectiveness of any arrester concept to arrest a propagating crack in a given design situation. This certainly does not mean that there is no one type that will be the most suitable for certain specified circumstances. What is meant is that the suitability of a candidate device will not hinge on whether it can be made to stop the crack--because, in principle, it can always be so constructed--but whether the resulting design will be both economically feasible and physically compatible with other structural features. Such considerations are beyond the scope of the work undertaken in connection with this report, however.

There are three stages of the hypothetical crack propagation/arrest problem that influence the proper design of a crack arrester system. These arise in the context of the most damaging situation that can be envisioned and, therefore, which must be addressed by the designers. The first is the stable crack growth of an initial flaw or defect to a critical size; the second is the rapid unstable crack propagation event itself, culminating in arrest; and third, the reinitiation and unstable growth of the arrested crack. While the second stage is obvious, the first and third can be equally important but are nevertheless easily overlooked. The first stage is important because it can strongly affect the crack driving force in stage two, particularly as the crack approaches the arrester. The third stage is important because it obviously will accomplish nothing to have arrested a crack if further unstable growth is not precluded. The precise position of the crack tip could be important in making such a determination and this, of course, will be affected by the dynamic features of the crack arrest process.

The numerical results given earlier in this section can be used to provide quantitative illustrations. Suppose that the hypothetical design problem is to arrest a crack propagating in a 1-inch thick steel plate having a speed-independent fracture toughness of 100 ksi $in.^{1/2}$ under a fixed displacement loading at a level such that at the time of crack growth initiation K = 200 ksi $in.^{1/2}$. Figure 3.6.6 indicates that the crack speed to be expected under these conditions is about 3000 ft/sec (i.e., at K_q/K_{IC} = 2.0, V = 1000 M/sec).

Assuming nearly complete utilization of kinetic energy by the propagating crack (an upper limit), the results of Figures 6.1.2, 6.1.3, and 6.1.4 can be used directly. Suppose that to preclude subsequent reinitiation of unstable growth, the crack must be stopped before completely penetrating the arrester section. To achieve this, the minimum toughness of an inserted 1-inch-thick tougher steel strip would have to be 160 ksi $in.^{1/2}$, cf, Figure 6.1.2(b). If an intermittently

TABLE 6.1.2. EXAMPLE CALCULATIONS FOR THE DESIGN OF THREE DIFFERENT CRACK ARRESTER SYSTEM TYPES

Crack Arrester System[a]	Design Variable	Minimum Value of Design Variable[b]	
		K_q = 200 ksi in.$^{1/2}$	K_q = 300 ksi in.$^{1/2}$
High toughness integral inserted 1-inch wide strip	Fracture toughness of arrester	160 ksi in.$^{1/2}$	270 ksi in.$^{1/2}$
Intermittently attached 1-inch wide stiffener	Stiffener thickness	0.35 inch	1.20 inch
Pretensioned cable 1-inch^2 cross section	Stress in cable	60 ksi	160 ksi

(a) Arrester system dimensions are relative to a 1-inch thick steel base plate having a speed-independent dynamic fracture toughness of 100 ksi in.$^{1/2}$

(b) The parameter K_q represents the applied load-flaw size combination that existed at the time of unstable crack growth initiation. Fixed displacement boundary conditions are assumed during crack propagation.

attached 1-inch-wide stiffener device is to be used, it would have to be 0.35 inch in thickness; cf, Figure 6.1.3(b). Finally, if a pretensioned cable with a cross-sectional area of 1 in.^{2} is to be used, it must be stressed to at least 60,000 psi; cf, Figure 6.1.4(b).

To further emphasize the key variables that influence the requirements for an arrester device, calculations have also been made for the higher initial load level of 300 ksi in.$^{1/2}$. The arrester parameters obtained for the three cases given in Figures 6.1.2, 6.1.3, and 6.1.4 are summarized along with the above results in Table 6.1.2. The significant effect of the load level (or, equivalently, the fracture speed) is obvious from these results. Note finally that these results are based on a geometric configuration that is a much more efficient utilizer of kinetic energy than are actual ship hull structures. But, while over-estimating the minimum arrester parameters, these results have the virtue of automatically incorporating a factor of safety which more than likely would always be inserted in any event.

7.0 RECOMMENDATIONS FOR FUTURE RESEARCH

There are two major points that have been identified in the work reported here that bear on the proper design and utilization of crack arrester systems for ship hulls. The first is that there is no general type of system that can be identified as being completely superior to all others in all circumstances. The reason is that, in principle, there is no upper limit to the crack arresting capability of most arrester systems.* By choosing materials and sizes properly, most systems can be made to have sufficient "stopping power" in any conceivable situation. Consequently, the choice of an arrester system probably rests mainly on economic considerations (e.g., cost of materials, installation and fabrication costs), material availability, and other design considerations (e.g., potential crack initiation sites introduced, the effect of the arrester on the performance of the vessel), not on any limits on the effectiveness of the arrester system.

The second major point is connected with the design of the arresters to be used in a given application. Once the particular arrester system has been selected, an exact quantitative evaluation must be performed. In performing this evaluation, numerical calculations based on a fully dynamic theory of elasticity solution procedure with boundary conditions properly taken into consideration are required. In short, statically based calculations can be highly misleading with regard to the crack arrest capability of a given arrester system and structural configuration. The extent to which this is true cannot be determined at this time and, in fact, is a highly appropriate area for further research, as described below.

In performing an analysis of a crack arrester device for a specific ship hull, it is obviously necessary to have a detailed, albeit preliminary, knowledge of the ship hull configuration (e.g., mechanical properties, plate thicknesses, stringer stiffnesses and spacings). A basis for estimating the severity of the loads that will be acting on the ship hull in the vicinity of the crack arrest device must also be known. It is then necessary to anticipate where an unstable crack might initiate and the direction in which it might be expected to propagate. These are pieces of information that a ship designer would normally have at hand. But, there are three additional general aspects of the problem in which a specific capability is also needed to properly design the arrester. These are

- A way of estimating the growth of a flaw by fatigue during anticipated service conditions for the ship
- A way of evaluating the mechanical and fracture properties of the ship hull and arrester device when presented with a fast-running crack
- A practical computational method for performing dynamic calculations for rapid crack propagation and crack arrest in a given structural configuration.

---

* All systems clearly have a practical limitation because of the mechanical properties of the materials that are available. Material considerations aside, with the further exceptional cases of devices such as the ditch-type arrester being excluded, an arrester system can always be adequately designed for a given situation.

In contrast, these capabilities are not ordinarily available to ship designers. In fact, it can be said that in none of these three areas has enough fundamental work been done to provide ship designers with the techniques required to do his job properly. These areas therefore represent potential topics in which research can be recommended to provide a design basis for the proper design of ship hull crack arrester systems.

In accordance with the conclusions that have been drawn from the work given in this report, a number of recommended research topics can be proposed. In no particular order, these are as follows.

1. A program of experiment and analysis to obtain a technique for estimating the rate of fatigue crack growth in ship hull materials for the load spectrum that a vessel would be expected to experience under severe, but probable, service conditions. The results of this work will likely show that fatigue crack-growth rates are primarily dependent on the type of ship and the geographical locations in which it is expected to serve. This work could take advantage of the large body of work already performed for aircraft structures.

2. A program of experiment and analysis aimed at determining the dynamic fracture properties of present-day and contemplated ship hull and arrester materials. This program will likely be based upon developing (or modifying) a standardized laboratory test specimen. Since there is no way to directly measure dynamic fracture-toughness values, these must be inferred from test quantities that are directly measurable. Hence, the need for an analysis capability in such a program. It should in any event be reemphasized that the dynamic fracture-toughness values are not generally the same as their static counterparts and, in some instances, can be quite different. Work in this area should draw upon the extensive progress that has been made on behalf of the NRC and others.

3. A program to develop a two-dimensional dynamic analysis capability for treating fast-moving cracks in real engineering structures. Because of the generality that is needed to treat arresters, the tool that must be evolved will be based on a numerical analysis technique (e.g., finite different method) and will take the form of a computer program. Such programs are already available. What is needed is that they be extended to explicitly treat arresters.

4. A program to develop an elastic-plastic dynamic fracture-mechanics capability for the initiation of unstable crack propagation from arrested cracks. With the high-toughness levels used in ship steels, particularly in arrester

sections, ordinary linear elastic fracture-mechanics treatments are quite inappropriate. In particular, stable crack growth cannot be treated within the linear elastic regime, and this may be a key factor in determining the point at which a fast fracture arrested at or near an arrester can become critical once again. Some work is under way in this area but has only scratched the surface of this formidable problem.

5. A research program to evaluate and make available the response of a ship under service conditions in a systematic manner. It is recommended that research programs be pursued using model and full-scale experiments to determine ship responses in random seas. These data should be utilized to advance the currently available linear strip theory programs on various ship classes. Then the research results in the areas of fracture mechanics and probabilistic design approaches can be integrated into useful tools for the ship designer. Currently, the ship designer is aware of meaningful research results in a number of areas, but he does not have the time or knowledge to apply these new data to his designs. The ship response effort is also required to determine ship springing and related elastic strains to predict the adequacy of crack arresters to stop dynamic cracking. A significant body of work already exists as a result of Ship Structure Committee work in this field, of course.

It might be noted that a research program confined to one of these topics and excluding other aspects of the problem could be quite ineffective. A research program that has proper design of crack arrester systems for ship hulls as its objective must be cognizant of all of the various aspects of the crack propagation-arrest problem to be truly beneficial.

Consider one example problem to help make these ideas more concrete. Figure 7.1.1 shows a section of a ship hull that is periodically reinforced by riveted stiffeners. Suppose that a crack initiates at the rivet hole (as they often do) and grows by fatigue under the normal loadings carried by the ship while in service. Further suppose that the ship is exposed to storm conditions severe enough to cause the crack to propagate unstably across the hull plate towards the most vulnerable part of the stiffener reinforced region--the point midway between the rivets in the adjacent stiffener. The first question is will the crack be stopped at the stiffener or will it pass under it and, likely, tear apart the entire hull in the process? The second question is, assuming that the crack has been arrested at the first stiffener, can unstable crack growth be subsequently reinitiated?

The ship designer can readily anticipate the scenario illustrated in Figure 7.1.1 and outlined above. The obvious problem that he is faced with in this circumstance is to insure that the crack is arrested at the stiffener. What he must do to achieve this is have the stiffener constrain the dynamic crack driving force as the propagating crack tip approaches it so that the dynamic stress-intensity

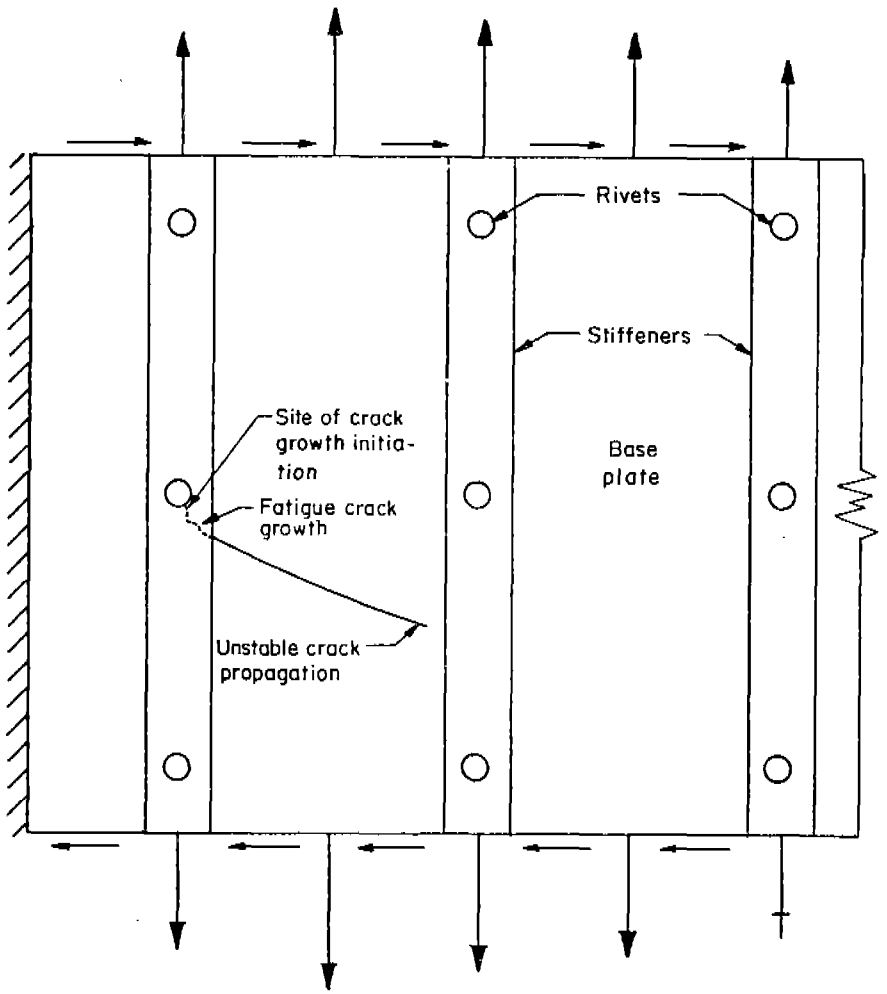

FIGURE 7.1.1. REINFORCED SHIP HULL

factor falls below the minimum value of the hull plate's dynamic fracture toughness in the vicinity of the arrester. It is perhaps less obvious that, having assured himself that an unstable crack would be quickly arrested, further analysis is still needed. The possibility of the arrested crack becoming critical once again still exists. A little thought will show that, to accomplish all of this, the designer will need to draw upon research results from all of the topics suggested above for future research.

Finally, it should be clear that the basic situation described here will not be essentially altered regardless of the arrester type considered, be it a weld-on stiffener, a tension device, or an integral high-toughness strip. The design problem for ship hulls or any other engineering structure where the possibility of flaw initiation, stable growth to a critical size, and rapid unstable growth under an abnormally high load involves both static and dynamic fracture-mechanics analysis employing properly determined material fracture properties. The essential research problem that presently exists is to put these into the hands of ship designers in a form that they can be used in a practical way in ship design.

8.0 REFERENCES

1. Hinners, R.A., contributed discussion to Reference 3, Soc. Naval Arch. Marine Eng. Trans. 75, 380 (1967).

2. Boyd, G.M., "Fracture Design Practices for Ship Structures", Fracture, H. Liebowitz (editor), 5, 383, Academic Press, New York (1969).

3. Heller, S.R., Jr., Lytle, A.R., Nielsen, R., Jr., and Vasta, Jr., "Twenty Years of Research Under the Ship Structure Committee", Soc. Naval Arch. Marine Eng. Trans., 75, p 332 (1967).

5. Chazal, E.A., Jr., Goldberg, J.E., Nachtsheim, J.J., Rumke, R.W., and Stavovy, A.B., "Third Decade of Research Under the Ship Structure Committee", presented at Ship Structure Symposium, Washington, D.C., October 6-8, 1975.

5. Rolfe, S.T., Rhea, D.M., Kuzmanovic, B.O., "Fracture-Control Guidelines for Welded Steel Ship Hulls", Ship Structure Committee Report SSC-244 (1974).

6. Kihara, Kanazawa, Ikeda, Okabe, Nakijima, Lajima, Mitsubishi Heavy Industries, Ltd., "Study on Welded-Type Crack Arrester (First Report)", June,1972.

7. Yajima, Nakajima, Okabe, Nagamoto, "Study on Welded-Type Crack Arrester, (First Report)", Tech. Review, Vol. 8, No. 2, June,1971.

8. Kanazawa, Machida, Yajima, Aoki, "Study on Brittle Crack Arrester-Considerations on the Arrest of a Very Long Crack", J.S.N.A., Japan, Vol. 131, June,1972.

9. Kanazawa, Machida, Matola, "Some Basic Considerations on Brittle Crack Arrester for Welded Steel Structures (First Report)", J. Soc. Naval Arch, Japan.

10. Kanazawa, et al., Ibid (2nd Report) - Patch Type, Vol. 116, 1964.

11. Yoshiki, et al., Ibid (3rd Report) - Experimental Checks, Vol. 118, 1964.

12. W.M. Hannan,"Classification Society Experiences in Today's Ships" presented at Ship Structures Symposium, Washington, D.C., October 6-8, 1975.

13. G. Buchanan, Jensen, C.J.G., Dolson, Dr.R., "Lloyd's Register of Shipping's Approach to the Control of the Incidence of Brittle Fracture in Ship Structures", Lloyd's Register Report No. 56, 1969.

14. Kanazawa, Machida, Yajima, Aoki, "Study on Brittle Crack Arrester - Considerations on the Arrest of a Very Long Crack", J.S.N.A., Japan, Vol. 130, December, 1971.

REFERENCES (Continued)

15. Kanazawa, Machida, Aoki, "Fracture Mechanics Analyses and Design of Stiffner-Type Crack Arrester", Japan Shipbuilding and Marine Engineering, Vol. 3, No. 6, November, 1968.

16. Yoshiki, Kanazawa, Machida, "Fracture Mechanics Analysis of Stiffner-Type Crack Arrester", J.S.N.A., Japan, Vol. 118, December,1965, Vol. 122, December,1967, Vol. 124, December, 1968.

17. Gammall, M.M.,"A New Method for Estimating the Fatigue Life of Ship Structures", University of Newcastle Upon Tyne, July, 1975.

18. Nibbering, J.J.W., "Fracture Mechanics and Fracture Control for Ships", Netherlands Ship Research Center TNO, Delft, Report No. 178 S(177/Sc) May, 1973.

19. "Brittle Fracture Tests for Weld Metal", Concept Final Report of IIW Working Group 2912, Report No. 185, Ship Structures Laboratory, Delft University of Technology, Doc. X-754-74, May, 1974.

20. Kavlie, Dag., "Notes on Steel Grades vs. Temperature and Thickness for Various Ship Hull Members", University of Trondheim, Norges Tekniske Hogskole, June, 1975.

21. Lerde, N.G., "Review of Crack Arresting Experience and Development from Kockums", September 17, 1975.

22. Stenberg, Per, Svetsaren, "Has the Experience of Recent Years Confirmed that All-Welded Ships are Ships of the Future?", No. 2-3, Vol. 15, p 32, 1950.

23. Liston, Haskins, "Tensile Testing of Steel", Lloyd's Register of Shipping Report No. 62, 1969.

24. Broek, D., Elementary Engineering Fracture Mechanics, Noordhoff, 1974.

25. Mott, N.F., Engineering 165, 16 (1948).

26. Kanninen, M.F., Int. J. Frac., 10, 415 (1974).

27. Freund, L.B., J. Mech. Phys. Solids, 20, 129 (1972).

28. Hahn, G.T., Gehlen, P.C., Hoagland, R.G., Kanninen, M.F., Popelar, C., Rosenfield, A.R., and de Campos, V.S., "Critical Experiments, Measurements and Analyses to Establish a Crack Arrest Methodology For Nuclear Pressure Vessel Steels", Report to Div. Reactor Safety Research, U.S. Nuclear Regulatory Commission, BMI-1937, August, 1975.

REFERENCES (Continued)

29. Eftis, J. and Krafft, J.M., J. Basic Eng., ASME 257, March, 1965.

30. Barton, F.W. and Hall, W.J., Weld. J. Res. Supp., 39, 379s, 1960.

31. Hahn, G.T., Hoagland, R.G., Rosenfield, A.R., and Sejnoha, R., Met. Trans., 5, 475, 1974.

32. Burns,S.J. and Bilek, Z.J., Metl. Trans., 4, 975, 1973.

33. Fearnehough, G.D., "Fracture Propagation Control in Gas Pipelines", Crack Propagation in Pipelines, Paper No. 1, The Institution of Gas Engineers, London, 1974.

34. Freed, C.N., Sullivan, A.M., and Stoop, J., "Effect of Sheet Thickness on the Fracture-Resistance Parameter K_c for Steels", NRL Report 7601, 1973.

35. Freed, C.N., Sullivan, and Stoop, J., "Effect of Sheet Thickness on the Fracture-Resistance Parameter K_c for Steels", NRL Report 7464, 1972.

36. Sullivan, A.M., Stoop, J., and Freed, C.N., "Influence of Sheet Thickness Upon the Fracture Resistance of Structural Aluminum Alloys", ASTM-STP, Vol. 536, pp 323-333, 1973.

37. Krafft, J.M., and Irwin, G.R., ASTM STP 381, 114, 1964.

38. Hahn, G.T., Hoagland, R.G., Kanninen, M.F., Rosenfield, A.R., "Crack Arrest in Steels, Eng. Fract. Mech., Vol. 2, p 583, 1975.

39. Irwin, G., Handbook of Physics, 6, 551, 1968.

40. Shabbits, W.O., Dynamic Fracture Toughness Properties of Heavy Section A533B Class 1 Steel Plate. WCAP-7623 (HSSTP-TR 13) Westinghouse, December, 1973.

41. Crosley, P.B., and Ripling, E.J., Trans., ASME 91, Series D, 525, 1969.

42. Irwin, G.R., and Wells, A.A., Met. Rev., 10, 223, 1965.

43. Crosley, P.B., and Ripling, E.J., Nucl. Engng Design, 17, 32, 1971.

44. Crosley, P.B., and Ripling, E.J., Materials Research Laboratory Report, Glenwood, Illinois, 1970.

45. Crosley, P.B., and Ripling, E.J., Proc. 2nd Int. Conf. Pressure Vessel Tech., October, 1973, San Antonio, Texas.

REFERENCES (Continued)

46. Yoshiki, M., Kanazawa, T., and Machida, S., "Fracture Mechanics Approach to Brittle Fracture Propagation-Arrest in Structural Steel," Proc. First Int. Conf. Fracture, 1965, Vol. 3, p 1711.

47. Kanazawa, T., "Recent Studies on Brittle Crack Propagation and Arrest for a Material having a Crack Speed Dependent Fracture Toughness", Presented at the Conf. on the Prospects of Fracture Mechanics, Delft, Netherlands June 24-28, 1974.

48. Kanninen, M.F., "An Analysis of Dynamic Crack Propagation and Arrest for a Material having a Crack Speed Dependent Fracture Toughness", Presented at the Conf. on the Prospects of Fracture Mechanics, Delft, Netherlands June 24-28, 1974.

49. Romualdi, G.P., Frasier, G.T., and Grwin, G.R., "Crack Extension Force Near a Riveted Stringer", NRL 4956, 1952.

50. Poe, C.C., "The Effect of Riveted and Uniformly Spaced Stringers on the Stress-Intensity Factor of a Cracked Sheet", AFFDL-TR-70-144, 1970, pp 207-216.

51. Poe, C.C., "Fatigue Crack Propagation in Stiffened Panels", ASTM STP 486, American Society for Testing and Materials, pp 79-97, 1971.

52. Vlieger, H., "Residual Strength of Cracked Stiffened Panels", NLR TR-71004, 1971.

53. Vlieger, H., "The Residual Strength Characteristics of Stiffened Panels Containing Fatigue Cracks", Eng. Fracture Mechanics, 5 pp 447-478, 1973.

54. Swift, T., and Wang, D.Y., "Damage Tolerant Design Analysis Methods and Test Verification of Fuselage Structure", AFFDL-TR-70-144, 1970, pp 653-683.

55. Swift, T., "Development of the Fail-Safe Design Features of the DC-10" ASTM STP 486, American Society for Testing and Materials, pp 164-214, 1971.

56. Swift, T.,"The Effect of Fastener Flexibility and Stiffener Geometry on the Stress Intensity Factor in Stiffened Sheet", Prospects of Fracture Mechanics, Sih et al editors, Noordhoff, 1974, pp 419-436.

57. Hahn, G.T., Hoagland, R.G., Kanninen, M.F., and Rosenfield, A.R., Sejnoha, R., "Fast Fracture Resistance and Crack Arrest in Structural Steels", Ship Structure Committee Report SSC-242.

REFERENCES (Continued)

58. Hahn, G.T., Hoagland, R.G., Kanninen, M.F., and Rosenfield, A.R., Dynamic Crack Propagation, edited by G.C. Sih (Noordhof), pp 649, 1973.

59. Hahn, G.T., Hoagland, R.G., Kanninen, M.F., and Rosenfield, A.R., A, Pressure Vessel Technology, Part II, ASME, New York, p 981-994, 1974.

60. Hahn, G.T., Hoagland, R.G., Kanninen, M.F., and Rosenfield, A.R., B, Pressure Vessel Technology, Part III, ASME, New York, p 121, 1974.

61. Hahn, G.T., Hoagland, R.C., Kanninen, M.F., and Rosenfield, A.R., "Pilot Study of Fracture Arrest Capabilities of A533B Steel", (to be presented at Ninth National Symposium Fract. Mech., Pittsburgh, 1975), 1975.

62. Hahn, G.T., Hoagland, R.G., and Rosenfield, A.R., "Dynamic Crack Propagation and Arrest in Structural Steels", Final Report on Project SR-201 to Ship Structure Committee, 1975.

63. Hoagland, R.G., Trans. ASME, Vol. 89, (Ser. D), p 525, 1967.

64. Hoagland, R.G., Kanninen, M.F., Rosenfield, A.R., and Hahn, G.T., "Rectangular-DCB Specimens for Fast Fracture and Crack Arrest Measurements, Topical Report to NRC, Div. Reactor Safety Research, 1974.

65. Hoagland, R.G., Rosenfield, A.R., and Hahn, G.T., Met. Trans., Vol. 3 p 123, 1972.

66. Kanninen, M.F., Int. J. Fract. Mech., Vol. 9, p 83, 1973.

67. Kanninen, M.F., B. Proc. Cont. on Prospects of Fracture Mech., G.C. Sih, et al., editors, Nordhoff, Leyden, The Netherlands, p 251, 1974.

68. Freund, L.B., B, J. Mech. Phys. Solids, Vol. 20, p 141, 1972.

69. Freund, L.B., J. Mech. Phys. Solids, Vol. 21, p 47, 1973.

70. Francis, P.H., Landford, J., and Lyle, F.F., "A Study of Subcritical Crack Growth in Ship Steels", Final Technical Report on SR-20, 1974.

71. Pelloux, R.M.N., "Review of Theories and Laws of Fatigue Crack Propagation", AFFDL-TR-70-144, 1970, pp 409-416.

72. Erdogan, F., "Crack Propagation Theories", NASA CR-901, 1967.

REFERENCES (Continued)

73. Toor, P.M., "A Review of Some Damage Tolerance Design Approaches for Aircraft Structures", Eng. Fracture Mechanics, 5, pp 837-880, 1973.

74. Schijve, J., and Broek, D., "Crack Propagation Tests Based on a Gust Spectrum with Variable Amplitude Loading", Aircraft Engineering, 34, pp 314-316, 1963.

75. Schijve, J., "Cumulative Fatigue Problems in Aircraft Structures and Materials", Aeronautical Journal, 74, pp 517-532, 1970.

76. Corbly, D.M., and Packman, P.F., "On the Influence of Single and Multiple Peak Overloads on Fatigue Crack Propagation in 7075-T6511 Aluminum", Eng. Fracture Mechanics, 5, pp 449-497, 1973.

77. Willenborg, J., Engle, R.M., and Wood, H.A., "A Crack Growth Retardation Model Using an Effective Stress Concept", AFFDL-TM-71-1FBR, 1971.

78. Landis, J.D., and Begley, J.A., "The Effect of Specimen Geometry on J_{Ic}", ASTM STP J14, p 24, 1972.

79. Robinson, J.N., and Tetelman, A.S., "The Critical Crack-Tip Opening Displacement and Microscopic and Macroscopic Fracture Criteria for Metals", UCLA-ENG-7360, Tech. Report No. 11 to U.S. Army Research Office, Durham on Contr. DAHC04-69-C-0008, August, 1973.

80. Shoemaker, A.K., and Rolfe, S.T., The Static and Dynamic Low-Temperature Crack-Toughness Performance of Seven Structural Steels", Eng. Fract. Mech., Vol. 2, p 319, 1971.

81. Barsom, J.M., and Rolfe, S.T., "K_{Ic} Evaluation-Temperature Behavior of A517-F Steel", Eng. Fract. Mech., Vol. 2, p 341, 1971.

82. Unpublished NRL data.

83. Hawthorne, J.R., and Loss, F.J., "Fracture Toughness Characterization of Shipbuilding Steels", SSC-248, 1974.

84 Nilsson, F., "A Note on the Stress Singularity at a Non-Uniformly Moving Crack Tip", J. Elasticity, 4, 73, 1974.

APPENDIX A

DERIVATION OF FRACTURE ENERGY, TOUGHNESS AND WIDTH REQUIREMENTS FOR IN-PLANE ENERGY-ABSORBING ARRESTER MODEL

An approximate expression of the fracture energy, fracture toughness and arrester width requirements can be derived for the case of plate that is large relative to the length of a centrally located, propagating and (ultimately) arrested crack as shown in Figure 5.1. The variation of the relevant energy terms with crack length are illustrated in Figure A-1. The model involves a number of simplifying assumptions: (1) the nominal applied stress is essentially constant, (2) the fracture energy of the arrester plate is large relative to the base plate and independent of crack velocity, (3) the external work and the strain energy terms, $\frac{dW}{dA} - \frac{dU}{dA}$, for the propagating crack can be approximated by the value for a stationary crack of the same length, (4) the fraction φ of the kinetic energy returned to the crack tip can be established independently, and (5) the thickness of the arrester plate is the same as the base plate. For this model, which is described in Figure A-1:

$\frac{dW}{dA} - \frac{dU}{dA}$ = external work and strain energy = $\frac{\sigma^2 \pi a}{E}$

$2a$ = crack length

$2a_o$ = crack length at the onset of fracture

$2a_a$ = crack length at arrest

E = Young's modulus

φ = fraction of kinetic energy stored that is returned to crack tip

$K_{D,AP}$ = propagating crack toughness of arrester plate, $K_{D,AP} = \sqrt{ER_{AP}}$

R_{BP} = fracture energy of base plate

R_{AP} = fracture energy of arrester plate

$2S$ = spacing between arresters

σ = nominal stress

W = arrester width corresponding to the nominal value of R_{AP}, $W = a_a - S$

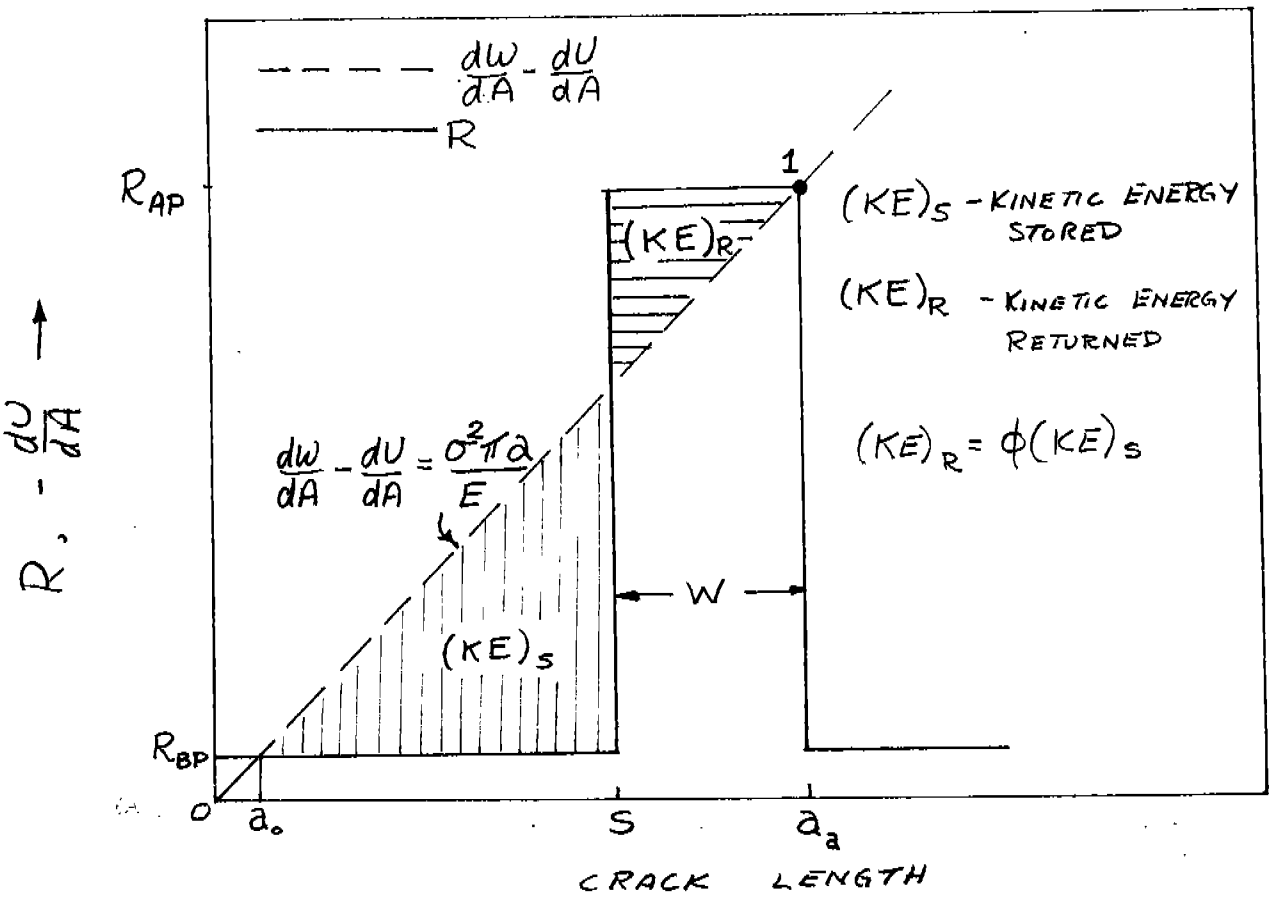

FIGURE A-1. VARIATION OF THE ENERGY TERMS FOR THE IN-PLANE ENERGY ABSORBING ARRESTER MODEL SHOWN IN FIGURE 5.1

The expressions for the conservation of energy

$$R = \mathcal{G} = \frac{dW}{dA} - \frac{dU}{dA} - \frac{dT}{dA} \tag{1A}$$

$$R\Delta a = \int \mathcal{G} da = \int \left[\frac{dW}{dA} - \frac{dU}{dA}\right] da - \int \frac{dT}{dA} da \tag{2A}$$

are valid while the crack is propagating. During the initial period, the interval $a_o \leq a \leq S$, the kinetic energy stored is

$$\int_{a_o}^{S} \frac{dT}{dA} da = \int_{a_o}^{S} \left[\frac{dW}{dA} - \frac{dU}{dA}\right] da - R_{BP}(s-a_o) \tag{3A}$$

which reduces to

$$\int_{o}^{S} \frac{dT}{dA} da \approx \int_{o}^{S} \left[\frac{dW}{dA} - \frac{dU}{dA}\right] da = \frac{\sigma^2 \pi S^2}{2E} \tag{4A}$$

for the simplifying assumptions listed above. For the period the crack propagates on the arrester, the interval $s \leq a \leq a_a$:

$$R_{AP}\, W = \int_{S}^{a_a} \left[\frac{\sigma^2 \pi a}{E}\right] da - \int_{S}^{a_a} \frac{dT}{dA} da \tag{5A}$$

where $a_a = S + W$. The last term of this equation is the kinetic energy returned to the crack tip which (by definition) is equal to the fraction φ of the kinetic energy stored given by Equation (4A):

$$R_{AP}\ W = \frac{\sigma^2\pi}{2E}\ (2SW+W^2) + \frac{\sigma^2\pi}{2E}\ (\varphi S^2) \qquad (6A)$$

The minimum arrester fracture energy corresponds with the value of $\frac{dW}{dA} - \frac{dU}{dA}$ at $a = a_a$ (the point 1 in Figure A-1):

$$R_{AP,minimum} = \frac{\sigma^2\pi a_a}{E} = \frac{\sigma^2\pi (S+W)}{E} \qquad (7A)$$

Substituting this into Equation (6A)

$$W = S\sqrt{\varphi} \qquad (8A)$$

$$R_{AP,minimum} = \frac{\sigma^2\pi S}{E}\ (1+\sqrt{\varphi}) \qquad (9A)$$

$$K_{D,AP,minimum} = \sigma\sqrt{\pi S}\ (1+\sqrt{\varphi})^{1/2} \qquad (10A)$$

where W is the arrester width corresponding to the minimum energy and toughness values. To stop a fracture with an arrester having a smaller width $W^* < W$, and for a finite values of φ, larger values of fracture energy are required:

$$R_{AP} = \frac{\sigma^2\pi S}{E}\ \left[1 + 0.5\left(\frac{W^*}{S}\right) + 0.5\left(\frac{W^*}{S}\right)^{-1}\varphi\right] \qquad (11A)$$

Unclassified

SECURITY CLASSIFICATION OF THIS PAGE *(When Data Entered)*

REPORT DOCUMENTATION PAGE		READ INSTRUCTIONS BEFORE COMPLETING FORM
1. REPORT NUMBER SSC-265	2. GOVT ACCESSION NO.	3. RECIPIENT'S CATALOG NUMBER
4. TITLE *(and Subtitle)* A STUDY OF SHIP HULL CRACK ARRESTER SYSTEMS		5. TYPE OF REPORT & PERIOD COVERED Final Report February 1975 to March 1976 6. PERFORMING ORG. REPORT NUMBER
7. AUTHOR(s) M. Kanninen, E. Mills, G. Hahn, C. Marschall, D. Broek, A. Coyle, K. Masubushi*, and K. Itoga* * Massachusetts Institute of Technology		8. CONTRACT OR GRANT NUMBER(s) N00024-75-C-4325
9. PERFORMING ORGANIZATION NAME AND ADDRESS Battelle Memorial Institute Columbus Laboratories 505 King Avenue, Columbus, Ohio 43201		10. PROGRAM ELEMENT, PROJECT, TASK AREA & WORK UNIT NUMBERS
11. CONTROLLING OFFICE NAME AND ADDRESS Commander, Naval Sea Systems Command Department of Navy Washington, D.C. 20362 Code N00024		12. REPORT DATE December 1976 13. NUMBER OF PAGES 98
14. MONITORING AGENCY NAME & ADDRESS*(if different from Controlling Office)*		15. SECURITY CLASS. *(of this report)* Unclassified 15a. DECLASSIFICATION/DOWNGRADING SCHEDULE
16. DISTRIBUTION STATEMENT *(of this Report)* Approved for Public Release Distribution - Unlimited		
17. DISTRIBUTION STATEMENT *(of the abstract entered in Block 20, If different from Report)*		
18. SUPPLEMENTARY NOTES		
19. KEY WORDS *(Continue on reverse side if necessary and identify by block number)* hull crack arresters, crack arresters, fast fracture arrest, fatigue crack propagation, arrester material characterization		

20. ABSTRACT

A world-wide survey of marine engineers, shipyards, and regulating agencies was conducted to ascertain both current and contemplated approaches to arresting cracks in ship hulls. As a result of this survey, a crack arrester classification system was developed. The classification was used to aid in a systematic investigation aimed at determining the most attractive practical schemes for arresting cracks in ship hulls. In addition to describing the classification system, example calculations showing quantitatively the effect of imposing various kinds of mechanical arrester devices in the path of a fast-moving crack

DD FORM 1 JAN 73 1473 EDITION OF 1 NOV 65 IS OBSOLETE

SECURITY CLASSIFICATION OF THIS PAGE *(When Data Entered)*

are given in the report. Considerable background material on the theoretical concepts and material characterizations required for the arrest of fast fractures and fatigue is also given. Taken together the work described in the report can be used as a first step in developing guidelines for ship designers in situations where structural perturbations for the purpose of arresting unstable crack propagation are envisioned.

☆U.S. GOVERNMENT PRINTING OFFICE: 1977—240-897:221

SHIP RESEARCH COMMITTEE
Maritime Transportation Research Board
National Academy of Sciences-National Research Council

The Ship Research Committee has technical cognizance of the interagency Ship Structure Committee's research program:

PROF. J. E. GOLDBERG, Chairman, *School of Civil Engrg., Georgia Inst. of Tech.*
DR. J. M. BARSOM, *Section Supervisor, U.S. Steel Corporation*
MR. D. P. COURTSAL, *Vice President, DRAVO Corporation*
MR. E. S. DILLON, *Consultant, Silver Spring, Maryland*
DEAN D. C. DRUCKER, *College of Engineering, University of Illinois*
PROF. L. LANDWEBER, *Inst. of Hydraulic Research, The University of Iowa*
MR. O. H. OAKLEY, *Consultant, McLean, Virginia*
MR. D. P. ROSEMAN, *Chief Naval Architect, Hydronautics, Inc.*
DEAN R. D. STOUT, *Graduate School, Lehigh University*
MR. R. W. RUMKE, *Executive Secretary, Ship Research Committee*

The Ship Materials, Fabrication, and Inspection Advisory Group prepared the project prospectus and evaluated the proposals for this project:

DR. J. M. BARSOM, Chairman, *Section Supervisor, U.S. Steel Corporation*
DR. J. N. CORDEA, *Senior Staff Metallurgist, ARMCO Steel Corporation*
MR. J. L. HOWARD, *President, Kvaerner-Moss, Inc.*
MR. J. G. KAUFMAN, *Manager, Technical Development, ALCOA*
MR. T. E. KOSTER, *Naval Architect, AMOCO International Oil Company*
DR. H. I. McHENRY, *Cryogenics Division, National Bureau of Standards*
PROF. S. T. ROLFE, *Civil Engineering Dept., The University of Kansas*
PROF. G. C. SIH, *Institute of Fracture & Solid Mechanics, Lehigh University*
PROF. J. H. WILLIAMS, JR., *Dept. of Mech. Engrg., Massachusetts Inst. of Tech.*

The SR-226 Project Advisory Committee provided the liaison technical guidance, and reviewed the project reports with the investigator:

MR. T. E. KOSTER, Chairman, *Naval Architect, AMOCO International Oil Company*
MR. G. E. LINNERT, *North American Representative, The Welding Institute*
PROF. W. H. MUNSE, *Dept. of Civil Engineering, University of Illinois*

SHIP STRUCTURE COMMITTEE PUBLICATIONS

These documents are distributed by the National Technical Information Service, Springfield, Va. 22151. These documents have been announced in the Clearinghouse journal U.S. Government Research & Development Reports (USGRDR) under the indicated AD numbers.

SSC-259, *Verification of the Rigid Vinyl Modeling Technique: The SL-7 Structure* by J. L. Rodd. 1976. AD-A025717.

SSC-260, *A Survey of Fastening Techniques for Shipbuilding* by N. Yutani and T. L. Reynolds. 1976. AD-A031501.

SSC-261, *Preventing Delayed Cracks in Ship Welds - Part I* by H. W. Mishler. 1976. AD-A031515.

SSC-262, *Preventing Delayed Cracks in Ship Welds - Part II* by H. W. Mishler. 1976. AD-A031526.

SSC-263, *Static Structural Calibration of Ship Response Instrumentation System Aboard the Sea-Land McLean* by R. R. Boentgen and J. W. Wheaton. 1976. AD-A031527.

SSC-264, *First Season Results from Ship Response Instrumentation Aboard the SL-7 Class Containership S.S. Sea-Land McLean in North Atlantic Service* by R. R. Boentgen, R. A. Fain, and J. W. Wheaton. 1976.

SL-7 PUBLICATIONS TO DATE

SL-7-1, (SSC-238) - *Design and Installation of a Ship Response Instrumentation System Aboard the SL-7 Class Containership S.S. SEA-LAND McLEAN* by R. A. Fain. 1974. AD 780090.

SL-7-2, (SSC-239) - *Wave Loads in a Model of the SL-7 Containership Running at Oblique Headings in Regular Waves* by J. F. Dalzell and M. J. Chiocco. 1974. AD 780065.

SL-7-3, (SSC-243) - *Structural Analysis of SL-7 Containership Under Combined Loading of Vertical, Lateral and Torsional Moments Using Finite Element Techniques* by A. M. Elbatouti, D. Liu, and H. Y. Jan. 1974. AD-A002620

SL-7-4, (SSC-246) - *Theoretical Estimates of Wave Loads on the SL-7 Containership in Regular and Irregular Seas* by P. Kaplan, T. P. Sargent, and J. Cilmi. 1974. AD-A004554.

SL-7-5, (SSC-257) - *SL-7 Instrumentation Program Background and Research Plan* by W. J. Siekierka, R. A. Johnson, and CDR C. S. Loosmore, USCG. 1976. AD-A021337.

SL-7-6, (SSC-259) - *Verification of the Rigid Vinyl Modeling Techniques: The SL-7 Structure* by J. L. Rodd. 1976. AD-A025717.

SL-7-7, (SSC-263) - *Static Structural Calibration of Ship Response Instrumentation System Aboard the SEA-LAND McLEAN* by R. R. Boentgen and J. W. Wheaton. 1976. AD-A031527.

SL-7-8, (SSC-264) - *First Season Results from Ship Response Instrumentation Aboard the SL-7 Class Containership S.S. SEA-LAND McLEAN in North Atlantic Service* by R. R. Boentgen, R. A. Fain, and J. W. Wheaton. 1976.